

Organic and molecular magnets

This article has been downloaded from IOPscience. Please scroll down to see the full text article.

2004 J. Phys.: Condens. Matter 16 R771

(<http://iopscience.iop.org/0953-8984/16/24/R03>)

View [the table of contents for this issue](#), or go to the [journal homepage](#) for more

Download details:

IP Address: 129.252.86.83

The article was downloaded on 27/05/2010 at 15:22

Please note that [terms and conditions apply](#).

TOPICAL REVIEW

Organic and molecular magnets

S J Blundell¹ and F L Pratt²¹ Department of Physics, Clarendon Laboratory, Oxford University, Parks Road, Oxford OX1 3PU, UK² ISIS Facility, Rutherford Appleton Laboratory, Chilton, Oxfordshire OX11 0QX, UK

E-mail: s.blundell@physics.ox.ac.uk and f.pratt@rl.ac.uk

Received 22 April 2004

Published 4 June 2004

Online at stacks.iop.org/JPhysCM/16/R771

doi:10.1088/0953-8984/16/24/R03

Abstract

Historically most materials in magnetic applications are based on inorganic materials. Recently, however, organic and molecular materials have begun to show increasing promise. Purely organic ferromagnets, based upon nitronyl nitroxide radicals, show long range magnetic order at very low temperatures in the region of 1 K, while sulfur based radicals show weak ferromagnetism at temperatures up to 36 K. It is also possible to prepare molecule based magnets in which transition metal ions are used to provide the magnetic moment, but organic groups mediate the interactions. This strategy has produced magnetic materials with a large variety of structures, including chains, layered systems and three-dimensional networks, some of which show ordering at room temperature and some of which have very high coercivity. Even if long range magnetic order is not achieved, the spin crossover effect may be observed, which has important applications. Further magnetic materials may be obtained by constructing charge transfer salts, which can produce metallic molecular magnets. Another development is single-molecule magnets, formed by preparing small magnetic clusters. These materials can show macroscopic quantum tunnelling of the magnetization and may have uses as memory devices or in quantum computation applications.

(Some figures in this article are in colour only in the electronic version)

Contents

1. Introduction	772
2. Organic magnets	774
2.1. Early attempts to produce organic ferromagnets	774
2.2. Nitronyl nitroxides	777
2.3. Other nitroxides	782
2.4. Verdazyl radicals	783

2.5. Sulfur based radicals	783
2.6. Fullerenes	785
3. Molecular magnets	786
3.1. Closed shell molecular systems	786
3.2. Open shell molecular systems	792
4. Two-dimensional systems	797
4.1. Layered hydroxides	797
4.2. Oxalates	798
4.3. BEDT-TTF salts	798
4.4. BETS salts	800
5. One-dimensional systems	803
5.1. Magnetic chains	803
5.2. Magnetic chains based on hexafluoroacetylacetonate	804
5.3. Spin–Peierls transition	805
5.4. First-order phase transitions in one-dimensional crystals	807
5.5. TMTSF salts and spin density waves	808
5.6. Polymeric magnets	808
6. Zero-dimensional systems: single-molecule magnets	808
6.1. Introduction	809
6.2. Mn ₁₂	812
6.3. Fe ₈	816
6.4. Other single-molecule magnets	818
6.5. Magnetic wheels	819
7. Conclusion	820
References	820

1. Introduction

Solid-state physics, and the study of ferromagnetism in particular, has been traditionally concerned almost exclusively with the study of *inorganic* elements (e.g. Fe, Co, Ni), alloys (e.g. permalloy) and simple compounds (e.g. transition metal oxides). This field of study has provided numerous technological rewards based upon the exploitation of such materials. But the underlying assumption that has driven much of the most basic research on solids is that the most fundamental physics research is best concentrated on *chemically simple* materials. This assumption is quite misplaced, and in fact some of the most exciting studies in condensed matter physics can now be attempted on certain *organic* materials which are *chemically very complicated* indeed. Their tunability, resulting from the rich structure of carbon chemistry which allows many small adjustments to be made to each molecule, means that in principle materials can be tailor-made to exhibit desired properties. This is only ‘in principle’ however, since the structure–property relations can turn out to be remarkably intricate. However there is an obvious advantage in choosing a route already favoured by biological systems.

The building blocks of these new organic materials are not atoms but molecules. Therefore many of the primary initiatives in this field have come from organic chemistry and coordination chemistry. A selection of molecules forming the basis of the materials to be discussed in this review can be found in figure 1. The shape of molecules and their electronic structure play a crucial role in determining the resulting crystallographic structure, and hence the observed physical properties. Intermolecular forces are typically weaker than interatomic forces and also rather short range. They differ markedly therefore from the type of strong, long range Coulombic forces found in ionic crystals. Molecular crystals are consequently rather soft and

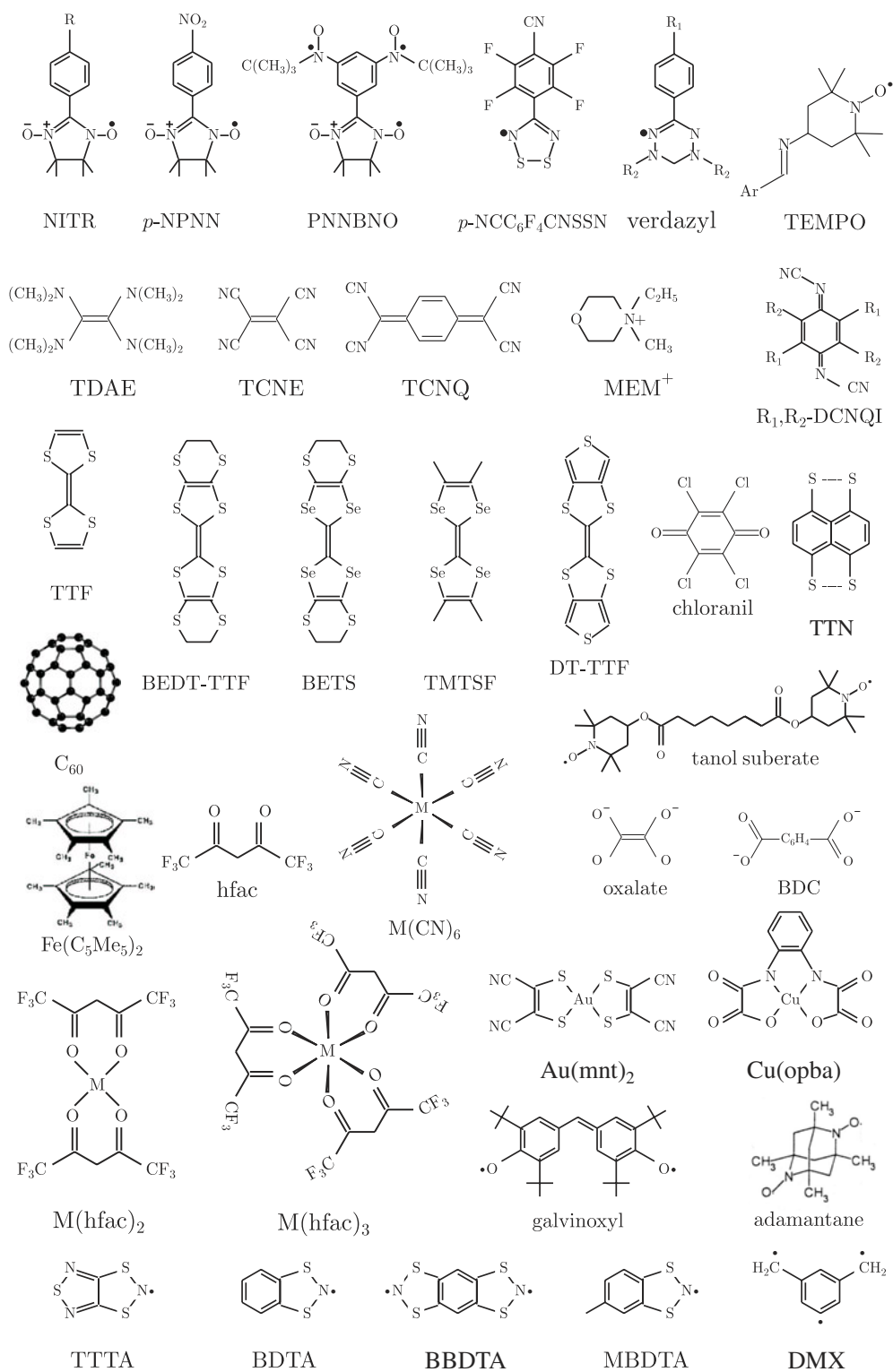


Figure 1. The molecular structure of some of the organic materials described in this review.

hence their properties can be extremely tunable using applied pressure. Molecular dimensions and vibrational frequencies typically resemble those of the free molecule because of the dominance of intramolecular forces over intermolecular forces. The latter do however strongly influence properties such as charge transport and can lead to large correlation effects (enhanced effective masses, superconductivity, density wave ground states [1]).

Organic materials can often possess interesting optical properties, thus allowing the possibility of devices which implement new functionality. The impetus to study organic materials in condensed matter physics stems particularly from the recent remarkable discoveries of three types of new material: first, conducting polymers which, despite their flexibility, can have electrical conductivities as high as conventional metals such as copper and which have been used in the fabrication of polymer transistors and light-emitting-diode devices; second, superconducting charge transfer salts which can exhibit superconducting transition temperatures approaching 15 K; third, carbon ‘buckyballs’ C_{60} , a newly discovered allotrope of carbon which when appropriately doped may exhibit superconductivity [2, 3] or even, as described below, unusual magnetic properties. These examples are well known and have been reviewed elsewhere. However, as described in detail in this review, organic and molecular materials have an extraordinarily diverse range of magnetic properties. In this review, we describe the main strands in this rapidly emerging field, though the choice of examples and topics in this broad and expanding field is inevitably a personal one. For further information the interested reader is referred to more specialized reviews which have recently appeared [4–10]. We do not aim to offer a comprehensive survey of all the materials which have been studied but instead focus on their most important physical properties.

The review is structured as follows. In section 2, we describe purely organic magnets in which it is only carbon based molecular species which bear an unpaired spin. Section 3 describes molecular magnets in which magnetic transition metal ions are introduced but organic molecules are used either to simply mediate the magnetic interactions or to also play a role in the magnetism themselves. The remaining sections focus on physical properties that are associated with particular reduced dimensionality, which can be two (section 4), one (section 5) or zero (section 6).

2. Organic magnets

The drive to produce purely organic ferromagnets comes partly from the desire to achieve something that was once thought impossible: making ferromagnetism in materials containing only s and p electrons. Heisenberg’s theory of ferromagnetism [11], which was formulated in the 1920s and which introduced the concept of exchange, explained this mandatory requirement for d and f electrons. Conventional wisdom has it that, for example, carbon (containing only s and p electrons) does not have a spontaneous magnetic moment in any of its allotropes.

Many organic radicals exist which have unpaired spins, but few are stable enough to be assembled into crystalline structures. Moreover, even when that is possible *aligning* these spins ferromagnetically is usually impossible. Ferromagnets are rather rare even among the elements and even there are exclusively found in the d or f block.

2.1. Early attempts to produce organic ferromagnets

Neutral organic radicals possess an odd number of electrons (and hence one unpaired electron) and are often highly chemically reactive. They can be made more stable by adding aromatic rings to delocalize the unpaired electron or by introducing bulky substituents. Crystals of neutral organic radicals exhibit paramagnetism at high temperatures, provided dimerization can be prevented. They then usually show a very small negative Weiss constant, indicating

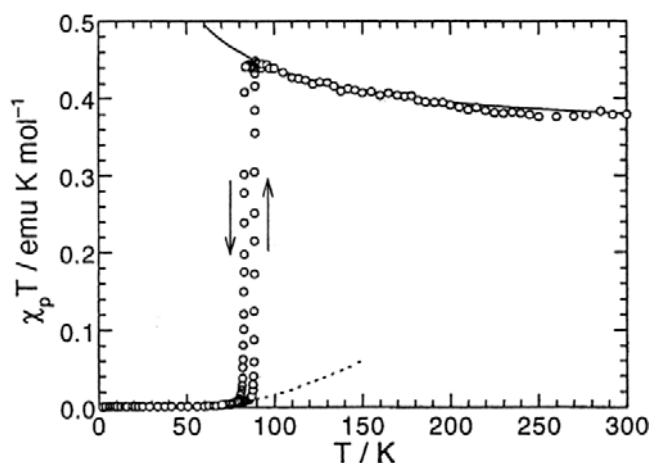


Figure 2. The magnetic susceptibility of galvinoxyl [12]. Ferromagnetic interactions dominate above the phase transition at 85 K. The high temperature behaviour fits to a one-dimensional ferromagnetic Heisenberg model and the low temperature behaviour fits to a singlet–triplet model.

weak antiferromagnetic interactions. This is to be expected, since the intermolecular overlaps of the singly occupied molecular orbitals (SOMO) will tend to lead to a state with the character of a bonding orbital, i.e. one in which one SOMO is spin up and the other is spin down.

Prospects for ferromagnetic interaction between organic molecules therefore seemed limited, but in 1969 ferromagnetic interactions were identified in crystals of galvinoxyl [13] (molecular structure shown in figure 1). Magnetic susceptibility measurements gave a positive Weiss constant (19 K), but the crystal undergoes a phase transition at 85 K to a low temperature phase with strong antiferromagnetic interactions [14, 15] ($J/k_B = -260$ K). In galvinoxyl, the almost planar radicals are arranged in stacks along the c axis, and in fact the high temperature susceptibility is well reproduced by a one-dimensional ferromagnetic Heisenberg model with $J/k_B = 13 \pm 1$ K [12] (see figure 2). The first-order phase transition is hysteretic (width 5 K) and the low temperature susceptibility is consistent with a singlet–triplet model with $J/k_B = -230 \pm 20$ K [12].

The magnetic moment on the galvinoxyl radical is due to the SOMOs. Galvinoxyl has a large spin polarization because the large intramolecular exchange means that the next-highest occupied molecular orbital (NHOMO) for \downarrow -spin (often denoted β) is higher in energy than the SOMO for \uparrow -spin (often denoted α), thus stabilizing the latter state (see figure 3). It is found that the intermolecular SOMO–SOMO overlap is very small (this is because the π -orbitals are spread out over the molecule, and the SOMO–SOMO overlap is positive in some regions and negative in others, so averages to a small value overall). Hence the SOMOs on neighbouring molecules are almost orthogonal.

In many organic radicals, a singlet state (i.e. antiferromagnetic alignment) is stabilized by resonance with an excited charge transfer configuration involving intermolecular SOMO–SOMO overlap. Because this overlap is small in galvinoxyl, the triplet state (i.e. ferromagnetic alignment) is stabilized by resonance with excited charge transfer configurations involving intermolecular interactions between the SOMO on one molecule and the fully occupied molecular orbital on the other [16]. Large spin polarization can be achieved by promoting intramolecular exchange, and this can be helped by using electronegative atoms such as oxygen or nitrogen, which lead to a large probability of occupation by an unpaired π electron. An extended π system also helps ferromagnetic interactions by promoting the SOMO–NHOMO interaction [17]. The crystal structure is also a vital ingredient and this must be such as to minimize the intermolecular SOMO–SOMO overlaps. The overlap between the SOMO on one molecule and the NHOMO/NLUMO (NLUMO = next-lowest unoccupied molecular

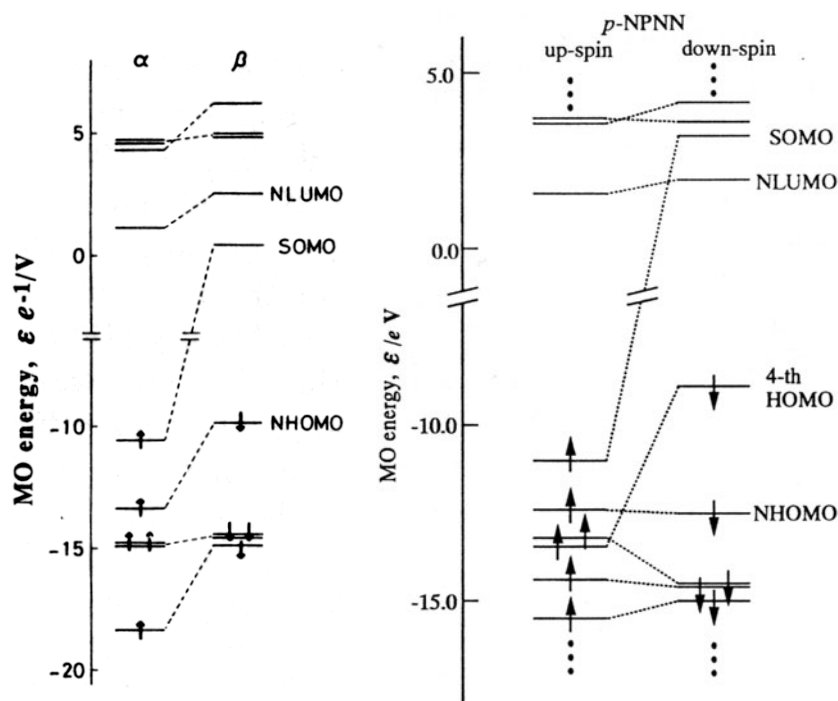


Figure 3. Energies of the molecular orbitals in galvinoxyl [17] (left) and *p*-NPNN (right) [30]. NLUMO = next-lowest unoccupied molecular orbital; SOMO = singly occupied molecular orbital; HOMO = highest occupied molecular orbital; NHOMO = next-highest occupied molecular orbital.

orbital) on the other can be such that regions of positive spin density on one molecule overlap with regions of negative spin density on the other molecule, thus promoting ferromagnetic interactions [18]. Galvinoxyl therefore fulfilled many of the conditions necessary to be an organic ferromagnet, but unfortunately only above the 85 K phase transition.

Another early candidate organic ferromagnet was tanol suberate (see figure 1), which is a biradical with formula $(C_{13}H_{23}O_2NO)_2$. The spin density is found to be located on the NO group and almost equally shared between the oxygen and the nitrogen atoms [19]. The magnetic susceptibility measured down to liquid helium temperatures follows a Curie–Weiss law with a positive Curie temperature (+0.7 K) and it therefore looked like a good candidate for an organic ferromagnet. The specific heat exhibits a λ anomaly [20] at 0.38 K, but tanol suberate was actually found to be an antiferromagnet with a metamagnetic transition in a field of 6 mT, resulting in ferromagnetic spin alignment [21, 22]; this accounts for the initial belief that it was an organic ferromagnet.

In tanol suberate the molecules are arranged in sheet-like layers in which the magnetic moments are almost localized [25]. Neutron scattering experiments confirm that the magnetic moments lie in the plane of the sheets and the directions of magnetic moments, aligning parallel to each other in a sheet, are antiparallel to those in adjacent sheets [21]. Although the susceptibility was originally analysed according to a model assuming one-dimensional ferromagnetic interactions associated with interchain interactions [22], a recent study has shown that the susceptibility is much better described by a two-dimensional ferromagnetic square lattice with interlayer coupling $J/k_B = 0.67$ K [26]. Muon spin rotation (μ SR) experiments [24] yield clear spin precession oscillations (see figure 4(b)). The temperature

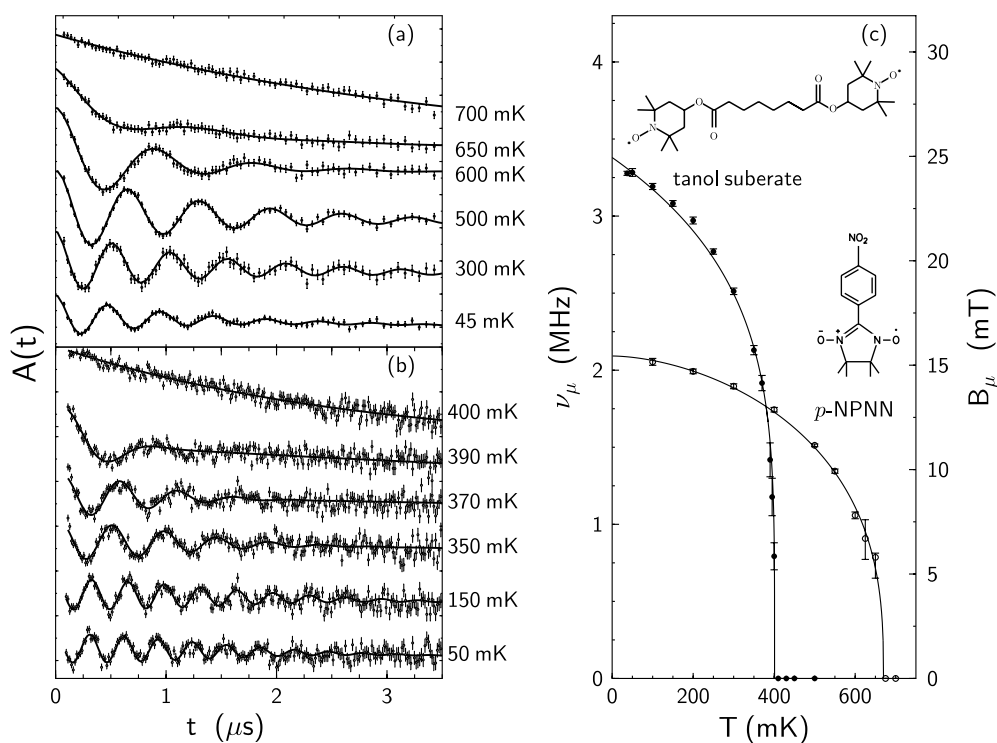


Figure 4. The zero-field muon spin rotation frequency in (a) the organic ferromagnet *p*-NPNN (after [23]) and (b) the organic antiferromagnet tanol suberate (after [24]). In both cases the data for different temperatures are offset vertically for clarity. (c) The temperature dependence of the zero-field muon spin rotation frequency in *p*-NPNN and tanol suberate.

dependence of the precession frequency (figure 4(c)) fits to $\nu_{\mu}(T) = \nu_{\mu}(0)(1 - T/T_c)^{\beta}$ where $\beta = 0.22$, consistent with a two-dimensional *XY* magnet [27] and also with the temperature dependence of the magnetic susceptibility [26], suggesting that the ordered state is dominated by two-dimensional interactions.

2.2. Nitronyl nitroxides

Following these early attempts, genuine organic ferromagnetism was first achieved using a member of a family of organic radicals called nitronyl nitroxides [6]. These have general molecular structure as shown by the molecule labelled NITR in figure 1. Different systems can be obtained by varying the chemical group R, as illustrated by the specific examples shown in the top row of figure 1. Nitronyl nitroxides are extensively used as spin labels to mark biological systems. The unpaired electron in nitronyl nitroxides is mainly distributed over the two NO moieties, although some unpaired spin density is also distributed over the rest of the molecule. The central carbon atom of the O–N–C–N–O moiety is a node of the SOMO. Nitronyl nitroxides are chemically stable but the vast majority of them do not show long range ferromagnetic order. Therefore, the discovery of long range ferromagnetism in one of the crystal phases (the β phase) of *para*-nitrophenyl nitronyl nitroxide (C₁₃H₁₆N₃O₄, abbreviated to *p*-NPNN; see figure 1 for molecular structure) was particularly exciting, even though the transition temperature was a disappointingly low 0.65 K [28] and only present in one of its crystal phases.

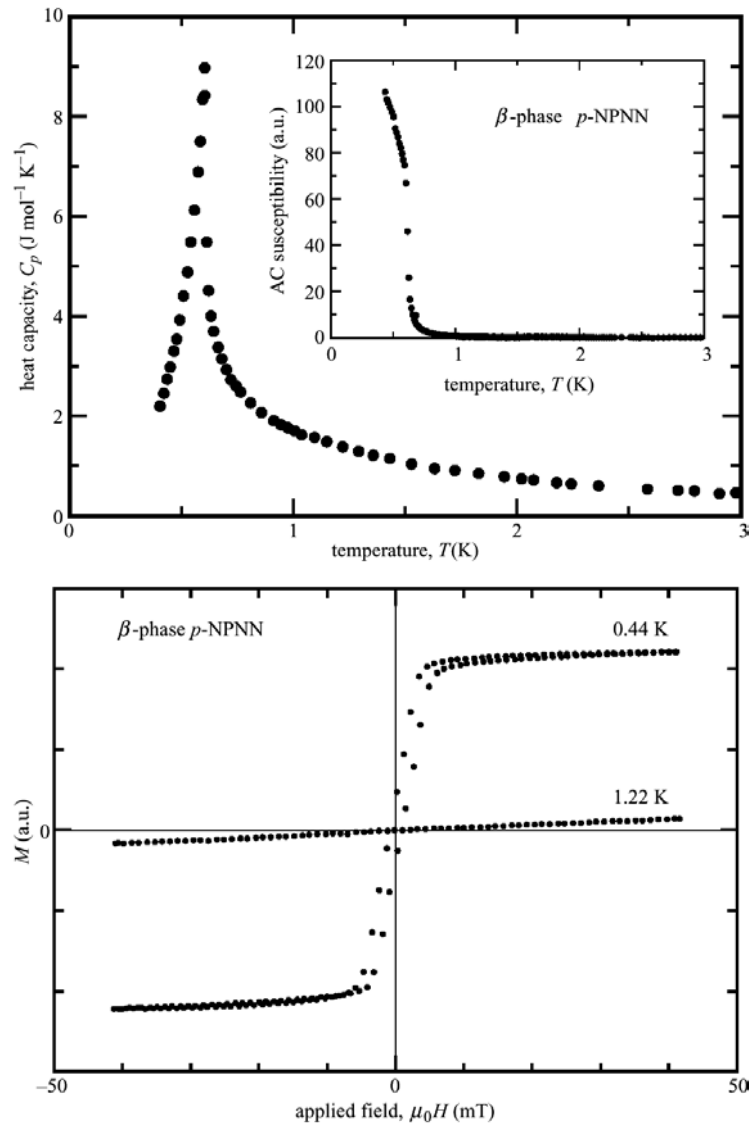


Figure 5. The upper figure shows the temperature dependence of the magnetic heat capacity of the β phase of p -NPNN. The inset shows the temperature dependence of the AC susceptibility. The lower figure shows the magnetization curves for the same material measured at temperature above and below the transition temperature (after [28–30]).

The transition to ferromagnetic order was indicated by a λ -type peak in the heat capacity (see figure 5) and a divergence in the AC susceptibility at the critical temperature [28, 29]. The magnetization below T_C saturates in a very small field (see figure 5), demonstrating that p -NPNN is a very soft ferromagnet. μ SR experiments on p -NPNN (figure 4(a)) show the development of coherent spin precession oscillations below T_C [31, 23]. The temperature dependence of the precession frequency and the corresponding local field at the muon site is shown in figure 4(c). This is fitted to a functional form $\nu_\mu(T) = (1 - (T/T_C)^\alpha)^\beta$ yielding $\alpha = 1.7 \pm 0.4$ and $\beta = 0.36 \pm 0.05$. In this expression, the parameter β controls the behaviour near T_C , while the parameter α determines the power law at $T \ll T_C$. This is consistent with

three-dimensional long range magnetic order [31, 23]. Near T_C the critical exponent is as expected for a three-dimensional Heisenberg model (one expects $\beta \approx 0.36$ in this case). At low temperatures the reduction in local field with increasing temperature is consistent with a Bloch $T^{3/2}$ law ($\alpha = 1.5$), indicative of three-dimensional spin waves.

The overlaps in all these materials which favour ferromagnetism appear to agree with the McConnell mechanism [18]: as a result of spin polarization effects, positive and negative spin density may exist on different parts of each molecule; intermolecular exchange interactions tend to be antiferromagnetic, so if the dominant overlaps are between positive (majority) spin density on one molecule and negative (minority) spin density on another molecule, the overall intermolecular interaction may be ferromagnetic. Though the mechanism for ferromagnetism is electronic, the low values of T_C imply that the magnetic dipolar interactions will play a role in contributing to the precise value of T_C . Dipolar interactions are also particularly important in determining the easy magnetization axis [30, 23]. This too depends on the crystal structure, which in turn depends on the molecular shape.

The energies of the molecular orbitals in *p*-NPNN are shown in figure 3 and demonstrate that the energy of the SOMO for \downarrow -spin is very high, so that the spin polarization in *p*-NPNN is expected to be very large. The spin density in nitronyl nitroxides can be studied using neutron scattering. Neutrons interact both with nuclei and with magnetic moments in a sample. These interactions can be separated by the use of spin-polarized neutrons. The scattered intensity $I(\mathbf{k})$ for scattering vector \mathbf{k} is given by

$$I(\mathbf{k}) = |F_N(\mathbf{k})|^2 + \mathbf{P} \cdot (\mathbf{F}_M^\perp(\mathbf{k}) F_N^*(\mathbf{k}) + \mathbf{F}_M^{\perp*}(\mathbf{k}) F_N(\mathbf{k})) + |\mathbf{F}_M^\perp(\mathbf{k})|^2 \quad (1)$$

where $F_N(\mathbf{k}) = \sum_j b_j e^{i\mathbf{k}\cdot\mathbf{r}_j} e^{-W_j}$ is the nuclear structure factor, $\mathbf{F}_M^\perp(\mathbf{k})$ is the projection of the magnetic structure factor $\mathbf{F}_M(\mathbf{k}) = \int_{\text{cell}} \mathbf{M}(\mathbf{r}) e^{i\mathbf{k}\cdot\mathbf{r}} d^3r$ on to the plane perpendicular to \mathbf{k} , \mathbf{P} is the polarization of the beam, W_j is a Debye–Waller factor for the j th atom in the unit cell at position r_j with scattering length b_j . The sample is magnetized by an external field and the intensity distribution of scattered polarized neutrons is measured. By measuring the scattered intensity with the polarization of the beam being either parallel or antiparallel to the magnetic field, the sign of the interference term in equation (1) can be measured, yielding an enormous sensitivity in determination of the magnetic structure factor. This can allow the mapping of the spin density distribution inside the unit cell, either by direct Fourier inversion or by MaxEnt reconstruction [33].

Figure 6 shows the spin density map of *p*-NPNN [32], which reveals a strong region of positive spin density which is delocalized over the nitronyl nitroxide group, as expected, but also a region of positive spin density on the nitrogen of the nitro group (labelled N2) corresponding to a *p* orbital perpendicular to the plane of the NO_2 group. The orthogonality of the *p* orbitals of N2 and O1 favours a ferromagnetic coupling between molecules. Each molecule of *p*-NPNN has a magnetic moment because of the radical (unpaired) electron which is delocalized over the O–N–C–N–O moiety (as shown in figure 6).

The importance of crystal structure is demonstrated by the fact that the only phase of *p*-NPNN which shows ferromagnetism is the (fortunately most thermodynamically stable) β phase (see figure 7(a)). At one stage it was thought that the γ phase of *p*-NPNN showed long range ferromagnetic order [34] but it later appeared that the γ phase gradually transforms into the β phase at room temperature, so that the signature of ferromagnetism in the γ phase of *p*-NPNN was in fact due to a small impurity of β phase [35]. The effect of pressure can be studied on *p*-NPNN, and such experiments show a reduction in the Curie temperature by nearly a factor of two to 0.35 K at 7.2 kbar. There is also evidence that the system becomes more anisotropic [36]. More recent studies have shown that this may be connected with a switch to antiferromagnetic order [37].

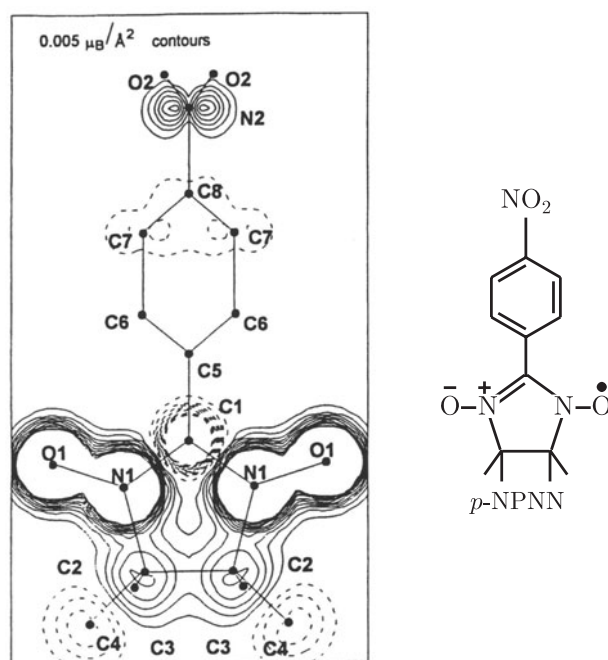


Figure 6. The spin density map obtained from polarized neutron diffraction experiments (after [32]) for *p*-NPNN (molecular structure shown to the right), contours at $0.005 \mu_B \text{ \AA}^{-2}$.

Various chemical modifications can be made to *p*-NPNN in order to change the properties, particularly substituting different groups for the para-nitrophenyl group. However, such small changes can lead to significant modifications of the crystal structure, thereby altering the intermolecular overlaps and thus the magnetic interactions between unpaired spins on neighbouring molecules. For example, the molecules 3-QNNN and 4-QNNN (QNNN is quinolyl nitronyl nitroxide; see figure 8 for molecular structures) are isomers, but the former is a weak ferromagnet with transition temperature close to 210 mK while the latter is non-magnetic [38, 39]. Similarly, 1-NAPNN shows a magnetic transition while its isomer 2-NAPNN does not [40] (NAPNN is naphthyl nitronyl nitroxide; see figure 8). In each case, the different isomers have different shapes and so pack in different ways, thus altering the intermolecular overlaps (see figures 7(b), (d) and (e)). The crystal structure of *para*-pyridyl nitronyl nitroxide (*p*-PYNN; see figure 8) consists of one-dimensional chains in which molecules are arranged side by side and head to tail [41]. This favours ferromagnetic interactions along the chain (see figure 7(c)) but the interchain interactions are thought to be antiferromagnetic, and a transition is observed at ~ 90 mK [41]. Thus, different compounds have greatly different magnetic ground states. The relationship between crystal structure and magnetic properties in these systems has been discussed in some detail elsewhere [42, 43].

Besides the usual ground states for these systems showing either magnetic order or non-magnetic singlet pairing, some examples of nitronyl nitroxides have also been found that show magnetic properties dominated by geometrical frustration. Salts of the molecule *m*-*N*-methylpyridinium nitronyl nitroxide (*m*-MPYNN; see figure 8) of the form *m*-MPYNN⁺M⁻, where M is typically BF₄, ClO₄ or I provide an example of the geometrically frustrated triangular Kagomé lattice [45]. In this salt pairs of $S = 1/2$ *m*-MPYNN molecules are ferromagnetically coupled to form an $S = 1$ dimer at each Kagomé lattice point (see figure 9).

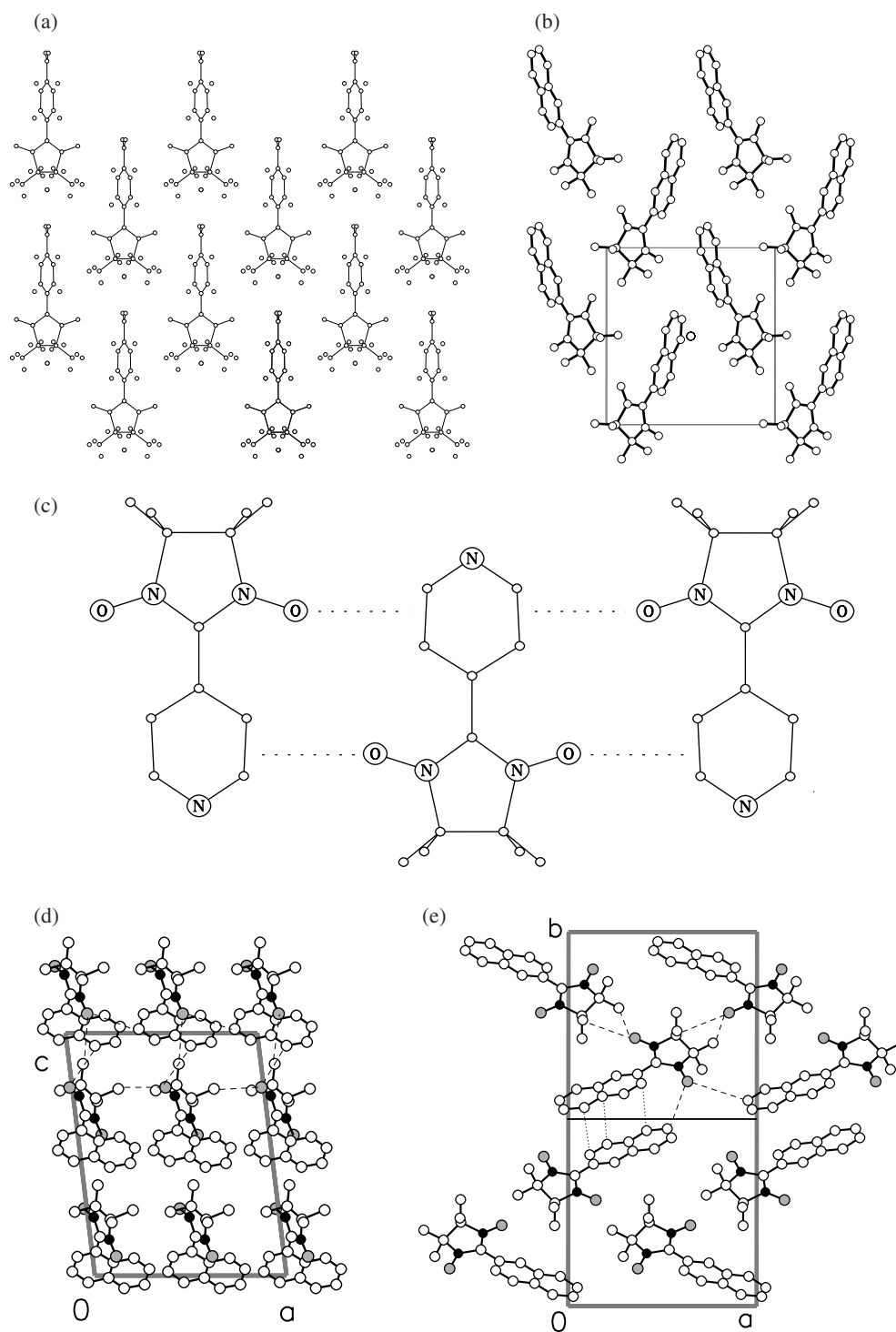


Figure 7. Pictures of the crystal structure of various nitronyl nitroxides: (a) *p*-NPNN (β phase), (b) 3-QNNN, (c) *p*-PYNN (shown along a particular direction and emphasizing the dominant intermolecular overlaps) and the isomers (d) 1-NAPNN and (e) 2-NAPNN. The molecular structures of these molecules are shown in figure 8.

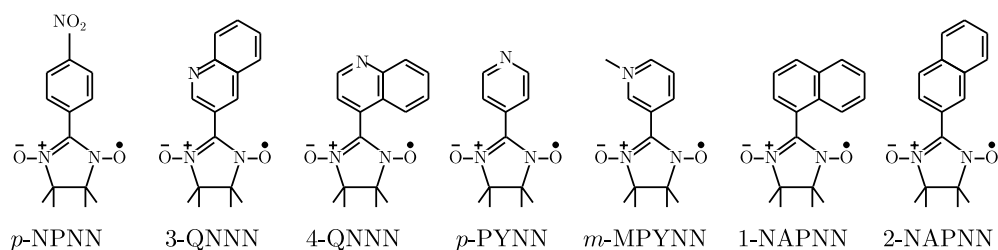


Figure 8. The molecular structure of some modifications of p -NPNN which are discussed in the text.

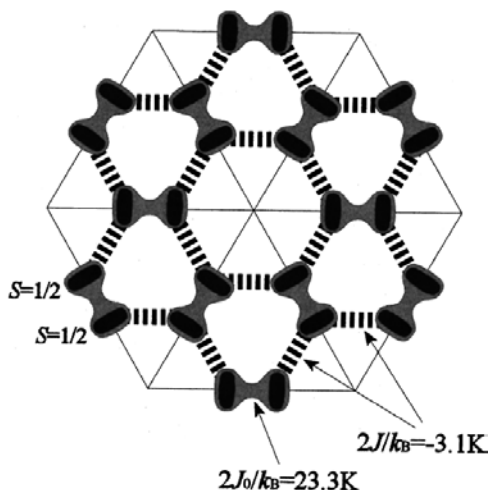


Figure 9. The Kagomé structure of m -MPYNN·BF₄. Two m -MPYNN molecules form an $S = 1$ dimer with a ferromagnetic intermolecular exchange interaction $2J_0$. Dimers are coupled by an antiferromagnetic interdimer exchange interaction $2J$. (Reprinted with permission from [44]. Copyright 1998, the American Physical Society.)

The interaction between adjacent dimers is antiferromagnetic, leading to frustration on the triangular lattice. However detailed magnetic susceptibility studies for the BF₄ salt taken to very low temperatures showed evidence for short range magnetic order and spin gap formation below 0.25 K [46, 47].

2.3. Other nitroxides

Forming polyradical molecules with ferromagnetic intramolecular coupling leads to high spin molecules with potential for improved transition temperatures. A biradical molecule currently holds the transition temperature record for a fully organic ferromagnet, which was measured at 1.48 K in the compound diazaadamantane dinitroxide (adamantane for short) [48] (see figure 1 for molecular structure). Triradicals have also been studied. One example is 1,3,5-tris(nitronyl nitroxide)benzene (abbreviated as TNN, see figure 1 for the molecular structure), which was reported to have an $S = 3/2$ ground state, however the intermolecular antiferromagnetic interactions between the radical spins were found to be stronger than the ferromagnetic coupling between the spins on the same molecule, producing a temperature dependent susceptibility characteristic of an antiferromagnetic chain [49].

Asymmetric molecular structure in a triradical can lead to a ferrimagnetic molecular moment. An example of such a nitroxide based organic ferrimagnet, PNNBNO (see figure 1 for molecular structure), has recently been prepared [50] with a three-dimensional phase transition at 0.28 K. The molecular triradical has two spins ferromagnetically coupled to give an $S = 1$

unit and a separate $S = \frac{1}{2}$ unit within a single molecule. The two units are connected by an antiferromagnetic intramolecular exchange. Coupling between molecules is dominated by antiferromagnetic interaction between the different types of spin, producing a bulk ferrimagnet.

Very recently, an organic triradical with an open shell doublet ground state has been discovered [51]. The material, 5-dehydron-*m*-xylylene (DMX; see figure 1 for molecular structure), is made from reacting a xylene compound with fluorine. It will be interesting to see if this new radical can be used as a building block in new non-metallic magnets.

Other stable nitroxide organic radicals showing ferromagnetic interactions have been found, including those based on imino nitroxides and TEMPO (see figure 1) [52, 53]. The highest ferromagnetic transition temperature for the family Ar-CH=N-TEMPO is 0.28 K for Ar=4-chloro-benzylidene; the magnetically ordered states for the series have been confirmed by μ SR [54]. These materials have a layered structure and the low transition temperatures are considered to be the result of weak dipolar coupling between ferromagnetic layers. Hydrostatic pressure was found to produce periodic variation in T_C and result in a switch from ferromagnetic to antiferromagnetic behaviour for pressures above 0.5 GPa [55]. Similar pressure studies on the β phase of *p*-NPNN produced a comparable ferromagnetic to antiferromagnetic crossover but no oscillations in T_C and just a general reduction in T_C . In the case of 2,5-difluorophenyl- α -nitronyl nitroxide, no T_C oscillations or crossover were observed but the ferromagnetic T_C was found to steadily increase from 0.45 to 0.57 K under 1.35 GPa [37].

2.4. Verdazyl radicals

Verdazyls provide another family of stable organic radicals (figure 10). Ferromagnetic intermolecular interactions were first demonstrated in 1,3,5-triphenylverdazyl [56], which showed a positive Weiss constant of 1.6 K. Some variants on the structure in the form of oxo-verdazyl and thioxo-verdazyl were reported [57]. For all these molecules, substitutions can be made on several different positions on the molecule, leading to a wide range of magnetic systems. Some examples of these materials and their magnetic properties are listed in figure 10. It is particularly notable that ferromagnetism has been observed in *p*-CDpOV with $T_C = 0.21$ K [58], in *p*-CDTV with $T_C = 0.68$ K [59] and in *p*-MeDpOV with $T_C = 0.67$ K [60]. These latter transition temperatures are comparable to that of the original *p*-NPNN nitronyl nitroxide organic ferromagnet. Examples of antiferromagnetism, weak ferromagnetism and spin–Peierls transitions have also been seen in verdazyl systems. Alloying between differently substituted oxo-verdazyl radicals has allowed the effect of randomly substituted antiferromagnetic and ferromagnetic Heisenberg interactions on a quasi-1D chain to be studied [61]. Although the number of different verdazyl materials is large, detailed crystal structures have only been obtained in a few cases, so it has not been possible so far to make the detailed studies of the structure–property relationships in verdazyls that have been made on other families of organic radical magnets.

2.5. Sulfur based radicals

Sulfur based radicals are emerging as important building blocks for molecular magnets; the magnetic properties of thiazyl radicals were recently reviewed in some detail by Rawson and Palacio [62]. Whereas the transition temperatures of the nitroxide based organic radicals showing long range magnetic order described in the previous section are very low, typically below 1 K, the recent discovery of spontaneous magnetization below 35 K associated with noncollinear antiferromagnetism in the β crystal phase of the dithia-diazolyl molecular radical *p*-NC(C₆F₄)(CNSSN) [63] (see figure 1 for molecular structure) has shown a viable route

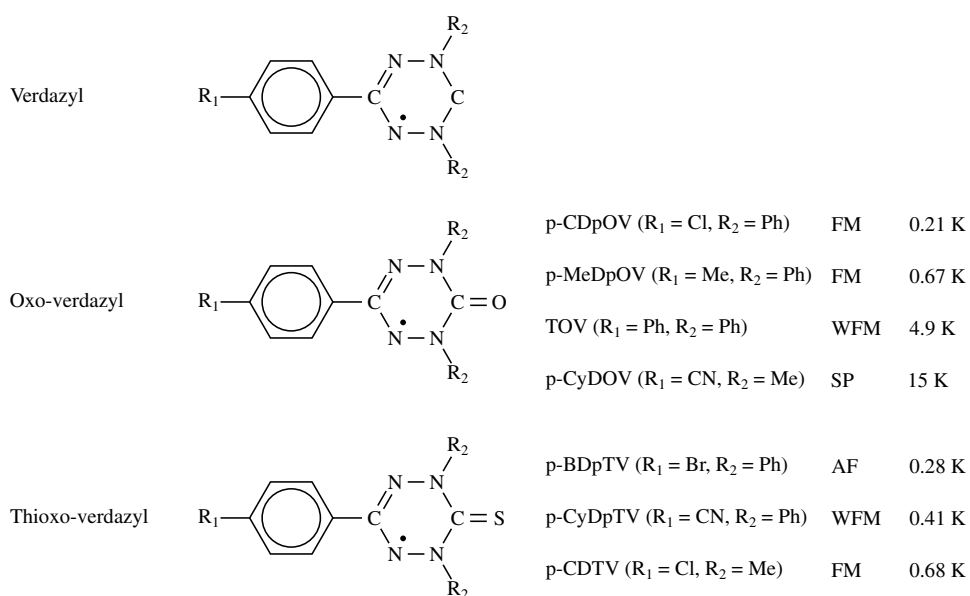


Figure 10. The molecular structure of several types of verdazyl radical along with some examples showing ferromagnetic (FM), weak ferromagnetic (WFM), antiferromagnetic (AF) and spin-Peierls (SP) transitions.

towards higher transition temperatures. In fact it was found that T_C for this material could be raised still further to 65 K by applying a hydrostatic pressure of 16 kbar [64].

Zero-field μSR has been used to study the internal field in this system [65]. Two distinct frequencies are resolved in the zero-field muon spin rotation signal, which have been assigned to muon states bonded at two different sites on the CNSSN ring. The muon data show that the easy direction for the spin structure is along the b axis, in agreement with neutron studies. Muon spin relaxation below the transition follows the power law expected for two-magnon scattering and also shows a distinct antiresonance feature just below the magnetic transition, which has been assigned to an interaction between magnons and low frequency intermolecular phonons [65].

The crystal structure of this material provides an elongated diamond-structure-like three-dimensional exchange pathway between the molecules, which is believed to be one of the reasons for the relatively high transition temperature. Thiazyl radicals appear to be particularly promising structural units for providing the multidimensional coupling needed for high magnetic transition temperatures. A number of substitutions on the dithia-diazolyl molecule have been reported and it was found that the molecular packing in the crystal and the corresponding magnetic properties are very sensitive to these substitutions. Dimerized structures are formed in many cases leading to singlet state formation and diamagnetic properties. Substituting the cyano group by a nitro group however produces an organic ferromagnet with an ordering temperature of 1.3 K. This represents only the second example of a purely organic ferromagnet to be found with a T_C above 1 K [66]. Substitution of the cyano group by bromine produces an undimerized paramagnetic system with antiferromagnetic interactions and no sign of long range magnetic order down to 1.8 K [67]. If the sulfur in the cyano dithia-diazolyl radical is substituted by selenium then a dimerized non-magnetic structure is produced, with an unusual perpendicular interaction between the CNSSN rings of the molecules forming the dimer [68].

Another group of sulfur containing molecular radicals is the series of dithiazolyl radicals. One of the first to be studied was benzodithiazolyl radical (BDTA; see figure 1 for molecular structure), which was found to be strongly dimerized and diamagnetic down to 4.2 K [69]. Methyl substitution of BDTA produces MBDTA (see figure 1 for molecular structure), which was found to have a regularly spaced molecular stacking structure with a paramagnetic state showing two-dimensional Heisenberg antiferromagnetic correlations down to 1.8 K [70]. Recent studies of BDTA [71] have shown a number of interesting new properties at high temperature, in particular that the paramagnetic state can be recovered by heating above 346 K and that supercooling of this paramagnetic state can be achieved, leading to antiferromagnetic ordering at 11 K.

An interesting thiazyl radical is TTTA (1,3,5-trithia-2,4,6-triazapentalenyl; see figure 1 for molecular structure). This material has a first-order spin–Peierls-like transition between a non-magnetic dimerized stack structure at low temperature and a paramagnetic regular stack structure at high temperatures [72–74]. The transition is hysteretic, resulting in magnetic bistability at room temperature [75]. Optical bistability and optical switching were also reported recently for this material [76]. We note that there are some similarities between these properties and those of the metal–organic hybrid spin crossover systems which will be discussed in section 4. Further discussion will be found of spin–Peierls transitions in section 5.3 and the TTTA transition in section 5.4.

Thiazyl radicals have been used to form cation radical salts [77]. Starting with the diradical BBDTA (benzo[1,2-*d*:4,5-*d'*]bis[1,3,2]dithiazole; see figure 1 for molecular structure), a 1:1 charge transfer salt can be formed between a monoradical cation BBDTA⁺ and a GaCl₄[−] anion, the crystal also containing a single molecule of acetonitrile solvent per formula unit. This material shows antiferromagnetic ordering at 6.6 K [77]. Recently it was reported by that removal of the solvent changes the sign of the magnetic interaction, resulting in a ferromagnetic transition at 6.7 K [78]. It was further reported that replacing the Ga by Fe and the acetonitrile solvent by acetone produced an antiferromagnetic transition at 6.3 K in the solvated system and a ferrimagnetic transition at 44 K in desolvated material [79].

2.6. Fullerenes

Much interest followed the discovery of ferromagnetism in TDAE-C₆₀, a compound of tetrakis(dimethylamino)ethylene (TDAE; see figure 1 for molecular structure) and buckminsterfullerene (C₆₀; see figure 1 for molecular structure) at the relatively high temperature of 16 K [80]. This discovery was soon followed by a characterization of the magnetic state by μ SR [81]; these experimental results supported the initial interpretation of ferromagnetism in TDAE-C₆₀ [81]. However, these results have remained controversial with successive experiments using a range of techniques pointing to a variety of possible types of ground state, including itinerant ferromagnetism [80], spin glass [82, 83], superparamagnetic [84], spin-canted ferromagnetism [85], 3D Heisenberg ferromagnetism [86] or non-magnetic down to low temperature [87].

It has become clear that the problem is related to sample preparation, but how? This puzzle has recently been resolved. It appears that a crucial ingredient is the way in which the sample is annealed. Annealing at 350 K leads to a well defined transition temperature at 16 K, while the as-grown crystal showed a glassy ground state with no magnetic ordering [87, 88]. This difference was posited to be connected with the orientation of the C₆₀ molecules in TDAE-C₆₀ and the way in which this might feed through to the magnetic properties [89, 90]. A very recent structural study [91] has confirmed this assumption: fresh single crystals can be grown below 10 °C, which show no ferromagnetic behaviour when cooled down to 2 K (this is the

α' phase) but on annealing at high temperature, they transform to the α phase which shows long range ferromagnetism below 16 K. The two forms appear structurally indistinguishable at room temperature, but small differences between the orientation of the C_{60} molecules in the two phases show up in structural data below 50 K [91]. In the α' phase the relative C_{60} orientations are similar to those encountered in other C_{60} solids with a hexagon on one molecule facing the double bond on another molecule. The α phase contains a new orientation, leading to various possible relative configurations.

Another set of magnetic fullerenes take the form AC_{60} (where $A = Rb$ [92, 93], Cs [94]) and these have a more quasi-one-dimensional structure than TDAE- C_{60} . These alkali fullerenes do not superconduct and μ SR experiments show random static magnetic order freezing in at low temperature [92–94]; there is a large distribution of internal fields in the magnetic ground state which could be consistent with a spin density wave. Antiferromagnetic transitions were found in the series $NH_3K_{3-x}Rb_xC_{60}$ with T_N ranging from 40 to 80 K [95].

A dramatic development in molecular magnetism was provided in 2001 by the report from Makarova *et al* of room temperature ferromagnetism in C_{60} fullerene polymerized at high temperature and pressure [96], which has since been reproduced by several other groups [97, 98]. The maximum remanent magnetization is found for samples polymerized around 800 K, just below the point at which the buckyballs collapse. Under these conditions a two-dimensional rhombohedral polymer phase is produced containing layers of covalently bonded C_{60} molecules. The spontaneous magnetization is stable up to very high temperatures and estimated Curie temperatures for different samples range from 500 K [96] to 820 K [97]. Using electron microscopy and x-ray diffraction Wood *et al* [97] showed that the buckyballs are undamaged in the most magnetic phase, suggesting that the magnetism is due to radical centres formed by the dangling bonds which are left over following the breaking up of the intermolecular bridging bonds in the polymer. The mechanism for the magnetic coupling between these radical centres is not yet elucidated and the magnetization is very small and far from being uniformly distributed throughout the sample. Nevertheless, the discovery that such a strong magnetic coupling is possible in a system purely containing s and p electrons is highly encouraging for those looking to develop further molecular ferromagnets with high transition temperatures.

3. Molecular magnets

One way to raise the magnetic ordering temperature to well above room temperature is by preparing ‘hybrid materials’ known as molecular magnets in which organic groups are combined with transition metal or rare earth ions [4, 5]. These materials can be broadly classified into two major categories. In one class of materials the organic groups essentially have a closed shell electronic structure and are not intrinsically magnetic, but are used to mediate the magnetism between transition metal ions. In the other class of materials the organic molecules have open shell electronic structure and there can be unpaired spins on the molecules as well as on the transition metal ions. This second set of materials contains a number of examples of metallic molecular magnets and we include here also a number of hybrid materials without metal ions, where the hybrid system contains two different types of molecular radical. In this section various families of molecular ferromagnets will be described in turn.

3.1. Closed shell molecular systems

3.1.1. *Prussian blues.* Prussian blue, $Fe_4^{III}[Fe^{II}(CN)_6]_3 \cdot 14H_2O$, was one of the first, modern, artificially manufactured pigments, and was made by the colourmaker Diesbach of Berlin in

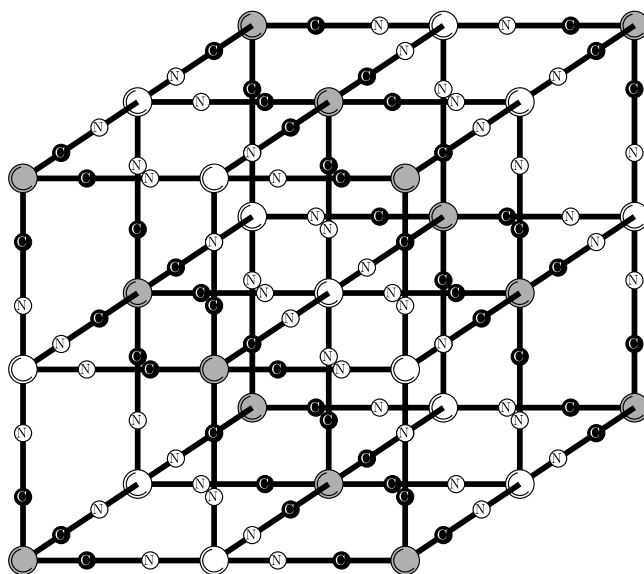


Figure 11. The crystal structure of generalized Prussian blue compounds $A_k[B(CN)_6]_l \cdot nH_2O$ (not showing the water of crystallization). The shaded ions are A (high spin) and the unshaded atoms are B (low spin).

about 1704 [99]. It is a deep blue colour due to an intense absorption band in which an electron is transferred from an Fe^{II} site to an Fe^{III} site. The Fe^{III} ($3d^5$) ions carry a spin, but the Fe^{II} ($3d^6$) ions are low spin $S = 0$. However, because of strong spin delocalization from the Fe^{III} ions onto neighbouring atoms, there is significant magnetic coupling through the $Fe^{III}-C-N-Fe^{II}-N-C-Fe^{III}$ linkages and the magnetic transition temperature is $T_C = 5.6$ K [100, 101]. Replacing the two metal ions (Fe^{II} and Fe^{III}) by other magnetic ions can be expected to increase the transition temperature and in fact high transition temperatures in compounds with the general formula $A_k[B(CN)_6]_l \cdot nH_2O$ have been found [102, 103] (see figure 11). In this formula, A is a high spin ion and B is a low spin ion (the environment of B, surrounded as it is by six cyano groups, leads to a large electron pairing energy, forcing B to be low spin). Varying the metals A and B leads to a variety of behaviours, and depending on the charges of A and B, structural defects (such as missing $B(CN)_6$ groups) can be introduced which can be filled with water [104]. One of the most spectacular examples of one of these compounds is that of $V[Cr(CN)_6]_{0.86} \cdot 2.8H_2O$ which has $T_C = 315$ K [105]. The vanadium is believed to be in a $V_{0.42}^{II}V_{0.58}^{III}$ state and the moments on both V^{II} and V^{III} ions are antiparallel to those on the Cr^{II} ions so that the system is a ferrimagnet. The saturation magnetization is around $0.15 \mu_B$ per formula unit, while the coercive field is a rather low 1 mT [105]. Prussian blue compounds with even higher transition temperatures have now been found [106, 107].

Because the magnetic properties of Prussian blues are now fairly well understood, their composition can be rationally designed in order to obtain desired properties, however unusual. To appreciate the following example of this, recall that in many ferrimagnets the magnetization in one sublattice dominates; however, sometimes the temperature dependences in each sublattice can be very different in such a way that the magnetization in one sublattice dominates at low temperatures but the other dominates at high temperatures. At the so-called compensation temperature, both have equal but opposite contributions and the net magnetization is zero. The Prussian blue $(Ni_{0.22}^{II}Mn_{0.60}^{II}Fe_{0.18}^{II})_{1.5}[Cr^{III}(CN)_6] \cdot 7.6H_2O$ is

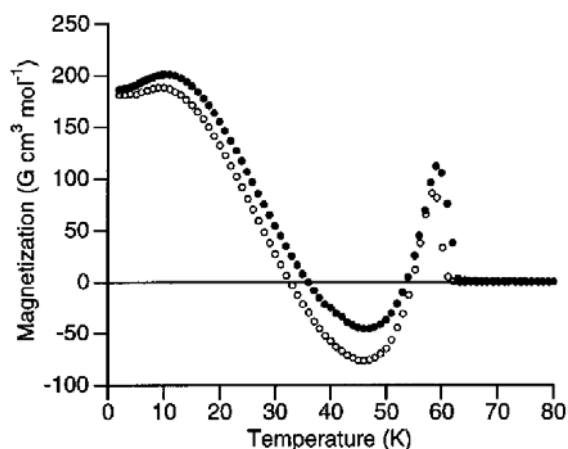


Figure 12. The measured magnetic susceptibility for the Prussian blue ferrimagnet $(\text{Ni}_{0.22}^{\text{II}}\text{Mn}_{0.60}^{\text{II}}\text{Fe}_{0.18}^{\text{II}})_{1.5} [\text{Cr}^{\text{III}}(\text{CN})_6] \cdot 7.6\text{H}_2\text{O}$. (Reprinted with permission from [108]. Copyright 1999, the American Physical Society.)

a mixed ferrimagnet which has been rationally engineered to exhibit two compensation temperatures [108] (see figure 12), a feat it achieves through the presence of four different metal ions, with the correct ratio being obtained by the use of a molecular field calculation. Another Prussian blue, $\text{Sm}_{0.52}^{\text{III}}\text{Gd}_{0.48}^{\text{III}}[\text{Cr}^{\text{III}}(\text{CN})_6] \cdot 4\text{H}_2\text{O}$ [109] was recently synthesized which exhibits an inverted hysteresis loop so that the magnetization becomes negative as the field is reduced, even when the applied field is still positive. Sm is chosen since it has a large uniaxial anisotropy, so that it remains coupled to the Cr moment as the field is reduced, and the flipping of the large Gd moment occurs first and dominates the magnetization [109]. These two examples demonstrate the possibilities for directly engineering molecular magnets in the Prussian blue family.

3.1.2. Polycyanamides. Cyanide ($-\text{C}\equiv\text{N}$), dicyanamide ($-\text{N}(\text{CN})_2$) and tricyanomethanide ($-\text{C}(\text{CN})_3$) are useful ligands because they are highly conjugated and can provide strong spin coupling between metal atoms. This has led to them producing a range of extended three-dimensional network structures [110]. These include the Prussian blue magnets described above, and also the family of transition metal dicyanamides. The dicyanamide ion, $[\text{N}\equiv\text{C}-\text{N}-\text{C}\equiv\text{N}]^-$, has been found to be a promising choice as a ligand in assembling novel metal-organic ferromagnets and ferrimagnets (see [111–116]) because it aligns divalent transition metal ions in such a way that their magnetic orbitals are approximately orthogonal. It is a small ligand and so can give rise to well defined structures with large orbital overlaps. It contains delocalized π electrons which enhance indirect exchange (principally superexchange) between metal sites. One can prepare pure metal complexes $\text{M}^{\text{II}}[\text{N}(\text{CN})_2]_2$, containing $\text{M}^{\text{II}} = \text{Ni}$ (d^8 , $S = 1$), $\text{M}^{\text{II}} = \text{Co}$ (d^7 , $S = 3/2$) or $\text{M}^{\text{II}} = \text{Mn}$ (d^5 , $S = 5/2$). X-ray diffraction [112] and neutron scattering experiments [118] suggest that these compounds are isostructural, and that they adopt an orthorhombic form of the rutile structure [111, 112] similar to those of CrCl_2 and CuF_2 (though see [117]). For the Ni and Co materials, the ground state is ferromagnetic. Below the ferromagnetic transition temperature the spins are ordered collinearly [118] with magnetic moments of $2.61 \mu_{\text{B}}$ ($\text{Co}[\text{N}(\text{CN})_2]_2$) and $2.21 \mu_{\text{B}}$ ($\text{Ni}[\text{N}(\text{CN})_2]_2$) oriented along the c axis. The magnetic structure of $\text{Mn}[\text{N}(\text{CN})_2]_2$ consists of two sublattices which are antiferromagnetically coupled and canted. The spin orientation is mainly along the a axis with a small component along b [119]. For a review of these compounds, see [120].

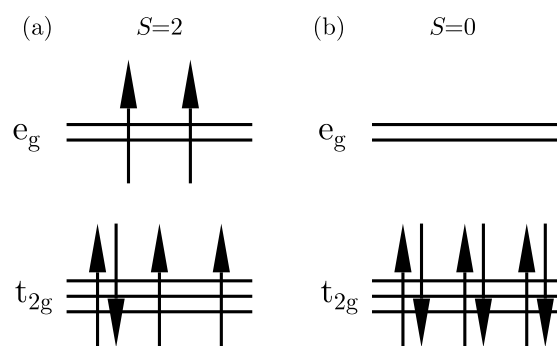


Figure 13. (a) The high spin and (b) the low spin configuration for Fe^{2+} ($3d^6$) ions.

3.1.3. Spin crossover. Even if there is no transition to long range magnetic order, a molecular magnetic material may yet exhibit bistability and hence be surprisingly useful in memory applications. A spectacular example of this bistability is the spin crossover effect, sometimes known as a spin transition. A transition metal ion of configuration $3d^n$ ($n = 4-7$) in octahedral surroundings can have a low spin (LS) or high spin (HS) ground state [121], depending on the magnitude of the energy gap Δ between e_g and t_{2g} orbitals compared to the mean spin pairing energy P . When Δ and P are of comparable magnitude, the energy difference between the lowest vibronic levels of the potential wells of the two states may be sufficiently small that a change in spin state may occur due to the application of a relatively minor external perturbation [122]. A spin crossover between the LS and HS states is associated with a change of magnetic properties and often by a change of colour. Iron (II) systems ($3d^6$) can show a crossover between LS ($S = 0$) and HS ($S = 2$) (see figure 13) induced by changes in temperature or by light irradiation [123]. In the HS and LS states there are different orbital occupancies and hence the metal–donor atom distance in complexes is very sensitive to spin state. For example, Fe–N bond lengths are often about 0.2 \AA longer in the HS state due to the occupancy of the antibonding e_g^* orbitals. This effect has important implications in biological systems: for example, a spin transition occurs in haemoglobin and the accompanying change in Fe–N bond length allows it to absorb or release oxygen [124].

The crossover as a function of temperature is relatively smooth and gradual in solution, and is driven only by the entropy gain for $\text{LS} \rightarrow \text{HS}$, due partly to a magnetic contribution $R[\ln(2S+1)_{\text{HS}} - \ln(2S+1)_{\text{LS}}]$, but mainly to a vibrational contribution. However, the crossover is very sharp in the solid state, showing that cooperativity plays an important role. The change in metal–donor atom distance accompanying the spin crossover sets up an internal pressure which is communicated to the surrounding molecules via phonons. As the transition progresses through the sample, those atoms which have switched spin state produce an increasing internal pressure which accelerated the transition on the other unswitched metal centres [125]. The sharpness of the transition therefore can be increased by enhancing the cooperativity of the transition. This can be achieved by linking the active sites by chemical bridges, designing polymeric structures, stacking aromatic groups and introducing hydrogen bonding [126].

The spin crossover can be followed using bulk measurements of the magnetic susceptibility χ as a function of temperature T (see figure 14). For Fe^{2+} ions, the molar fraction of molecules in the HS state, x , is given by $x = \chi T / (\chi T)_{\text{HS}}$ where $(\chi T)_{\text{HS}}$ is the value of χT when all molecules are in the HS state. Usually $x = 0$ at low temperatures and $x = 1$ at high temperatures, reflecting the fact that the HS state maximizes entropy while the LS state minimizes energy. However, the energy difference is often very small and often the spin crossover is incomplete at low temperatures so that $x \neq 0$ as $T \rightarrow 0$. The spin crossover can

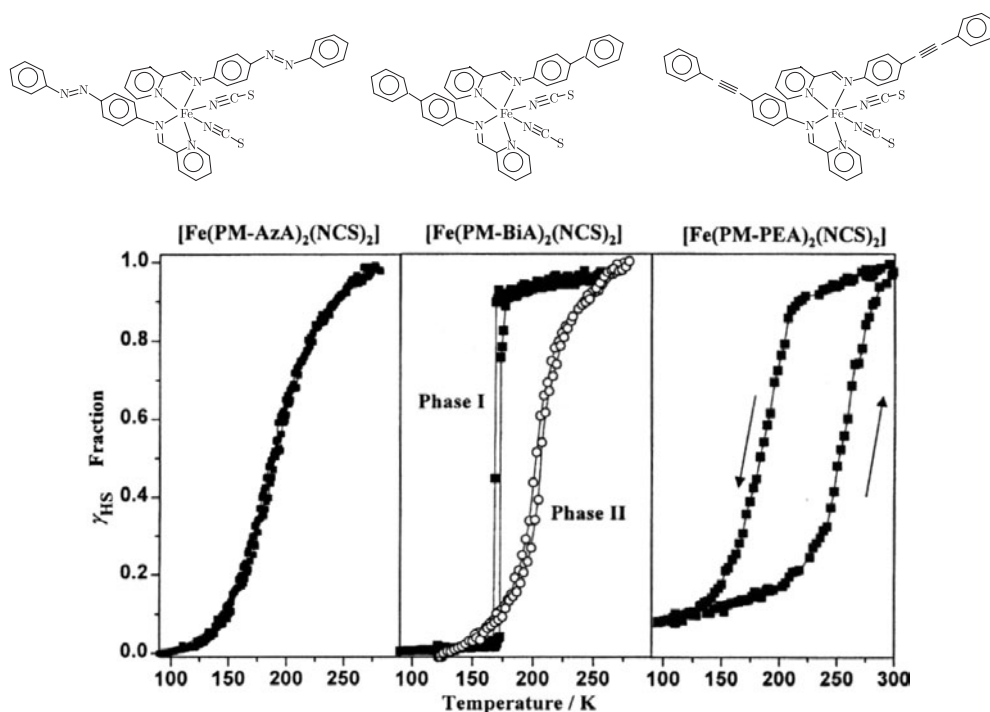


Figure 14. The measured susceptibility for the spin crossover compounds $\text{Fe}(\text{PM-AzA})_2(\text{NCS})_2$, $\text{Fe}(\text{PM-BiA})_2(\text{NCS})_2$ and $\text{Fe}(\text{PM-PEA})_2(\text{NCS})_2$ [127, 128]. (Reprinted with permission from [127]. Copyright 1997, the American Physical Society.)

be hysteretic so $T_C(\uparrow) \neq T_C(\downarrow)$ where $T_C(\uparrow)$ and $T_C(\downarrow)$ are the transition temperatures for warming and cooling respectively.

Subtle changes between the low spin and high spin states are also visible in the XANES spectra, illustrating that the Fe–N distances are shortened during the transition from HS to LS, enhancing the hybridization and mixing the N (2p) ligands with the metal Fe (4s, 4p) [129]. Mössbauer spectroscopy is also highly valuable for the study of the spin crossover in Fe(II) complexes. The quadrupole splittings and isomer shifts are much higher in HS Fe(II) than LS Fe(II), allowing the spin state to be easily followed [122]. The switching process in dinuclear Fe(II) compounds can also be measured in this way, and since Mössbauer spectroscopy gives local information, the number of LS–LS, LS–HS and HS–HS pairs can be extracted. The cooperative process can then be followed by measuring the probability of the second spin in a dinuclear pair undergoing a transition if the first one has already done so [130].

Strong intrasheet and intersheet interactions have been found in $\text{Fe}(\text{PM-PEA})_2(\text{NCS})_2$ by crystal structure determination [131]. In $\text{Fe}(\text{PM-AzA})_2(\text{NCS})_2$ the intersheet interactions are relatively weak. There is no structural phase transition at T_C (the space group is monoclinic $P2_1/c$ above and below T_C) for $\text{Fe}(\text{PM-AzA})_2(\text{NCS})_2$, but $\text{Fe}(\text{PM-PEA})_2(\text{NCS})_2$ undergoes a change of symmetry from monoclinic $P2_1/c$ (HS) to orthorhombic $Pccn$ (LS) [131], corresponding to a large rearrangement of the iron atom network. This symmetry change is responsible for the large hysteresis of the spin transition observed in $\text{Fe}(\text{PM-PEA})_2(\text{NCS})_2$. We note that the spin crossover in these compounds can be tuned by pressure [132], reflecting the fact that the structural and magnetic properties in these systems are coupled [133]. This also shows that it is plausible to ascribe a structural origin to the observed differences in spin

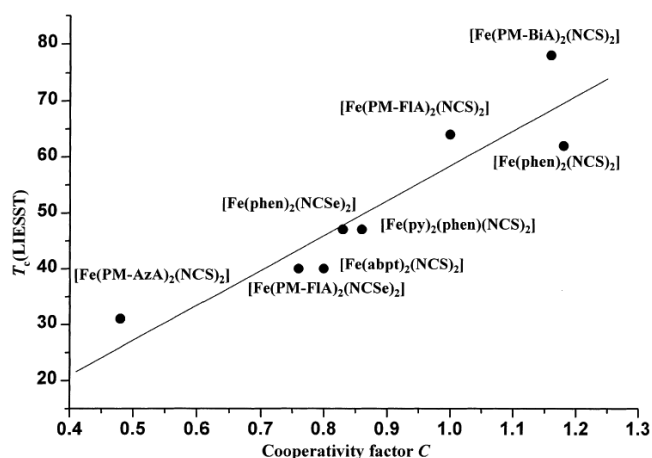


Figure 15. The magnitude of T_C (LIESST) scales with the strength of the cooperative interactions, parametrized by the parameter C (which is equal to the ratio of the strength of the intermolecular interactions in kelvins divided by the inversion temperature, the temperature at which half of the molecules are in a LS state and half are in a HS state) [136].

dynamics in the HS state between these two compounds. Other types of spin transition are also possible, such as ones introduced by a crystallographic phase transition [134], or those involving electron transfer from metal ion to ligand [135].

The optical properties of molecular magnets are one of their attractive features. The importance of the interaction between magnetic and optical behaviour was realized early on following the preparation of transparent ionic ferromagnets A_2CrCl_4 , where $A = Rb, CH_3NH_3, C_2H_5NH_3$, in which a colour change on passing through T_C resulted from exciton–magnon coupling [138–140]. The spin crossover can in fact also be induced by light, and at low temperature it is possible to convert a LS state into a metastable HS state using light of a particular wavelength. This is known as the light-induced excited spin state trapping (LIESST) effect [123, 141]. The reverse process is also possible using light of different wavelength. The metastable state needs to be prepared at low temperatures otherwise its lifetime becomes very small, and vanishes at a temperature T_C (LIESST). The magnitude of T_C (LIESST) seems to scale with the strength of the cooperative interactions [136] (see figure 15), though see [137]. The photoswitching process can exhibit nonlinear characteristics [142] and evidence is emerging that the photoinduced HS phase is structurally different from the thermally induced HS phase [143].

Prussian blue compounds have also attracted attention due to photoswitching effects such as photoinduced valence tautomerism [144, 145]. For example, red light can be used to transfer an electron from Fe to Co in the Prussian blue $K_{0.2}Co_{1.4}[Fe(CN)_6] \cdot 6.9H_2O$, changing a $Fe^{II}-C \equiv N-Co^{III}$ moiety (in which both transition metal ions are low spin and diamagnetic) into a $Fe^{III}-C \equiv N-Co^{II}$ moiety (in which both transition metal ions are high spin and have moments), and increasing the magnetization in the process [144]. Blue light switches it back again. This effect only occurred below 19 K, but it has recently been obtained above 200 K, producing accompanying changes in colour and magnetization [146]. Disorder is also thought to play an important role in these systems [147].

The spin crossover effect has also recently been used to produce a nanoporous metal–organic framework material which displays reversible uptake and release of guest molecules as the crossover proceeds [148].

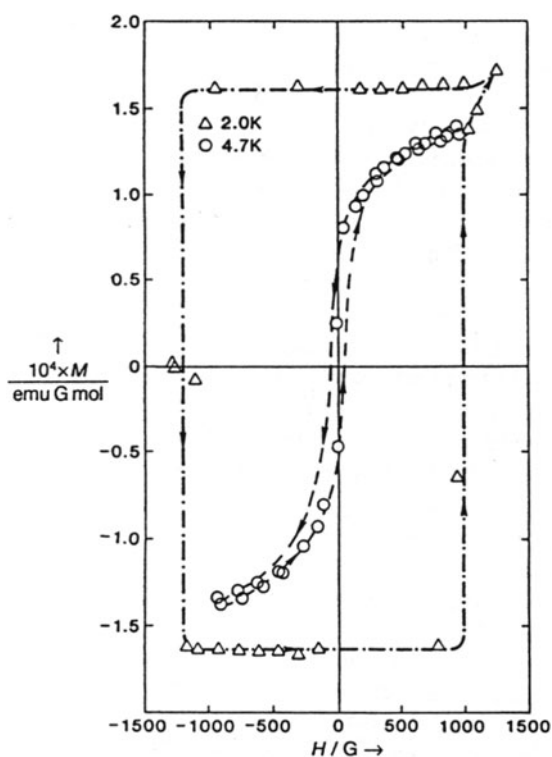


Figure 16. Magnetization data for [FeCp*₂]TCNE. (Reprinted with permission from [149]. Copyright 1987, the American Physical Society.)

3.2. Open shell molecular systems

3.2.1. TCNE salts. Magnetic ordering was found in metallocene TCNE based magnets, specifically in [FeCp*₂]TCNE [149] (sometimes known as (DMeFc)TCNE) where Cp* = C₅Me₅ = pentamethylcyclopentadienide and TCNE is an acceptor (see figure 1 for molecular structures). This charge transfer salt contains parallel chains of alternating [FeCp*₂]⁺ cations and TCNE⁻ anions and undergoes a phase transition to a ferromagnetically ordered state at $T_C = 4.8$ K [149]. There is a sharp anomaly in the specific heat at T_C and a broad maximum at 15 K, corresponding to an exchange interaction of $J \approx 35$ K along the chain axis [150]. The coercive field is large, ~ 0.1 T at 2 K (see figure 16). The transition temperature increases with pressure, reaching 7.8 K at 14 kbar [151]. Single-crystal polarized neutron diffraction studies [152] confirm that the spin density of TCNE⁻ is delocalized over all atoms. Muons have been used to measure the development of short range spin correlations above this temperature which are very slow in this quasi-1D material and follow an activated temperature dependence [153] (see figure 17), as expected in a spin chain with Ising character. The extracted activation energy E_a is 57.8 K, which is consistent with $E_a = 2J$ where $J/k_B = 28$ K was estimated from specific heat measurements.

Various similar salts were subsequently prepared and [MnCp*₂]TCNE [154] has a transition temperature of 8.8 K, which is consistent with a mean field treatment [155] which takes account of the larger moment on the Mn site than on the Fe site. The transition temperature can be reduced by doping with non-magnetic donors. For example, non-magnetic sites can be introduced into [FeCp*₂]TCNE by replacing some of the $S = \frac{1}{2}$ [FeCp*₂]⁺ sites by $S = 0$ [CoCp*₂]⁺ sites. Replacing only 14.5% of [FeCp*₂]⁺ by [CoCp*₂]⁺ causes the transition temperature to drop from 4.8 to 0.75 K [156]. This sudden drop is due to the break-up of

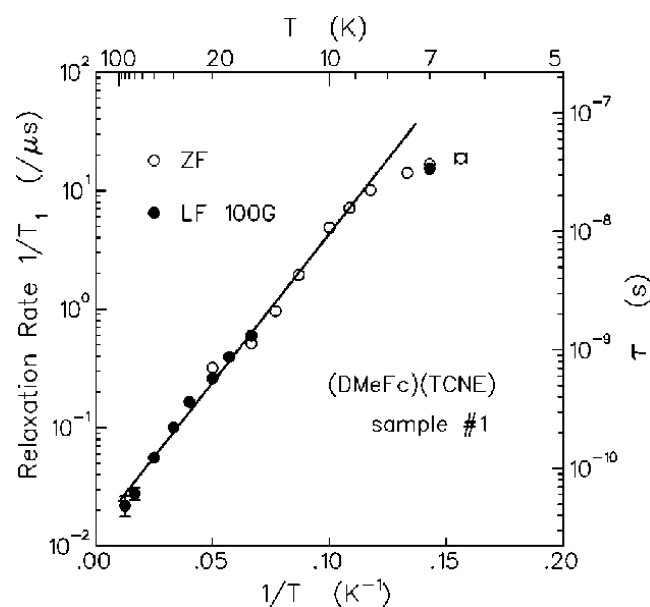


Figure 17. Relaxation rate and correlation time versus reciprocal temperature in the paramagnetic phase of $[\text{FeCp}_2^*]\text{TCNE}$ (after [153]).

the chains into finite segments, reducing the correlation length. This allows an estimate to be made of the ratio of the intrachain and interchain exchange coupling strength, which turns out to be ~ 14 [156].

The attempt to synthesize new TCNE magnets has led to some interesting materials. Since $[\text{V}^{\text{I}}(\text{C}_6\text{H}_6)_2]^+$ is an $S = 1$ cation like $[\text{Mn}^{\text{III}}\text{Cp}_2^*]^+$, this was mixed with TCNE in dichloromethane in the hope of making a new molecular magnet. The resulting black precipitate had formula $[\text{V}(\text{TCNE})_x] \cdot y\text{CH}_2\text{Cl}_2$ with $x = 2$ and $y = \frac{1}{2}$ and showed ferromagnetism at room temperature [157]. The critical temperature exceeds 350 K, the thermal decomposition temperature of the compound. The coercive field at room temperature is quite small (~ 6 mT; see figure 18). Frustratingly, the crystal structure of this material has proved elusive. It is thought that $S = \frac{3}{2}$ V^{II} and the two $S = \frac{1}{2}$ TCNE ligands are antiferromagnetically coupled, so that the system is probably a ferrimagnet. Substituting V by Fe in this material reduces the ferrimagnetic transition to 100 K [158]. Although the transition temperatures are impressively high for these materials, their structures are rather disordered and not yet properly determined. This structural disorder may be responsible for some glassy aspects of the magnetic behaviour. Recently some new TCNE magnets based on the rare earth lanthanide ions were reported [159]. The exchange couplings were found to be considerably lower than for the transition metals and transition temperatures below 10 K were reported for $\text{Gd}(\text{TCNE})_3$ ($T_C = 3.5$ K) and $\text{Dy}(\text{TCNE})_3$ ($T_C = 8.5$ K). For a more detailed review of TCNE magnets, see [160].

3.2.2. TCNQ salts. The TCNQ molecule has a similar shape to TCNE, but has a larger central section (see figure 1). TCNQ analogues of the TCNE salts generally have lower transition temperatures, e.g. $[\text{FeCp}_2^*]\text{TCNQ}$ has $T_N = 2.5$ K [161], compared with 4.8 K in the TCNE salt [149], and $\text{Fe}(\text{TCNQ})_2$ orders ferrimagnetically at 35 K [158], compared with 100 K in the TCNE salt [158]. The Mn based ferromagnet $[\text{MnCp}_2^*]\text{TCNQ}$ has $T_C = 6.2$ K [162], which is much closer to the 8.8 K transition of the TCNE variant [154]. Magnetic systems combining TCNQ directly with other transition metals have recently been reported [163],

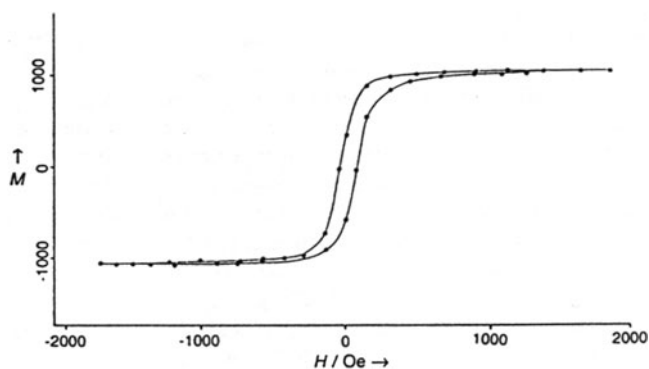


Figure 18. Magnetization data for $[V(TCNE)_x] \cdot yCH_2Cl_2$ with $x = 2$ and $y = \frac{1}{2}$ measured at room temperature (Professor J S Miller, private communication).

transition temperatures range from 7 K for $Co(TCNQ)_2$ up to 44 K for $Mn(TCNQ)_2$. Like the TCNE based magnets, these systems show spin-glass-like behaviour in the ac susceptibility, suggesting the presence of disorder and/or frustration.

There are also many examples of systems where TCNQ is combined with non-magnetic anions to provide paramagnetic spins on the TCNQ. These tend to form rather one-dimensional structures which are susceptible to spin-Peierls magnetoelastic instabilities (see section 5.3). One-dimensional spin chains are covered in more detail in section 5.

One intriguing system is $Cs_2(TCNQ)_3$, which was reported to be a room temperature ferromagnet, but with an extremely small moment corresponding to a spin concentration of 0.1% per formula unit [164]. This magnetic behaviour can be compared to that of the magnetic fullerene discussed in section 2.6. As in that case, the origin of the magnetism is not at all clear. As long as ferromagnetic impurities can be eliminated as a source, the magnetism must originate from some type of molecular defect or else be the result of a so far unidentified intrinsic mechanism with a weak associated moment. In this material the two $TCNQ^-$ molecules form a dimer, leaving the third $TCNQ^0$ as formally neutral. An explanation based on an intrinsic mechanism would require some unpaired spin density on at least one of the TCNQ molecules. There is in fact spectroscopic evidence that the charge partitioning between TCNQ molecules is not complete, with the average charge density on the 'neutral' TCNQ being 0.1 rather than 0 [165]. Recent studies showed that the magnetization disappears above 320 K and that for crystals grown in a magnetic field of 5 T, magnetization can be maintained up to a temperature of 420 K [166].

3.2.3. DCNQI salts. High conductivity molecular metals can be made from Cu salts of R_1, R_2 -DCNQI (see figure 1) which is a flat molecule with large electron affinity (a good acceptor). The properties of DCNQI salts have been reviewed recently by Kato [167].

The salts consist of face to face stacks of R_1, R_2 -DCNQI molecules next to chains of Cu ions (figure 19). By changing the groups R_1 and R_2 , by applying pressure or by selective deuteration, large changes in the electrical and magnetic properties may be produced, including metal-insulator transitions and charge and spin ordering. Antiferromagnetic ordering takes place below 8 K in region II of the phase diagram (figure 19) and a small canting is observed, resulting in a weak ferromagnetic state. The strong interaction between the d electrons of the Cu and the $p\pi$ electrons of the DCNQI is one of the characteristic features of this system. The importance of this interaction in producing the three-dimensional electronic structure

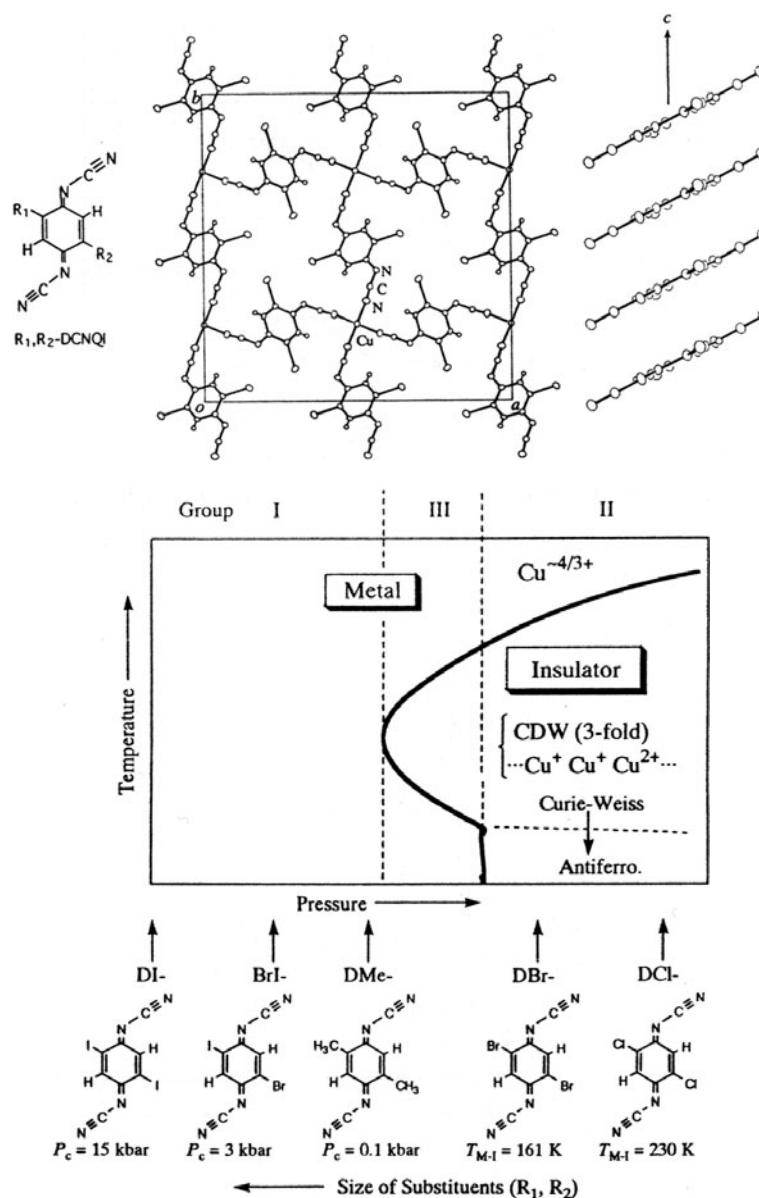


Figure 19. The crystal structure and schematic phase diagram of $(R_1, R_2\text{-DCNQI})_2\text{Cu}$ [167].

which can stabilize the metallic state to low temperatures is emphasized when the properties are compared to those of the isostructural $(\text{DMe-DCNQI})_2\text{Li}$ salt. Without the 3d electrons the electronic properties revert to those of a highly 1D chain and the salt undergoes a spin-Peierls transition at 65 K. The motion of spin solitons in this Li salt has been a topic of recent interest [168].

3.2.4. TTF salts. TTF is an electron donor (see figure 1 for molecular structure), so it can be combined with a transition metal M cation to form an anionic complex such as MCl_4^- to

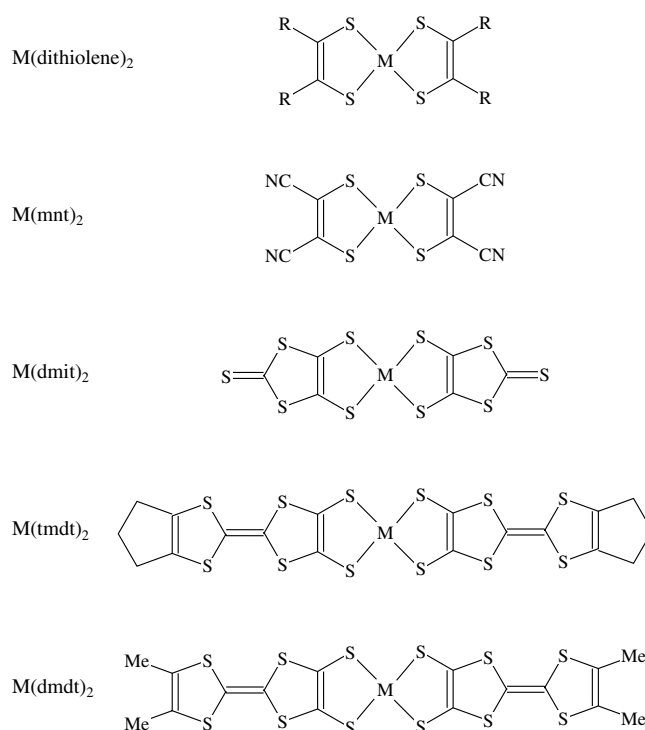


Figure 20. Some metal dithiolate molecules commonly used in constructing molecular magnets. The generic metal dithiolate molecule is $M(\text{dithiolene})_2$ and various modifications are also shown.

provide a series of magnetic charge transfer salts. The magnetic compounds $\text{TTF}_{14}(\text{MCl}_4)_4$ ($M = \text{Co}, \text{Mn}$) were reported in 1988 [169] and more recently the FeCl_4 salt [170]. These materials all behave as two-dimensional magnetic semiconductors with an energy gap around 0.2 eV.

Derivatives of TTF, such as BEDT-TTF, DT-TTF, BETS and TMTSF (see figure 1 for molecular structures) are well known as forming the basis for many organic metals and superconductors. These molecules have also provided an interesting range of magnetic materials and phenomena which will be described in sections 4 and 5.

3.2.5. Metal dithiolate based systems. Metal dithiolates build a transition metal directly into the central structure of a molecule. There are many variations on this theme which provide a flexible set of components for constructing systems of molecular magnets (see figure 20). Instabilities associated with one-dimensionality are often a problem in such systems but, under the right conditions, ferromagnetic ordering is possible and the $\text{NH}_4\text{Ni}(\text{mnt})_2 \cdot \text{H}_2\text{O}$ salt was observed to have an ferromagnetic transition below 4.5 K [171]. Also of interest is the salt $(\text{DT-TTF})_2\text{Au}(\text{mnt})_2$ which is a molecular spin ladder [172–174]. Here the Au is diamagnetic and the moment is on the DT-TTF donor molecule.

Magnetic order has also been observed in $\text{Pd}(\text{dmit})_2$ salts with tetrahedral anions, which provide a set of antiferromagnetic insulators with T_N up to 35 K [175]. Their structure consists of layers of dimers, each having a single spin and forming a triangular lattice on which magnetic frustration was demonstrated to be significant [176].

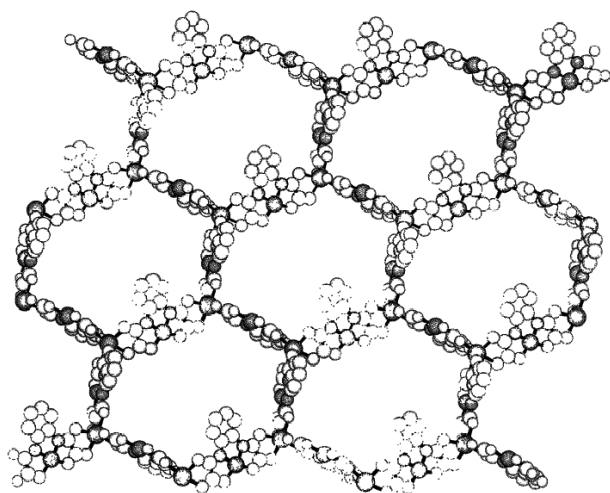


Figure 21. One layer of $\text{NITR}_2\text{Mn}_2[\text{Cu}(\text{opba})]_3(\text{DMSO})_2 \cdot 2\text{H}_2\text{O}$ showing the $\text{Mn}^{\text{II}}\text{Cu}^{\text{II}}$ hexagons. (Reprinted with permission from [179]. Copyright 1993 AAAS.)

The chemistry of the dithiolates is a very active area; one particularly interesting recent development has been the synthesis of the first single-component molecular metal $\text{Ni}(\text{tmdt})_2$ [177]. By extending the size of the molecule and increasing the delocalization of the molecular orbitals, the ratio of the intramolecular HOMO–LUMO separation and the intermolecular bandwidth was reduced sufficiently to produce overlap of the bands and so create a single-component organic metal. Although in the Ni form the molecule is diamagnetic, Ni can be replaced by Cu in the variant $\text{Cu}(\text{dmdt})_2$, resulting in a paramagnetic metal [178]. No information about the magnetic ground state is available so far for this material, but the progress in this area indicates one way in which magnetically ordered molecular metals might be produced.

3.2.6. Interlocked networks. Molecular magnets with a fully interlocked three-dimensional structure have been prepared using the ion $[\text{Cu}(\text{opba})_2]^{2-}$, together with MnCl_2 and nitronyl nitroxide radicals (NITR; see figure 1) with $\text{R} = \text{methylpyridinium}$ [179]. The structure of the resulting compound is shown in figure 21 and consists of two nearly perpendicular graphite-like networks with edge-sharing $\text{Mn}^{\text{II}}\text{Cu}^{\text{II}}$ hexagons. These layers actually interpenetrate each other with a full interlocking of the hexagons. The magnetic moments are on the Mn^{2+} ions, the Cu^{2+} ions and the NITR radicals. The compound orders below 22.5 K and behaves as a soft magnet with a small coercive field [180].

4. Two-dimensional systems

Following the survey of organic and molecular magnets in the preceding sections, we now turn to focus on particular features associated with low dimensionality. In this section, we concentrate on the novel properties that can be obtained in various layered compounds.

4.1. Layered hydroxides

A novel hydrothermal synthesis has led to a new family of layered molecular magnets containing interlayer dicarboxylate or terephthalate ($\text{BDC} = \text{O}_2\text{CC}_6\text{H}_4\text{CO}_2$) [181]. The interlayer separation has been tuned from 9.9 to 13.8 Å. One example of this family is

$\text{Co}_2(\text{OH})_2\text{BDC}$ which consists of two types of edge-sharing CoO_6 chains that are connected to each other by OH (Co–O–Co bridges) to form layers that are further joined together through terephthalate. It exhibits unusual magnetic properties: above 48 K it displays paramagnetism, between 44 and 48 K it behaves as a collinear antiferromagnet and below 44 K a weak spontaneous magnetization is observed in very low applied fields. At higher fields metamagnetic behaviour is observed. The critical field and the hysteresis width increase as the temperature is lowered; remarkably, the latter exceeds 5 T at 2 K [181]. The unusual large coercivity may be due to the large single-ion anisotropy of Co^{II} . By replacing BDC with a longer connector, one can tune the critical field but not the coercive field. The wide variety of organic pillars that can be used to separate the layers of metal hydroxide or metal hydroxysulphate (varying pillar rigidity, length and connectivity), together with possible metal substitutions at various sites in the layers, offers the possibility of tailoring the magnetic and porous properties of these materials [182, 183].

4.2. Oxalates

The oxalate ligand (see figure 1) is a good mediator of both antiferromagnetic and ferromagnetic interactions, and this has led to its use in preparing various mixed metal assemblies which order magnetically (see e.g. [184]). Many magnetic oxalates have been prepared, but we restrict our discussion to one series of hybrid organometallic–inorganic layered magnets which has been prepared with the formula $[\text{Z}^{\text{III}}\text{Cp}_2^*][\text{M}^{\text{II}}\text{M}^{\text{III}}(\text{ox})_3]$, where ox = oxalate, Cp^* = pentamethylcyclopentadienyl, $\text{Z} = \text{Co}, \text{Fe}$, $\text{M}^{\text{II}} = \text{Mn}, \text{Fe}, \text{Co}, \text{Cu}, \text{Zn}$ and $\text{M}^{\text{III}} = \text{Cr}, \text{Fe}$ [185] (see figure 22). They show a variety of magnetic behaviour, including ferromagnetism, ferrimagnetism or canted antiferromagnetism (the highest transition is 44 K). Note that $[\text{FeCp}_2^*]^+$ is paramagnetic while $[\text{CoCp}_2^*]^+$ is diamagnetic so that one has the possibility of turning a spin ‘on and off’ in the organometallic layers. These are, therefore, chemically prepared magnetic multilayers (in contrast with artificially deposited multilayers).

Oxalates have also turned out to be very flexible building blocks for forming molecular magnets in the form of metallic charge transfer salts when combined with radical cations such as BEDT-TTF. These materials will be discussed further in the following section.

4.3. BEDT-TTF salts

The electronic donor TTF was discussed in section 3.2.4 above. As described there, various modifications of the TTF molecule can be made (see figure 1) and one of the most important is the molecule BEDT-TTF (short for bis(ethylenedithio)tetrathiafulvalene, sometimes also known as ‘ET’). This molecule turns out to be a very versatile donor and a number of charge transfer salts derived from BEDT-TTF have been found to be very good organic metals and sometimes superconductors [1]. The BEDT-TTF molecules contain sulfur atoms on the side, and intermolecular S–S overlaps are the most important in these salts.

The basic structure of BEDT-TTF salts is illustrated by the example shown in figure 23. These materials are naturally layered, with alternating layers of the BEDT-TTF molecules, stacked side to side so that the molecular orbitals overlap, and layers of anions. In this way, the charge transfer salts are ‘organic–inorganic molecular composites’ or ‘chemically constructed multilayers’ [188]. Within the BEDT-TTF layers, the molecules are in close proximity to each other, allowing substantial overlap of the molecular orbitals. Usually 2 (or sometimes 3) BEDT-TTF molecules will jointly donate an electron to the anion, and the charge transfer leaves behind a hole on the BEDT-TTF molecules. This means that the bands formed by the overlap of the BEDT-TTF molecular orbitals will be partially filled, leading

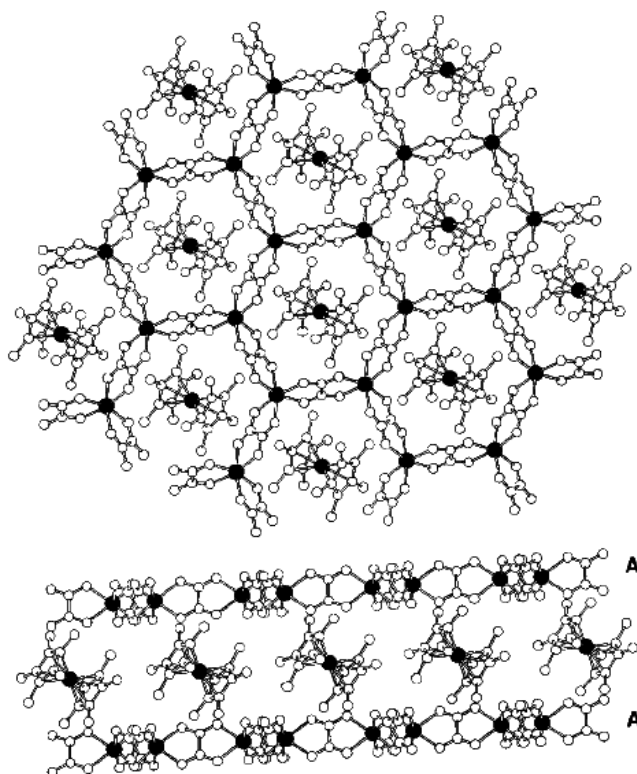


Figure 22. The structure of $[Z^{III}Cp_2^*][M^{II}M^{III}(ox)_3]$ [185].

to the possibility of metallic behaviour. The transfer integrals which parametrize the ease of hopping of electrons between BEDT-TTF molecules, will be relatively large within the BEDT-TTF planes. Conversely, in the direction perpendicular to the BEDT-TTF planes, the BEDT-TTF molecules are well separated from each other; the transfer integrals will be much smaller in this direction. This results in electronic properties which for many purposes can be considered to be two dimensional [189, 190]. In the Mott insulator regime of these metals, the π system can be regarded as having a localized $S = \frac{1}{2}$ on each BEDT-TTF dimer, and magnetic interactions between BEDT-TTF dimers are important for understanding the system [191, 192] (see also [193]).

Introduction of magnetic ions into the anion layer can lead to some interesting compounds. The compound $(BEDT-TTF)_3CuCl_4 \cdot H_2O$ was an early example of this idea, combining a localized moment on the Cu ion and delocalized electrons in the BEDT-TTF layer. The salt remains metallic down to 0.4 K while distinct magnetic resonances from the localized spins and conduction electrons can be resolved [194]. The interest here is that the electrons close to the Fermi surface are largely confined to the frontier orbitals of the BEDT-TTF, while the magnetic moments are localized on the anions, providing a degree of spatial separation between the two.

Very often, the introduction of magnetic anions produces insulating salts (e.g. [195]), though this is true of non-magnetic anions as well. Therefore, an important breakthrough was the discovery of $(BEDT-TTF)_2H_2OFe(C_2O_4)_3C_6H_5CN$, which is a superconductor with a transition temperature of 7 K and was the first discovered molecular paramagnetic superconductor [196]. Various other closely related superconductors have now been

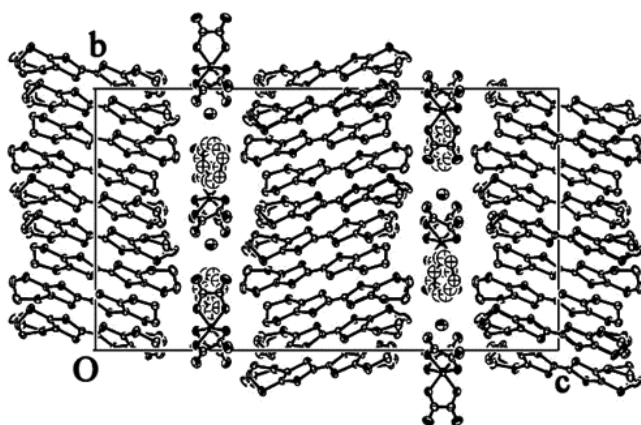


Figure 23. The monoclinic crystal structure of β'' -(BEDT-TTF)₄[(H₃O)M(C₂O₄)₃]·C₅H₅N projected along the *a* axis [186, 187]. (Reprinted with permission from [187]. Copyright, the American Physical Society.)

discovered, and although there is no long range magnetic order in these systems, they have interesting magnetotransport properties [187].

Long range magnetic order has now been achieved in the compound (BEDT-TTF)₃[MnCr(C₂O₄)₃] [197], in which layers consisting of an oxalate-bridged hexagonal network alternate with layers containing the β -packed BEDT-TTF molecules (see figure 24). This salt is a good metal but shows weak ferromagnetic order below $T_C = 5.5$ K. It has a small coercive field (0.5–1 mT) and is the first molecule based ferromagnetic metal. It is essentially a hybrid material which owes its metallic properties to the organic BEDT-TTF layers and its magnetic properties to the inorganic oxalate-bridged layers.

4.4. BETS salts

An entirely different family of organic metals can be obtained when the innermost four sulfur atoms of BEDT-TTF are replaced by selenium. The resulting molecule is BEDT-TSF (short for bis(ethylenedithio)tetraselenafulvalene), which is usually known by the name BETS (see figure 1 for molecular structure). The selenium atoms are larger than the sulfur atoms and tend to broaden the electronic bands. Several salts based on the BETS molecular donor have been found to be metallic and superconducting, with several salts of the form BETS₂X, where X is a magnetic anion, maintaining good metallic and superconducting properties in the presence of magnetism.

A particularly interesting example is λ -BETS₂GaCl₄ (here λ refers to a particular crystallographic packing type) which was found to be metallic with a superconducting transition at ~ 6 K [198, 199]. The isostructural salt λ -BETS₂FeCl₄ shows a metal–insulator transition at around 8 K, which is associated with antiferromagnetic order of the Fe³⁺ ($S = \frac{5}{2}$) spins [198, 200, 201]. However, the antiferromagnetic insulating phase can be destabilized by the application of a magnetic field of ~ 10 T which stabilizes a paramagnetic metallic phase due to the gain of Zeeman energy of the Fe³⁺ moments. Below 1 K, and with a field applied parallel to the layers, superconductivity is induced above 17 T (and then destroyed above 42 T) [202, 203]. The field-induced superconductivity appears to involve a Jaccarino–Peter [204] mechanism in which the exchange field is cancelled by the applied field. Precise orientation of the field is important to avoid orbital dissipation in the superconducting phase. There is also some evidence that the superconducting phase may be connected with

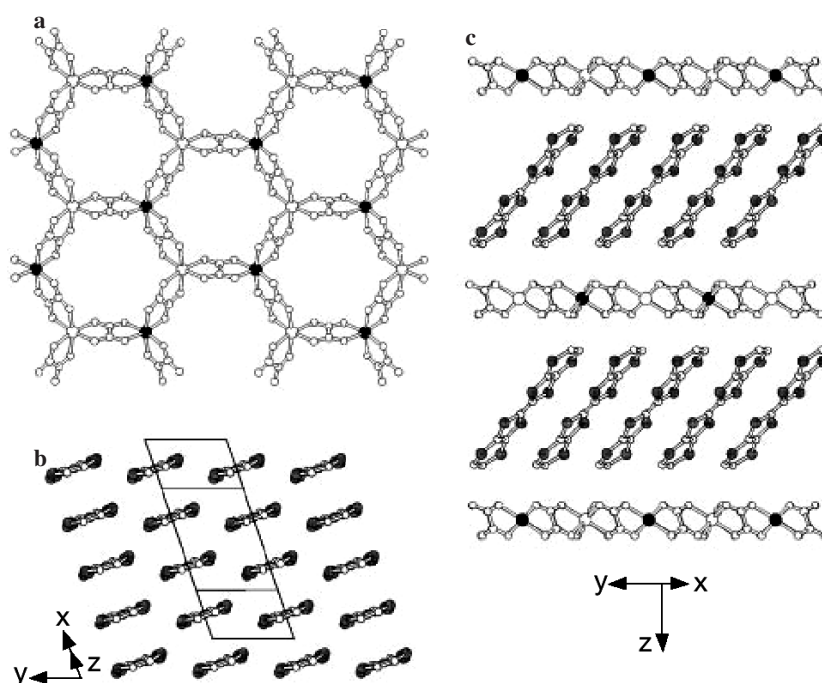


Figure 24. The structure of $(\text{BEDT-TTF})_3[\text{MnCr}(\text{C}_2\text{O}_4)_3]$ [197]. Views of (a) oxalate layers, (b) BEDT-TTF layers (illustrating the β -packing), (c) the hybrid structure (showing the alternating organic/inorganic layers) (reprinted with permission from [197]).

a spatially modulated order parameter [205, 206] (the Fulde–Ferrell–Larkin–Ovchinnikov state [207, 208]) though a direct observation is still needed [209].

Alloying of the Fe and Ga salts produces an extremely rich phase diagram (shown in figure 25) and allows the field-induced superconductivity phase to be brought down to lower magnetic fields [210]. This phase diagram can be understood in terms of the Jaccarino–Peter compensation mechanism.

The interplay between coexisting magnetism and superconductivity is particularly interesting. Magnetic spin fluctuations of band electrons have been considered to play an important role in many organic metals, however materials where localized moments coexist with metallic and superconducting properties have been less common. The salts κ -BETS₂FeBr₄ and κ -BETS₂FeCl₄ are of interest in this context. The κ crystal phase is an orthorhombic layered structure in which the BETS molecules are arranged in 2D sheets of interacting dimers in the ac plane. These sheets alternate with layers of magnetic anions as one goes along the b axis. The spatial separation of the highly conducting molecular layers and the strongly magnetic layers is a key feature of this structure. Magnetic and transport measurements on the FeBr₄ salt indicate that the Fe³⁺ is in a high spin state ($S = \frac{5}{2}$) with an antiferromagnetic transition at $T_N = 2.5$ K and a superconducting transition taking place at $T_C = 1$ K [211].

Zero-field muon spin relaxation measurements on the organic metal κ -BETS₂FeCl₄ clearly show the formation of an antiferromagnetically ordered state below $T_N = 0.45$ K. The magnetic order remains unperturbed on cooling through the superconducting transition $T_C \sim 0.17$ K, providing unambiguous evidence for the coexistence of antiferromagnetic order and superconductivity in this system. The internal field seen at a muon site depends on its

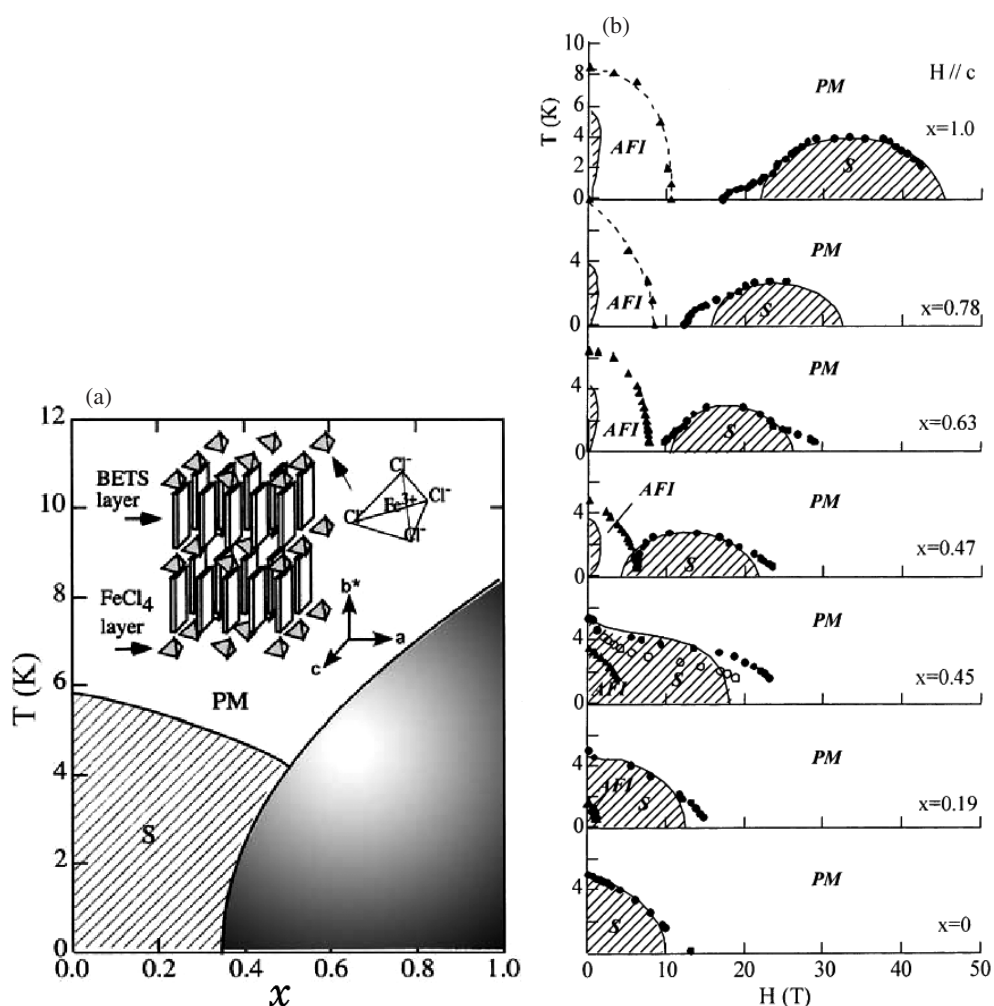


Figure 25. The phase diagram of λ -BETS₂Fe_xGa_{1-x}Cl₄ (a) in zero magnetic field as a function of x and (b) as a function of magnetic field for different values of x (after [210]).

position with respect to the magnetic structure and hence a number of different frequencies are to be expected from the large low symmetry unit cell of this material. The precession amplitude observed for each site depends both on the probability of occupancy of the site and on the alignment of the internal field at the site with respect to the polarization of the incoming muon. Two clear precession frequencies are observed (see figure 26, [212]). The antiferromagnetic nature of the Fe ordering means that high local fields such as reflected by the higher frequency can only be present close to the anion plane. For the lower frequency, sites arranged between FeCl₄ along the c axis are a possibility, however the local field in the region round the centre of the BETS sheets is also consistent. Superconductivity is expected to modify any spin modulation of the π -system, so the drop in frequency seen on entering the superconducting state may provide evidence for the presence in the normal state of a weak spin density wave within the BETS layers, as previous calculations have suggested [213]. It is clear that the BETS salts provide plenty of intriguing phenomena to be explored concerning the interaction of magnetism and superconductivity and further advances are to be expected.

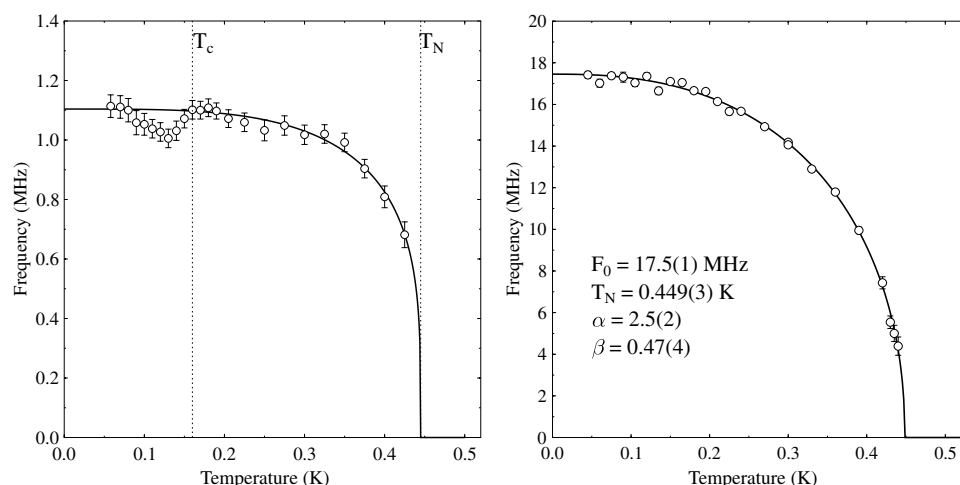


Figure 26. The temperature dependence of the two muon precession frequencies measured in κ -BETS₂FeCl₄ (after [212]).

5. One-dimensional systems

In this section, we discuss various one-dimensional aspects of molecular systems and outline properties which occur because of the one-dimensional nature of the interactions.

5.1. Magnetic chains

Low dimensional magnetic systems, in particular one-dimensional magnets, have attracted much attention because they are, in principle, easier to treat theoretically than three-dimensional systems [214]. In addition, low dimensional strongly correlated systems are of interest because of the discovery of high temperature superconductivity in cuprates. In this respect, the chain compound Sr₂CuO₃ has become much studied as it is an excellent realization of a one-dimensional spin- $\frac{1}{2}$ Heisenberg model [215, 216]. The value of the spin on a magnetic chain has a dramatic effect on the magnetic properties; for example, half-integer spin chains are gapless, but integer spin chains possess a spectrum with a non-zero energy gap (the Haldane gap) between the ground state and the lowest lying energy states [217].

An isolated one-dimensional spin chain will never show long range magnetic order, but because real crystal systems contain many chains and have non-zero interchain interactions, they will generally show long range three-dimensional magnetic ordering, albeit at very low temperature (unless there is large magnetoelastic coupling; see section 5.3 below). For example, Sr₂CuO₃ has a Néel temperature (T_N) of 5 K, despite having an intrachain exchange interaction $J \sim 1300$ K [215, 218]. The strong quantum fluctuations due to the one-dimensionality renormalize the moment on the Cu cation down to $\sim 0.06 \mu_B$ [218]. In isostructural Ca₂CuO₃ the chain separation is slightly smaller and hence the interchain interaction is larger, so that both T_N and the ordered moment are somewhat larger (11 K and $\sim 0.1 \mu_B$ respectively [218]).

If the interchain interactions are sufficiently weak, a spin- $\frac{1}{2}$ Heisenberg antiferromagnet will show magnetic susceptibility $\chi(T)$ with a broad peak around $1.282J/k_B$ (see figure 30), as given by Bonner and Fisher [219], although at very low temperatures there may be expected to be a departure from this behaviour with a singularity in $d\chi/dT$ as the temperature approaches zero [220]. Molecular magnets can be expected to provide good opportunities for studying

magnetic chains as the intrachain and interchain exchange interactions can be controlled using chemical modifications.

There are a number of realizations of one-dimensional chains, including those based on purely organic ferromagnetic radicals (see e.g. [221]) or Cu chains bridged by organic groups (see e.g. [222–224]). Cu chains bridged by organic groups can even be made to make spin ladders [225]. Some of the materials discussed in earlier sections also fall into the class of magnetic chain compounds. In the following sections we will restrict our discussion to several examples which exhibit properties of particular physical interest.

5.2. Magnetic chains based on hexafluoroacetylacetonate

A large number of magnetic spin chains can be produced using organic ligands and metal ions [4]. We will not attempt to review all the progress in this area, but instead concentrate on compounds based on one particular ligand, hexafluoroacetylacetonate (hfac; see figure 1), which has proved to be very versatile. An interesting family of magnetically ordered materials can be prepared by combining hfac, nitronyl nitroxides (NITR; see figure 1, using different substituents R) and transition metal or lanthanide ions. Each nitronyl nitroxide radical can bind to two different ions leading to compounds with a chain-like structure [226].

One such example is $\text{Mn}(\text{hfac})_2\text{NITPhOMe}$ [227] where NITPhOMe is a nitronyl nitroxide with methoxyphenyl attached to the carbon of the O–N–C–N–O moiety. The structure consists of helices in which $\text{Mn}(\text{hfac})_2$ moieties are bridged by the radicals coordinated through two equivalent oxygen atoms [227] (see figure 27(a)). It orders ferrimagnetically below 4.8 K with a moment corresponding to $S = 2$, as expected for antiparallel alignment of $S = \frac{5}{2}$ (Mn^{2+}) and $S = \frac{1}{2}$ (nitronyl nitroxide radical). The helical structure provides natural optical activity which may lead to interesting magneto-optical properties. Using other groups on the nitronyl nitroxide, different crystal structures may be obtained and hence different magnetic behaviour. $\text{Mn}(\text{hfac})_2\text{NITEt}$ (Et is ethyl) and $\text{Mn}(\text{hfac})_2\text{NIT-}n\text{-Pr}$ ($n\text{-Pr}$ is n -propyl) form zigzag chains (see figure 27(b)) and have a phase transition at 8.1 and 8.6 K respectively [228]. $\text{Mn}(\text{hfac})_2\text{NIT-}i\text{-Pr}$ ($i\text{-Pr}$ is isopropyl) forms straight chains [229] (see figure 27(c)) and orders ferromagnetically at 7.6 K [231].

Because the interchain contacts are very weak, and there are no superexchange pathways between different chains, it was believed that the ordering in these systems is driven by dipolar coupling [227]. The strong intrachain metal–radical coupling leads to long spin correlation lengths $\xi(T)$ at low temperature. Hence the critical temperature T_C can be estimated by the relation

$$k_B T_C = \xi(T_C) |E_{\text{dip}}|, \quad (2)$$

where E_{dip} is the dipolar energy in the preferred spin orientation [232]. However, the single-ion anisotropy is also believed to play a role in determining the three-dimensional ordering [233].

It is also possible to include lanthanide ions in magnets with NITR and hfac, thereby opening up the possibility of incorporating large anisotropy via the unquenched angular momentum of the lanthanides [234]. One family which has been extensively studied is $\text{Ln}(\text{hfac})_3\text{NITEt}$ where Ln is a lanthanide ion. The compound with the lanthanide ion is Y^{3+} [235] behaves as a one-dimensional antiferromagnet and does not order. Using other lanthanides, a magnetic phase transition is only found with anisotropic rare earth ions [236] such as Tb^{3+} , Dy^{3+} , Ho^{3+} and Er^{3+} . Of these the highest transition temperature (4.3 K) is found for $\text{Ln} = \text{Dy}^{3+}$ [237] which has a large anisotropy (isolated Dy^{3+} is ${}^6\text{H}_{15/2}$ which has $g_J = \frac{4}{3}$; a low symmetry environment yields a Kramers doublet ground state and hence an effect $\tilde{S} = \frac{1}{2}$ with $g_{\parallel} \gg g_{\perp}$ and thus an Ising-type interaction). The shortest Dy–Dy distance is

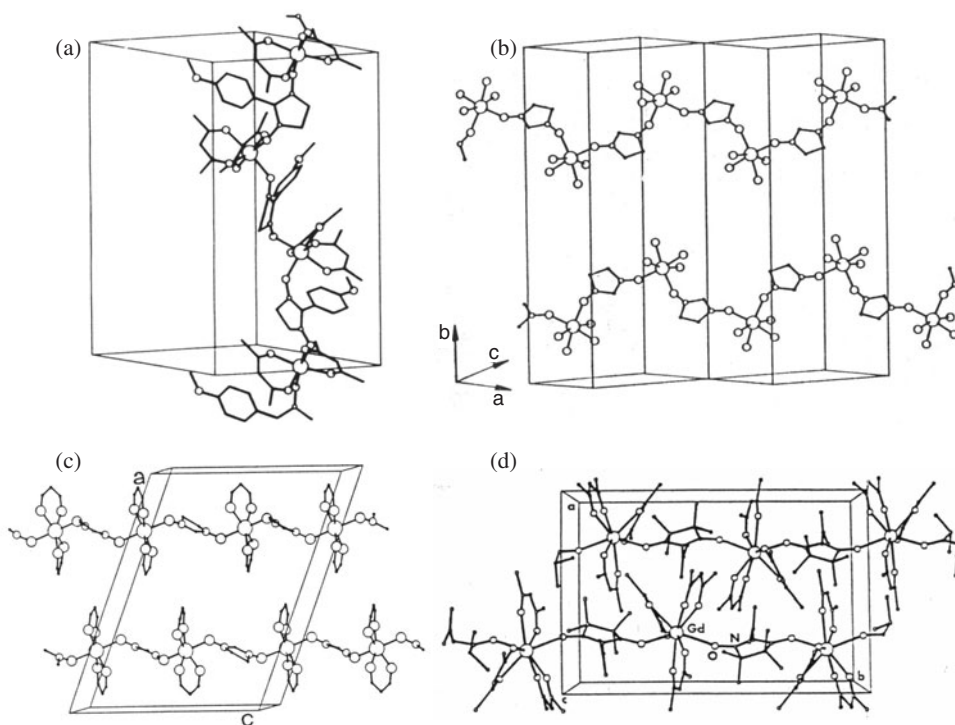


Figure 27. The crystal structure of (a) $\text{Mn}(\text{hfac})_2\text{NITPhOMe}$ [227], (b) $\text{Mn}(\text{hfac})_2\text{NITEt}$ [228], (c) $\text{Mn}(\text{hfac})_2\text{NIT-}i\text{-Pr}$ [229], and (d) $\text{Gd}(\text{hfac})_3\text{NiT-}i\text{-Pr}$ [230]. (Reprinted with permission from [227–230]. Copyright, American Chemical Society.)

8.74 Å along the chains and 10.76 Å between the chains, so that Dy^{3+} ions are well separated; hence strong correlations must be operative between the chains to produce magnetic order.

A particularly interesting case is that of $\text{Gd}(\text{hfac})_3\text{NITR}$ with $\text{R} = \text{Et}$ or $i\text{-Pr}$, both of which are chain compounds (see figure 27(d)) and both of which show a peak in the specific heat at 2 K [239] which disappears with the application of a 5 T field [238] (see figure 28), demonstrating that the peak is of magnetic origin. The one-dimensional character of these compounds is confirmed by single-crystal EPR spectra [230]. Because the Gd^{3+} ($S = \frac{7}{2}$) ions and NITR ($S = \frac{1}{2}$) radicals alternate along each chain, the magnetic behaviour in these compounds is dominated by a competition between nearest-neighbour and next-nearest-neighbour interactions. This can give rise to a helically ordered phase, but the 2 K peak in the specific heat does not signify the onset of three-dimensional long range helical order in this case [240]. μSR measurements show no evidence for long range order below 2 K [238]. Instead, below 2 K a chiral phase is believed to occur [241]. This can be described by considering the chains as a collection of parallel corkscrews, all turning clockwise (or anticlockwise) but with random phases. Chiral order has no measurable effect on magnetic susceptibility or μSR relaxation, which is related to spin-pair correlation functions, but does lead to an anomaly in the specific heat, which is related to four-spin correlation functions [240].

5.3. Spin–Peierls transition

It is possible to avoid a three-dimensional magnetically ordered ground state if the magnetoelastic coupling in a spin chain is large. In this case, a spin–Peierls transition may

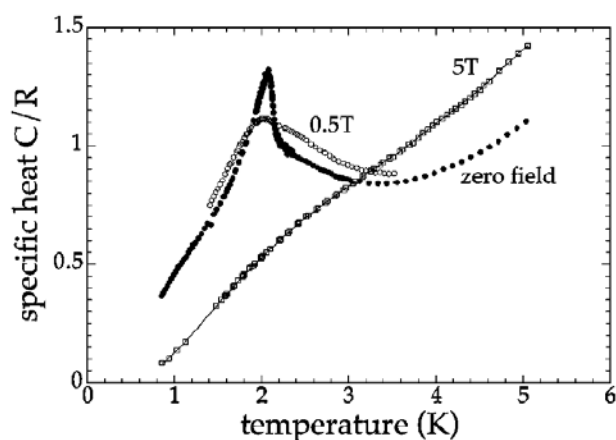


Figure 28. The specific heat of $\text{Gd}(\text{hfac})_3\text{NIT-i-Pr}$ [238] measured in zero field and in various applied magnetic fields. (Reprinted with permission from [238]. Copyright 2003 the American Physical Society.)

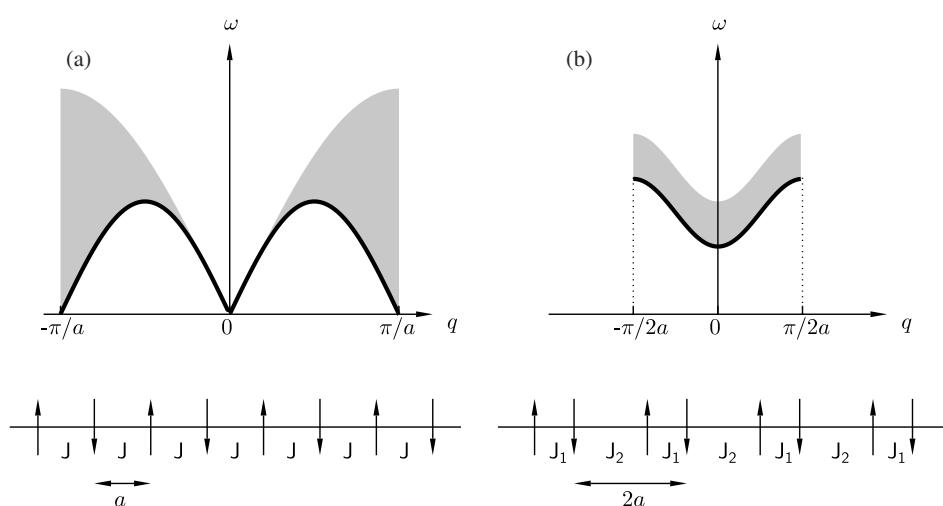


Figure 29. Schematic representations of the elementary excitations in (a) a uniform Heisenberg antiferromagnetic chain and (b) an alternating chain (for which the ground state is a singlet state at $q = 0$), and for which the unit cell is doubled (after [121]).

occur. This is an intrinsic lattice instability in $\text{spin-}\frac{1}{2}$ antiferromagnetic Heisenberg chains. Above the transition temperature T_{SP} , there is a uniform antiferromagnetic next-neighbour exchange in each chain; below T_{SP} there is an elastic distortion resulting in dimerization and hence two, unequal, alternating exchange constants (see figure 29). The alternating chain possesses an energy gap between the singlet ground state and the lowest lying band of triplet excited states which closes up above T_{SP} . The transition temperature may be related to the relevant coupling constants; whereas the conventional Peierls distortion is expected at a temperature $T_{\text{P}} \sim (E_{\text{F}}/k_{\text{B}}) \exp(-1/\lambda)$, where E_{F} is the Fermi energy of the system and λ is the electron-phonon coupling constant, the spin-Peierls transition is expected at $T_{\text{SP}} \sim (J/k_{\text{B}}) \exp(-1/\lambda)$. Since $J \ll E_{\text{F}}$, this implies that $T_{\text{SP}} \ll T_{\text{P}}$ [242].

One example is $\text{MEM}(\text{TCNQ})_2$, which consists of one-dimensional stacks of planar TCNQ molecules, each of which has a charge of $-\frac{1}{2}e$ associated with it. Adjacent stacks are separated by arrangements of MEM molecules (see figure 1 for the molecular structure of both MEM and TCNQ), each of which possess a localized charge of $+e$. It undergoes two structural

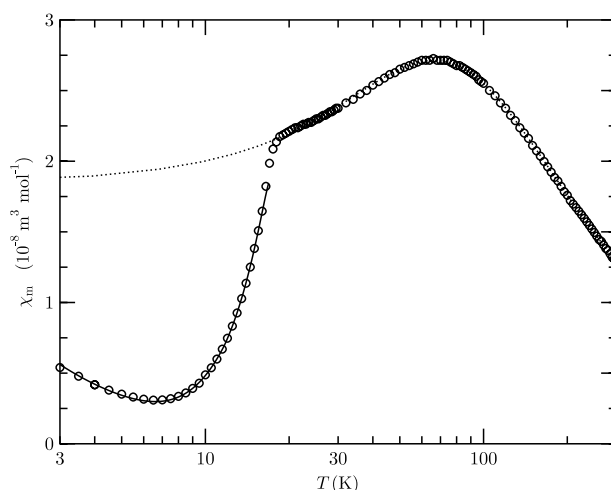


Figure 30. The bulk magnetic susceptibility for $\text{MEM}(\text{TCNQ})_2$. The dotted curve represents a fit to a Bonner–Fisher expression [219] at high temperature, which yields an exchange constant of 46 K. Note the knee at 18 K, indicative of a spin–Peierls transition. The low temperature fit (solid curve) is to a combination of Curie impurity and spin gap terms (after [243]).

distortions. The first, which occurs at 335 K, is a conventional Peierls transition in which the TCNQ chains dimerize. This results in a change from metallic to insulating behaviour as a single electronic charge becomes localized on each TCNQ dimer; the single spin on each dimer couples antiferromagnetically to its neighbours. This phase persists down to the spin–Peierls transition at 18 K, where a further dimerization of the TCNQ stacks takes place (this is a tetramerization of the original chain).

Magnetic susceptibility data for $\text{MEM}(\text{TCNQ})_2$ are shown in figure 30 (first measured by [244], but the data shown are from [243]). The high temperature dependence is well fitted by a Bonner–Fisher [219] expression for a uniform Heisenberg antiferromagnet, with a J of 46 K. There is a rapid drop in the susceptibility at 18 K, which is indicative of the opening of a gap in the magnetic excitation spectrum. The size of the BCS pair excitation gap, $2\delta(0)$, at absolute zero can be estimated by using the result of Bulaevskii [245] who calculated the temperature dependence of χ in the dimerized state; this yields a value of 56 K. It is necessary to include a contribution from paramagnetic defect spins at the lowest temperatures. These may arise, for instance, from chain ends where there are some spins which do not go into a dimerized configuration.

Other examples of spin–Peierls systems include salts of TTF (or molecules modified from TTF), such as $\text{TTF-CuS}_4\text{C}_4(\text{CF}_3)_4$ ($T_{\text{SP}} = 12$ K) [246], $\text{TTF-AuS}_4\text{C}_4(\text{CF}_3)_4$ ($T_{\text{SP}} = 2$ K) [246, 247], α' -(BEDT-TTF) $_2\text{Ag}(\text{CN})_2$ ($T_{\text{SP}} = 7$ K) [248–250] and $(\text{BCPTTF})_2\text{X}$ with $\text{X} = \text{PF}_6, \text{AsF}_6$ ($T_{\text{SP}} = 36$ K, 32.5 K) [251, 252]. A common feature of such materials is that they contain flat organic molecules in columnar stacks. The large interchain separation and weak van der Waals intermolecular interactions favour the dominance of magnetoelastic effects over interchain ordering. In contrast the chains in corresponding inorganic materials, such as copper chain compounds, are quite rigid due to the ionic bonding and only a single example of an inorganic spin–Peierls material is known (CuGeO_3 , with $T_{\text{SP}} = 14$ K [253]).

5.4. First-order phase transitions in one-dimensional crystals

A structural phase transition in the one-dimensional stacks of galvinoxyl has already been discussed in section 2.1. In that case, the phase transition prevented a ferromagnetically

ordered state from being observed at low temperatures. Such an effect has also been found in other systems. For example, potassium chloranil (chloranil is an organic radical; see figure 1) is a radical ion salt in which the chloranil molecules form regular stacks [254]. It behaves as a one-dimensional Heisenberg antiferromagnet down to 225 K at which point it shows a phase transition to a non-magnetic low temperature state in which the singlet ground state is separated from the triplet excited state by $J/k_B = 445$ K [12].

A particularly spectacular structural phase transition has been found in the organic radical TTTA (see figure 1, briefly mentioned in section 2.5) which occurs over a wide thermal hysteresis loop from 230 to 305 K [72]. In the high temperature phase, TTTA molecules stand face to face forming stacks, but a spin–Peierls-like dimerization occurs in the low temperature singlet phase. The structural phase transition is first order (conventional spin–Peierls transitions are second order) and may be the result of a competition between exchange and electrostatic energies, the former dominating at low temperatures [75].

It has recently been shown that the transition can be driven using a nanosecond laser pulse, both inside (290 K) and outside (11 K) the hysteresis loop [76]. It has been suggested that the effect is due to photocarriers suppressing the spin–Peierls-like instability, in much the same way as non-magnetic Zn impurities do in CuGeO_3 [255].

5.5. TMTSF salts and spin density waves

Charge transfer salts based on the organic donor TMTSF show an extraordinary range of properties. These salts consist of one-dimensional chains of TMTSF molecules. They can form metals with a formally $\frac{3}{4}$ filled conduction band, but the actual band filling is $\frac{1}{2}$ due to a weak dimerization along the chains. The metals are very anisotropic, so that the bandwidth along the chains is ~ 1 eV, while in the two perpendicular directions it is ~ 0.1 and ~ 0.003 eV. The high degree of one-dimensionality leads to these salts being susceptible to various instabilities, including the formation of density wave and superconducting ground states.

$(\text{TMTSF})_2\text{ClO}_4$ is the only compound in this family which at ambient pressure stays metallic down to 1 K where it becomes superconducting. Most of the others undergo a metal–insulator transition (at temperatures around 10 K) which in some cases, as for $(\text{TMTSF})_2\text{PF}_6$, can be suppressed by external pressure. As a function of field and pressure, the salts can have quite extraordinary phase diagrams, and that for $(\text{TMTSF})_2\text{PF}_6$ is shown in figure 31(b). It contains, in addition to a superconducting phase, both a spin density wave (SDW) phase and a cascade of field-induced spin density wave (FISDW) phases [256]. The SDW state in $(\text{TMTSF})_2\text{X}$, where $\text{X} = \text{PF}_6$, NO_3 and ClO_4 , has been detected using μSR with similar amplitude for all three compounds [257] (see figure 31(a)).

5.6. Polymeric magnets

A possible route to the production of one-dimensional magnets is via the use of π -conjugated polymers [258]. However, it has proved to be extremely difficult to prepare well defined materials with reproducible properties. Recently, an example of a magnetic polymer was reported which contained a large number of cross-links and alternating connectivity of radical molecules with $S = 2$ elements and cross-linking $S = \frac{1}{2}$ elements [259]. An effective magnetic moment corresponding to an average spin of ~ 5000 was found, so that the magnetic properties at low temperature resembled that of a spin glass.

6. Zero-dimensional systems: single-molecule magnets

We now turn to what are effectively zero-dimensional magnets, small molecular clusters which bear large spins which do not exist naturally in any of the elements in the periodic table. They

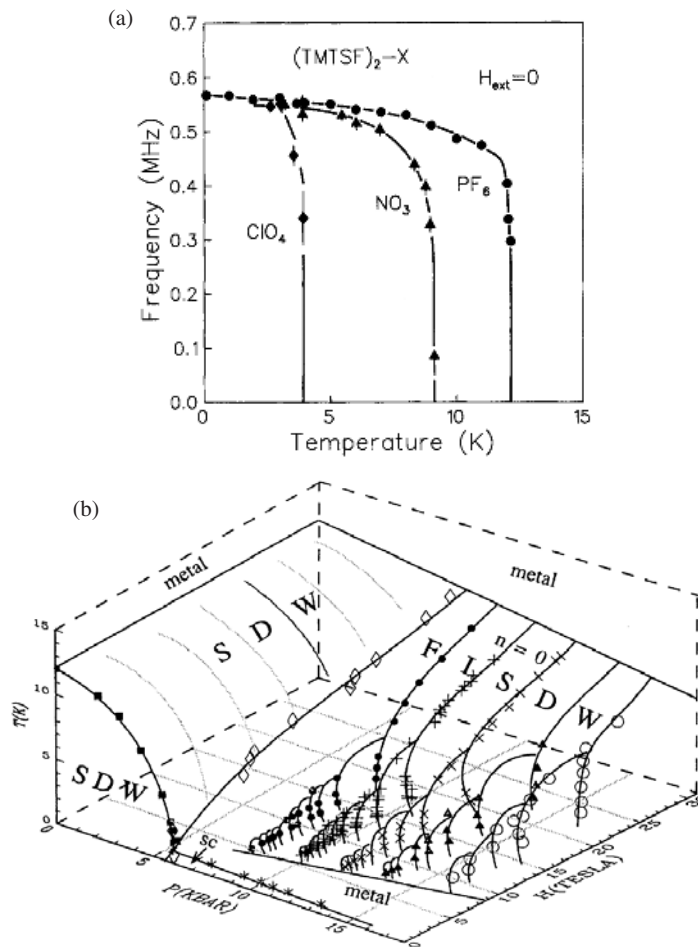


Figure 31. (a) The temperature dependence of the muon precession frequency in $TMTSF_2X$ where $X = PF_6, NO_3$ and ClO_4 [257]. (b) The pressure–magnetic field–temperature phase diagram of $TMTSF_2PF_6$ [256]. SDW = spin density wave; FISDW = field-induced spin density wave. (Reprinted with permission from [256, 257]. Copyright, the American Physical Society.)

tend to have large Ising-type anisotropy, and the magnetization relaxes very slowly at low temperature.

6.1. Introduction

The magnetic properties of small magnetic particles have been studied for a long time [260, 261], originally in the context of the switching of minute magnetic grains in rocks in the Earth’s magnetic field (which is a function of geological time). A small magnetic particle with uniaxial anisotropy will have its magnetization parallel to an easy axis. Switching between one easy axis direction and another will take place via thermal activation in a time τ given by

$$\tau = \tau_0 \exp\left(\frac{U}{k_B T}\right), \tag{3}$$

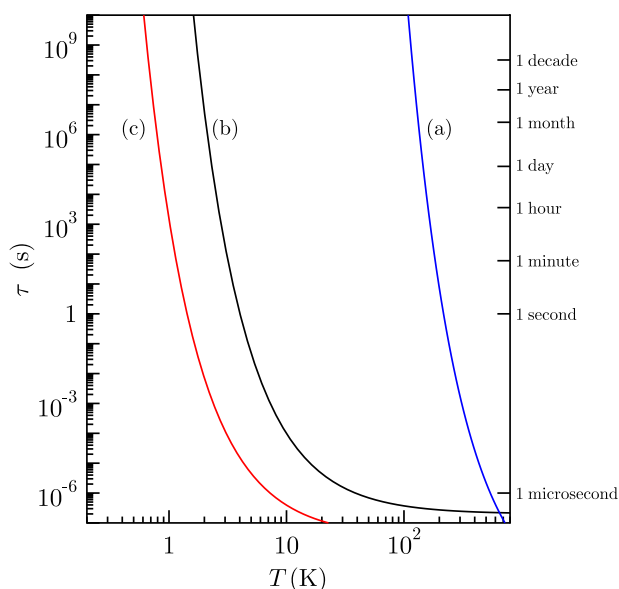


Figure 32. The correlation time of thermally activated fluctuations following equation (3) for (a) a small magnetic particle with energy barrier $U = 5000$ K, (b) Mn_{12} and (c) Fe_8 .

where U is the energy barrier, which is equal to KV where K is the anisotropy energy density and V is the volume. The prefactor τ_0 is usually in the range 10^{-9} – 10^{-11} s. When the temperature T is much larger than U/k_B , the magnetization can fluctuate readily, but when T is much smaller than U/k_B the fluctuations become ‘blocked’. The blocking occurs quite suddenly as the particles are cooled (because of the exponential in equation (3)), and sets in at a temperature determined mainly by $U \propto V$ but also by the timescale of the experiment (albeit only logarithmically). This behaviour is shown in figure 32.

Thermal activation is not the only way to cross the barrier; another possibility is quantum tunnelling, in an analogous manner to the tunnelling of an alpha particle from a radioactive nucleus [262]. The exchange interaction constrains all the electronic spins inside the particle to remain parallel with one another, but the ‘macro-spin’ can coherently tunnel from one state to the other. This coherent process of a macroscopic system undergoing a tunnelling process is known as macroscopic quantum tunnelling (MQT) [263, 264] or quantum tunnelling of magnetization (QTM).

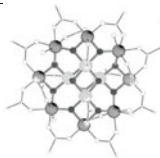
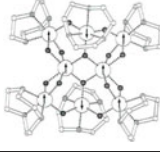
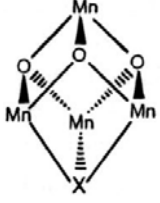
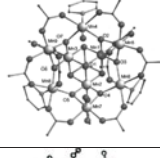
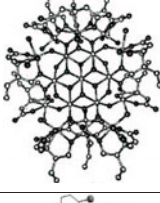

Conventional methods of preparing small magnetic particles suffer from a rather broad range of particle sizes which leads to a broad distribution of intrinsic switching rates, complicating the interpretation (though ingenious methods have been used to synthesize nanoparticles of a relatively controlled size; see e.g. [265, 266]). On the other hand, the chemical synthesis of polynuclear cage compounds is an attractive route to prepare identical molecular clusters [267]. The resulting molecular clusters turn out to be appealing systems in which to study these effects since the molecular approach provides ensembles of completely identical, iso-oriented nanomagnets [268].

A few examples of these clusters are shown in table 1. Each one has a large spin S which results from the intramolecular exchange between the transition metal ions in the cluster. In zero applied field, to a first approximation the Hamiltonian of this system can be written as

$$\mathcal{H} = -DS_z^2, \quad (4)$$

so that for $D > 0$ the lowest energy states have $M = \pm S$. At low temperatures ($k_B T \ll D$), only the states with $M = \pm S$ are thermally accessible. Moreover, if a molecule has $M = -S$,

Table 1. Examples of single-molecule magnets and their properties.

Molecule	Name	S	D (K)	Reference
	“Mn ₁₂ ” Mn ₁₂ O ₁₂ (CH ₃ COO) ₁₆ (H ₂ O) ₄	10	0.56	[269, 270, 271]
	“Fe ₈ ” [(tacn) ₆ Fe ₈ O ₂ (OH) ₁₂] ⁸⁺	10	0.275	[272]
	“Mn ₄ ” Mn ₄ O ₃ X(O ₂ CMe) ₃ (dbm) ₃	8	0.39–0.53	[273]
	“Mn ₉ ” Mn ₉ O ₇ (OAc) ₁₁ (py) ₃ (H ₂ O) ₂	$\frac{17}{2}$	0.42	[274]
	“Fe ₁₉ ” Fe ₁₉ (metheidi) ₁₀ (OH) ₁₄ O ₆ ⁻ (H ₂ O) ₁₂ NO ₃ •24H ₂ O	$\frac{33}{2}$	0.56	[275]
	“Ni ₁₂ ” Ni ₁₂ (chp) ₁₂ (thf) ₆ (H ₂ O) ₆	12	0.067	[276]

there is an activation energy barrier equal to $|D|S^2$ if S is an integer (or $|D|(S^2 - \frac{1}{4})$ if S is a half-integer) which separates the $M = +S$ state from the $M = -S$ state (see figure 33(a)). Molecules with $D > 0$ are known as single-molecule magnets (SMMs).

If a field is applied in the z direction to a SMM, the Hamiltonian becomes

$$\mathcal{H} = -DS_z^2 + g\mu_B S_z, \quad (5)$$

which causes the levels with $\pm M$ to no longer be degenerate (see figure 33(b)). In fact, the $M = -S$ and the $M = S - n$ levels have the same energy when the resonant field B_n given by

$$B_n = \frac{nD}{g\mu_B} \quad (6)$$

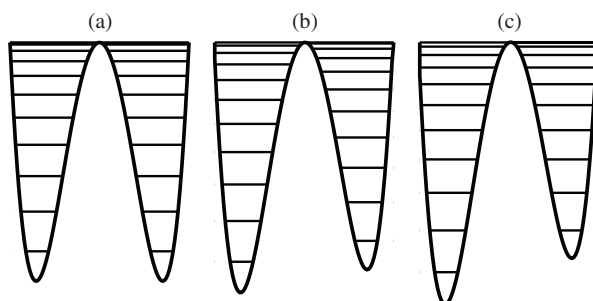


Figure 33. The energy levels in a single-molecule magnet with the Hamiltonian given by $\mathcal{H} = -DS_z^2 + g\mu_B BS_z$ with $D > 0$ for (a) $B = 0$, (b) $B = D/2g\mu_B$ and (c) $B = D/g\mu_B$.

is applied (see figure 33(c) for the case of $n = 1$). In real single-molecule magnets, there are usually additional small terms in the Hamiltonian, so that it should be written in general as

$$\mathcal{H} = -DS_z^2 + g\mu_B \mathbf{S} \cdot \mathbf{B} + \mathcal{H}', \quad (7)$$

where \mathcal{H}' is an anisotropy term such as $E(S_x^2 - S_y^2)$. These additional terms can be (as is the case for $E(S_x^2 - S_y^2)$) symmetry violating, and hence induce tunnelling between states on opposite sides of the barrier. Such tunnelling becomes enhanced when resonant magnetic fields described by equation (6) are reached [277].

Terms such as $E(S_x^2 - S_y^2)$ act like a transverse field in the Hamiltonian in that they mix states with different M . The field dependence of the energy for two molecular magnets, Mn_{12} and Fe_8 , is shown in figure 34 for two orientations of the magnetic field B , parallel and perpendicular to the easy axis which is assumed to lie along z . Both these systems have an $S = 10$ ground state, but different values of D and different forms of \mathcal{H}' as described below. When B is parallel to z , the states can be labelled by M , but when B is parallel to x , significant mixing of states occurs, except at high field.

As an example of SMM behaviour, consider the mixed-valence manganese cage Mn_9 (see table 1) which possesses an $S = 17/2$ ground state as a result of an antiferromagnetic interaction between three ferromagnetically coupled Mn^{4+} ions and a wheel of four Mn^{3+} and two Mn^{2+} ions. Data for this compound are shown in figure 35 and demonstrate the Arrhenius behaviour of the relaxation time as a function of $1/T$. The hysteresis loops are not smooth, but show steps in the magnetization at regular intervals of field, indicative of resonant QTM. As the applied field changes, the magnetization does not respond unless the field passes through a resonant field B_n . These steps in the magnetization show up more when the field sweep rate is faster, so that there is less time for all the tunnelling to take place at zero applied field and therefore a step becomes resolved. The field separation between the zero-field resonance and the next gives a value of D which is in good agreement with that obtained from the bulk DC measurements [278].

In the following two sections, our discussion concentrates on the two clusters which have received the greatest experimental attention, Mn_{12} and Fe_8 .

6.2. Mn_{12}

The most studied high spin molecule is Mn_{12} (full name $\text{Mn}_{12}\text{O}_{12}(\text{CH}_3\text{COO})_{16}(\text{H}_2\text{O})_4$), which appears in the first row of table 1. This molecule contains a cluster of twelve Mn ions. The moments of the four inner Mn^{4+} ions are parallel to each other (yielding a total spin of $4 \times \frac{3}{2} = 6$) and the remaining eight Mn^{3+} ions are also parallel (yielding a total spin of $8 \times 2 = 16$) with

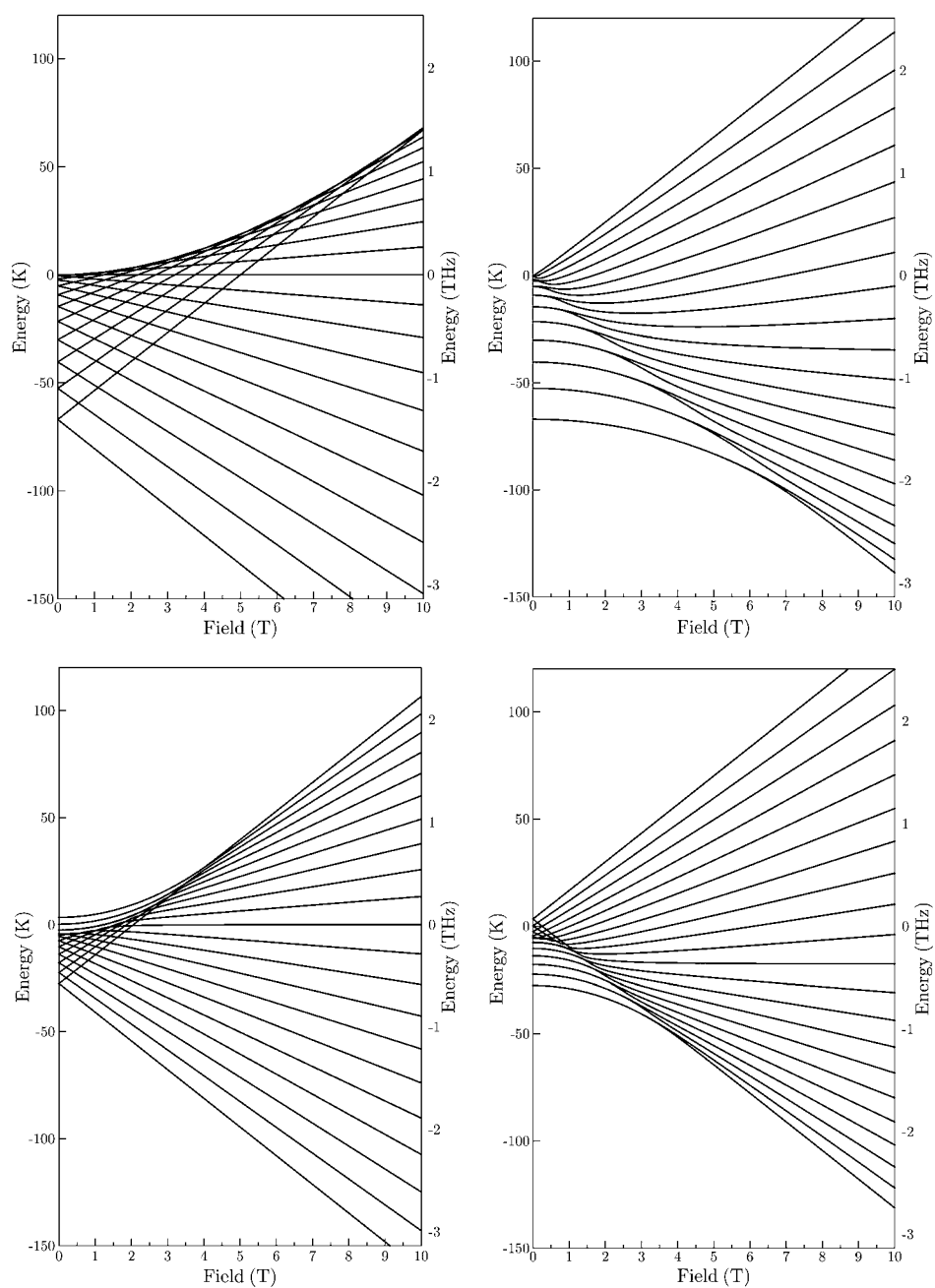


Figure 34. Calculated energy spectra for Mn_{12} (top) and Fe_8 (bottom) as a function of field applied parallel (left) or perpendicular (right) to the easy axis.

the two groups antiparallel (thus the net spin is $S = 10$). The system can thus be described as a single $S = 10$ spin system split by anisotropy terms [269] (there may be several $S = 9$ excited state manifolds at least 40 K above the $S = 10$ manifolds [279]). This material was the first to attract considerable attention following the observation of steps at regular intervals

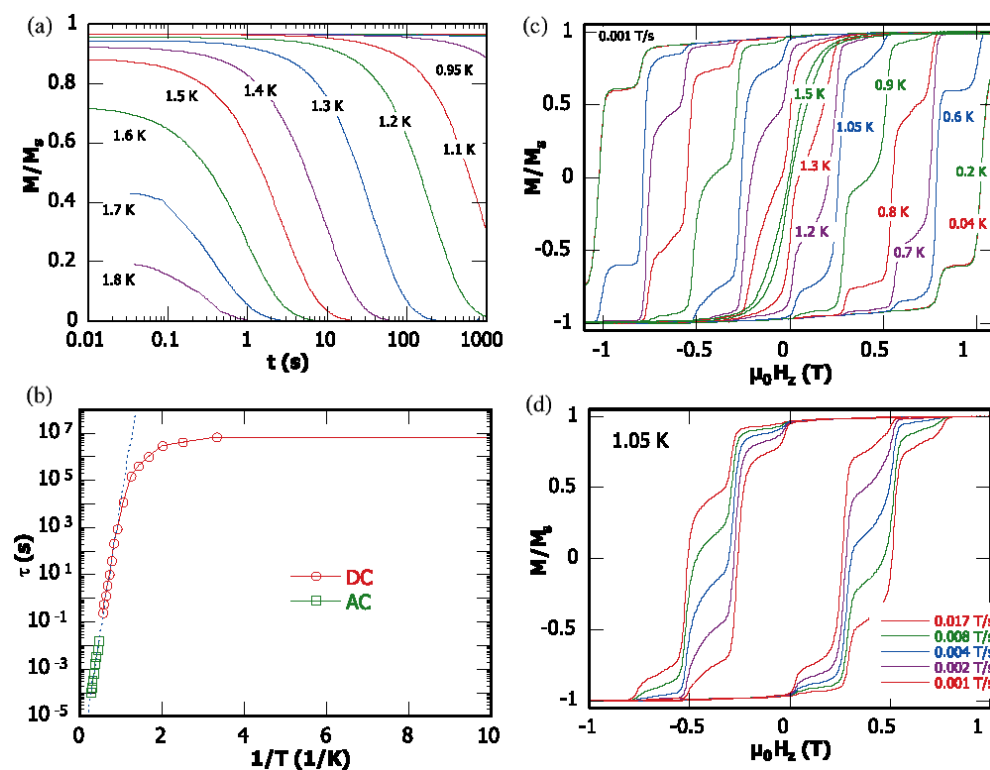


Figure 35. SMM behaviour in ‘Mn₉’, i.e. Mn₉O₇(OAc)₁₁(py)₃(H₂O)₂. (a) Relaxation data, plotted as the fraction of the maximum value M_s versus time. (b) An Arrhenius plot using AC data and DC decay data on a single crystal. The solid curve is the fit of the data in the thermally activated region and the dashed curve the fit of the temperature independent data. (c), (d) Magnetization versus applied magnetic field. The resulting hysteresis loops are shown at (c) different temperatures and (d) different field sweep rates (after [278]).

in the magnetic field of a sample of Mn₁₂, [271, 270], results which were interpreted in terms of field-tuned resonant tunnelling between quantum spin states, with the resonant fields given by equation (6).

Inelastic neutron scattering measurements on this molecule [280], performed in the absence of an applied magnetic field, are shown in figure 36 and illustrate quite beautifully the energy levels in this molecule. At low temperature, only one inelastic peak is observed, attributed to an excitation from the ground state ($M = \pm 10$) to the first excited state ($M = \pm 9$). As temperature increases, higher energy levels are populated and more inelastic peaks are observed. The shape and position of the peaks allow higher order terms in the Hamiltonian to be determined with some precision [280].

Mn₁₂ can be described by a Hamiltonian for which $\mathcal{H}' = -BS_z^4 + C(S_+^4 - S_-^4)$ where $B = 1.1$ mK and $C = 0.03$ mK [280, 281]. The fourth-order anisotropy term may arise largely from vibrationally induced distortions in the molecule [282]. Such a spin–vibron coupling can be expected on the basis of the magnetic field dependence of the infrared spectra [283]. However, the fourfold symmetry of the crystal precludes a term such as $E(S_x^2 - S_y^2)$ which would allow $\Delta M = 2$ transitions. The only remaining term which permits tunnelling is $C(S_+^4 - S_-^4)$, which allows $\Delta M = 4$ transitions. However, all transitions are nevertheless observed with equal intensity. One approach to explain the observed resonances is to include

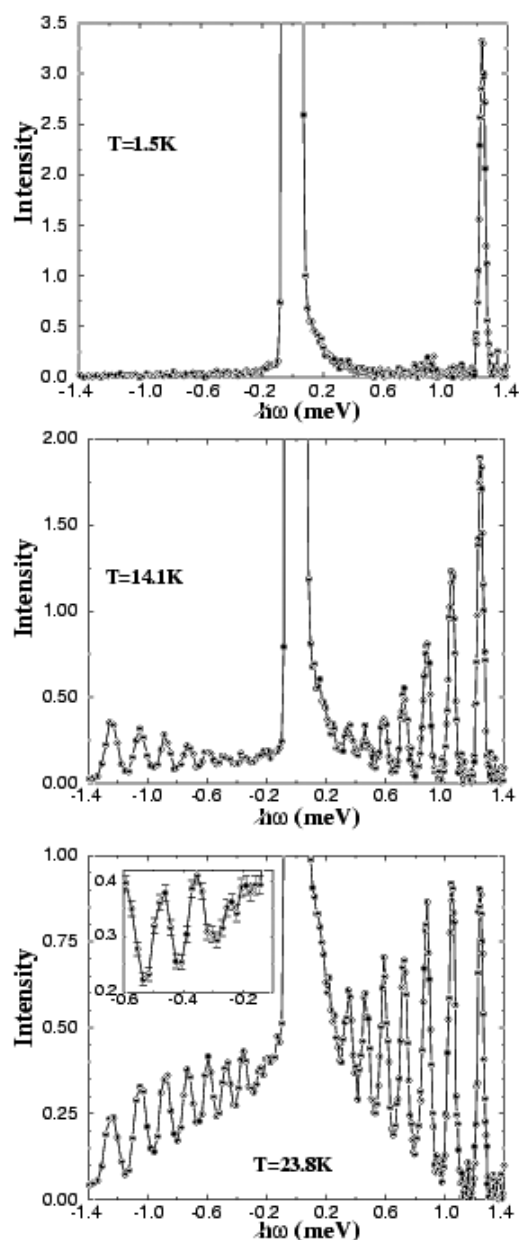


Figure 36. Inelastic neutron scattering data for Mn_{12} measured at three different temperatures. (Reprinted from [280] with permission. Copyright 1999 the American Physical Society.)

the magnetoelastic coupling in the Hamiltonian and model a dislocation [284]. This procedure results in local rotations of the magnetic anisotropy, and hence an effective local transverse magnetic field that unfreezes the odd tunnelling resonances. Recent structural data points to another origin of the effect: disorder of the acetic acid of crystallization is the main source of anisotropy and results in the Mn_{12} molecules experiencing an environment which is lower in symmetry than tetragonal [285]. This view has been supported by micro-Hall effect measurements [286].

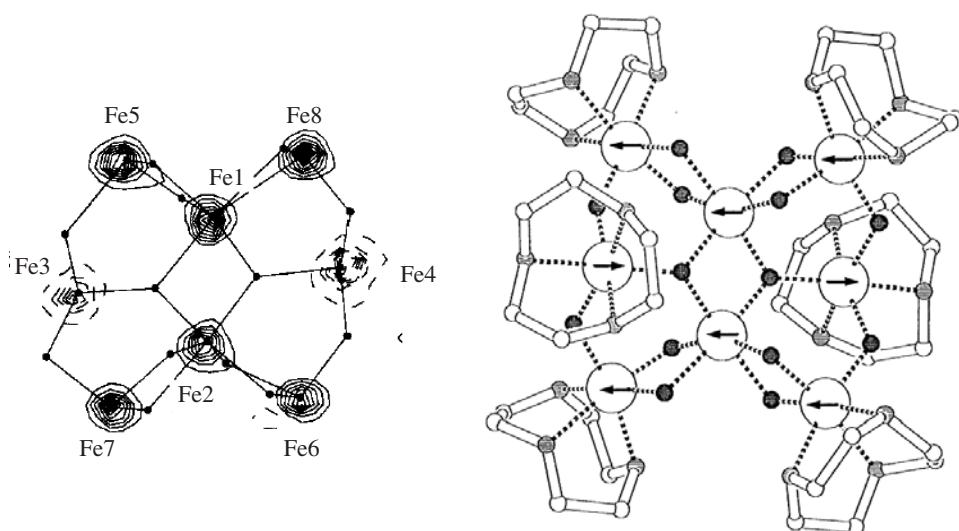


Figure 37. The MaxEnt reconstructed spin density of the Fe_8 cluster, from polarized neutron scattering data (after [287]; molecular structure shown schematically). (Reprinted with permission from [287]. Copyright 1999 the American Chemical Society.)

6.3. Fe_8

A second system which has been heavily studied is the octanuclear Fe(III) cluster $[\text{Fe}_8\text{O}_2(\text{OH})_{12}(\text{tacn})_6]^-$ (abbreviated to Fe_8) which is shown in the second row of table 1. This molecule has an $S = 10$ ground state due to interactions between the $\frac{5}{2}$ spins of the eight Fe(III) centres. The MaxEnt reconstructed spin density shown in figure 37 [287] demonstrates that the Fe atoms can be grouped into two sets, one set (Fe_3 and Fe_4) with moments opposing the field and the other set (Fe_1 , Fe_2 , Fe_6 , Fe_7 and Fe_8) with moments parallel to the field. This combination explains the $S = 10 = 6 \times \frac{5}{2} - 2 \times \frac{5}{2}$ ground state.

This cluster has no axial symmetry and hence its spin Hamiltonian does contain a term $E(S_x^2 - S_y^2)$. The ESR data were satisfactorily simulated with $D = 0.27$ K and $E = -0.046$ K [288]. Below 0.4 K, temperature dependent tunnelling through the barrier (of magnitude $DS^2 \approx 27$ K) is observed, corresponding to a quantum tunnelling of the magnetization [272]. This is a more clear-cut case than Mn_{12} in which temperature dependent (i.e. non-quantum) relaxation is observed even down to 0.06 K [289].

When two levels begin to cross, there is actually an avoided level crossing characterized by an energy gap called a tunnel splitting. This tunnel splitting can be tuned by a small transverse field. In fact, the tunnel splitting is an oscillatory function of the transverse field with period $2k_B[2E(E + |D|)]^{1/2}/g\mu_B$ [290], as has been demonstrated experimentally in Fe_8 using an array of micro-SQUIDS [291]. These oscillations result from a Berry phase [292] which enters the spin tunnelling probability and leads to radically different behaviour for integer and half-integer spins [293] (see also [294]).

At very low temperature, phonon-mediated relaxation can be neglected and in zero field the $M = \pm 10$ states are coupled by a tunnelling matrix element $\Delta \sim 10^{-7}$ K. The local dipolar magnetic fields induce an energy bias $\xi = g\mu_B SB \sim 10^{-1}$ K which forces almost all molecules off resonance. Magnetization relaxation can therefore only occur if there is some process, such as fast dynamic nuclear fluctuations, which acts to broaden the resonance [295]. This scenario can be described using a ‘spin-bath’ model [296], and this leads to the prediction of a relaxation

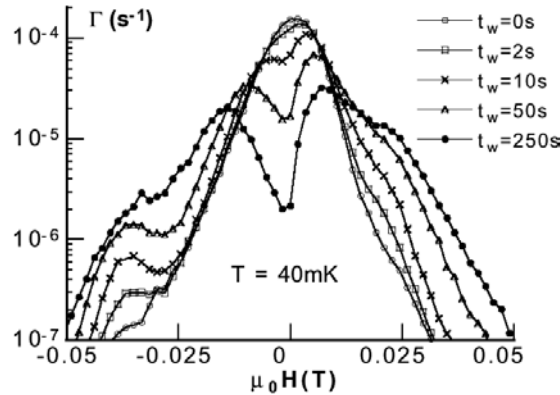


Figure 38. The field dependence of the short time square-root relaxation rate Γ in Fe_8 , showing the depletion of the molecular spin states by quantum tunnelling at $\mu_0 H = 0$ for various waiting times, t_w . The sample was magnetized at -1.4 T at 2 K and then rapidly cooled to 0.04 K. The sample was left at $H = 0$ for time t_w and then a small field was applied to measure the square-root relaxation. (Reprinted with permission from [297]. Copyright 1999 the American Physical Society.)

time with a ‘square-root time’ dependence, so that at short times t , the magnetization $M(t)$ is given by

$$M(t) = M(0) + [M_{\text{eq}} - M(0)]\sqrt{\Gamma t}, \quad (8)$$

where M_{eq} is the equilibrium magnetization, $\Gamma \sim \Delta^2 P(\xi)/\hbar$ and $P(\xi)$ is the distribution of energy bias in the sample [297]. Note that in equation (8), the quantities M_{eq} , $M(t)$ and Γ are functions of the applied field. This behaviour has been observed in crystals of Fe_8 [298], and the distribution $P(\xi)$ has hence been studied as a function of temperature [297].

Moreover, $P(\xi)$ is found to evolve during relaxation in a non-trivial way, illustrating how the tunnelling is proceeding in the sample. This gives rise to the so-called ‘hole-digging’ method, in which a hole in $P(\xi)$ is ‘dug’ by depleting the population of certain spins at a given applied field [297] by letting the relaxation occur (see figure 38). The hole linewidth is found to be independent of the initial value of the magnetization and is related to the inhomogeneous level broadening arising from the nuclear spins [295, 297]. This interpretation has been confirmed by studying samples with ^{56}Fe replaced by ^{57}Fe , and also those in which ^1H is partially replaced by ^2H . In each case, the width of the hole in $P(\xi)$ agrees with numerical simulations of the level broadening arising from the altered hyperfine couplings [299]. The hole-digging method has also now been performed for Mn_{12} [300], with similar results obtained at low temperature. At much higher temperatures, the effect of the nuclear spins on the relaxation is much less important, and the spin-phonon effect is expected to be dominant.

Monte Carlo simulations of the relaxation also support the hole-digging picture [301] and also the ‘square-root time’ relaxation in Fe_8 [302]. They also suggest that it arises from correlations that develop between the spins while the sample is cooled [302]. Moreover, $M(t) - M(0) \propto t^p$ relaxation is expected in general, where $p \approx 0.5$ for simple cubic lattices, but $p \approx 0.7$ for body-centred and face-centred cubic lattices [302]. This result depends on the samples being annealed by the magnetic field so that the spin-up and spin-down populations are unequal and this drives the magnetization process [303, 304].

These experiments have motivated a comprehensive set of studies exploring the tunnelling, relaxation and coherence in Mn_{12} and Fe_8 as a function of field, temperature and orientation of the magnetic field (see e.g. [305–309]). It has recently been predicted that the effects of

quantum tunnelling would lead to stepwise behaviour if the conductance of a SMM which could be measured by placing the SMM between an STM tip and a metallic substrate [310].

6.4. Other single-molecule magnets

The most detailed studies on SMMs so far have focused on Mn_{12} and Fe_8 . Nevertheless, many other SMMs have been discovered, and we briefly review some of these in this section.

A number of SMMs, such as Mn_4 [273] shown in schematic form in table 1, have been prepared based on a cubane structure. Four transition metal ions sit on four opposite corners of a distorted cube (to describe an inscribed pyramid), and three oxygens and a further bridging ion (such as Cl^- , F^- or one atom from a N_3^- , NCO^- or O_2CMe^- ligand) sit on the remaining four corners of the distorted cube. Stable complexes can be obtained by surrounding the cubane core with ligands. This structure can easily be modified and a number of clusters containing cubane cores can be prepared, some of them showing SMM behaviour ($D > 0$) with an $S = \frac{9}{2}$ ground state [273, 311–313]. Other variants can be obtained by flattening the cubane core, producing a layered core; see e.g. the cluster Fe_4 with $S = 5$ [314], or the related mixed-valence Mn_4 rhombus at the centre of the a cluster with $S = 8$ [315].

Although the intermolecular interactions between single-molecule magnets can usually be ignored, this is certainly not the case in a supramolecular dimer. In one such system, known as $[\text{Mn}_4]_2$, two Mn_4 cubane based molecules, each with ground state $S = \frac{9}{2}$, are coupled antiferromagnetically ($J = 0.1$ K) resulting in an $S = 0$ ground state [316] (see figure 39). The coupling results in an exchange bias of the tunnelling transitions [316] and also in additional quantum resonances associated with spin–spin cross-relaxation [318], allowing the effective exchange coupling to be deduced [319]. ESR transitions involve well defined superposition states on both molecules [317] and the measured hysteresis loops demonstrate quantum tunnelling of the magnetization via entangled states of the dimer [320].

The preparation of clusters with different spins is of interest because the tunnelling rate can be studied as a function of D , S and other terms in the Hamiltonian. One intriguing study has demonstrated that quantum tunnelling is suppressed at zero transverse field if the total spin of the magnetic system is half-integer (as a consequence of the Kramers degeneracy [321]) but allowed in integer spin systems [322].

An Mn_6 cluster with a total spin of $S = 12$ has a rather small anisotropy ($|D| \ll 0.05$ K), so that spin–lattice relaxation is fast down to the lowest temperatures and long range ferromagnetic dipolar order is found at $T_C = 0.16$ K [323]. The V_{15} cluster [324] has spin $S = \frac{1}{2}$ and has no anisotropy barrier, making it ideal to study direct phonon activation between the two levels [325].

At the opposite extreme are the very high spin states that can be obtained with a family of disc-like molecular clusters which have been prepared which contain either 17 or 19 iron atoms linked by oxygen atoms with organic ligands arranged around the edge [326, 275]. The highest spin of this family is $S = \frac{33}{2}$ exhibited by the complex $\text{Fe}_{19}\text{metheidi}$ (see table 1). This material has an anisotropy barrier of 15.7 K [327], and shows a transition to long range magnetic order at 1.17 K, probably due to superexchange between the clusters.

Other clusters of interest include a Ni_{12} cluster with an $S = 12$ ground state (see table 1), a Mn_9 cluster with an $S = \frac{17}{2}$ ground state [274, 278] (see table 1), an Fe_{10} cluster with an $S = 11$ ground state [328], a Cr_{12} cluster with an $S = 6$ ground state [329], and a V_4 cage has a butterfly-shaped core and an $S = 3$ ground state [330].

These clusters can all be extensively studied using magnetization measurements, but local probe techniques are also of use, including high frequency EPR (see e.g. [281, 331–336]), NMR (see e.g. [337–340]) and μSR (see e.g. [337, 338, 341–344]).

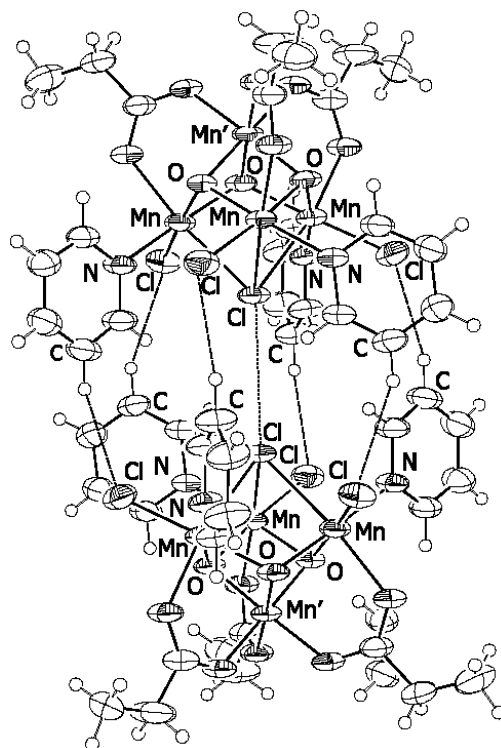


Figure 39. The $[\text{Mn}_4\text{O}_3\text{Cl}_4(\text{O}_2\text{CEt})_3(\text{py})_3]_2$ dimer; the Mn^{3+} and Mn^{4+} ions are labelled Mn and Mn', respectively. The dashed lines represent the C–H...Cl hydrogen bonds holding the dimer together, and the dotted line is the close approach of the central bridging Cl atoms believed to be the main pathway for the exchange interaction between the two Mn_4 molecules. (Reprinted with permission from [317]. Copyright 2003 AAAS.)

6.5. Magnetic wheels

Another recent development has been the synthesis of various cyclic polynuclear wheels (see e.g. [276, 345, 346]). In some of these systems, antiferromagnetic exchange renders the ground state spin $S = 0$, but a strong magnetic field can induce a level crossing to a non-zero-spin ground state [347]. The energy separation between the two lowest levels at an energy crossing vanishes in a centrosymmetric cluster (giving rise to a true level crossing) but anticrossings are produced in a non-centrosymmetric clusters (because of higher order terms in the Hamiltonian which mix states) and this can be observed using heat capacity measurements [347] or magnetometry [348–350]. The simple circular geometry makes these systems very attractive for theoretical treatment [351, 352]. Quantum coherence has been proposed to be observed in this class of nanomagnets [353–355], and the tunnelling dynamics of the Néel vector can be directly measured via the static magnetization and specific heat [353, 356]. Furthermore, the tunnelling of the Néel vector can also be detected using NMR and ESR [354], and some NMR studies on these systems have been performed [357]. The excitations in these antiferromagnetic wheels can be determined using inelastic neutron scattering, and although classical spin waves are found, the lowest excitations relevant for explaining low temperature data are quantized rotations of the Néel-type ground state configuration [358].

A variant on such wheels includes 2×2 squares of spins [359, 360] containing metal ions. Recently the first 3×3 grid complexes have been synthesized [361, 362] and show interesting

properties, including a field-induced level crossing between states of different S at which point the anisotropy changes sign [363]. They also show oscillations in the field dependence of the magnetic torque which is associated with an interesting level crossing effect [364].

Wheel systems may find applications in quantum computing applications. It was proposed recently [365] that molecules such as Fe_8 and Mn_{12} might be used to implement Grover's algorithm [366] for searching through a database (this algorithm was also applied to nuclear spins in GaAs [367]). Unfortunately, ferromagnetic clusters suffer from large matrix elements coupling their large spin to the environment, and hence tend to have short decoherence times. Antiferromagnetic systems, such as the ring compounds discussed above, do not suffer from this drawback, and quantum computing applications have been proposed for these systems [368, 369]. For an odd number of sites on a ring, a spin cluster qubit can be defined in terms of the ground state doublet and this turns out to be rather insensitive to the placement and coupling anisotropy of spins within the cluster [368]. The main advantage of spin clusters compared to single spins is that longer gate time operation times can be obtained [369]. Spin chains have also been proposed as possible quantum computation architectures, primarily for facilitating quantum communication between quantum computers [370]. So far these schemes remain to be implemented. A crucial component of any scheme to link SMMs is a patterning scheme, and some progress has begun to be made in this direction [371].

7. Conclusion

This review has shown that the use of organic and molecular building blocks can lead to new magnetic materials with intriguing properties which have, on occasion, led to the discovery of new physics. Organic groups can provide the source of the magnetic moment or mediate magnetic exchange interactions. In fact, even a simple hydride ion is now known to be an effective mediator of exchange interactions [372]. Molecular systems are attractive and are often praised for their 'spontaneous self-assembly'. This effect of course often frustrates the aim of performing 'crystal engineering', and many of the breakthroughs described above have come about somewhat serendipitously. Nevertheless, there is an undercurrent of rational design and once a new material with desirable properties is found, subtle chemical changes can be used to optimize it in a manner which is becoming increasingly predictable and understood [373]. The search is currently on for new materials with higher coercivities, higher transition temperatures, more pronounced anisotropies, or larger magnetoresistance. Many puzzles remain to be solved in, for example, the behaviour of single-molecule magnets and the relationship between magnetism and superconductivity. Moreover, little has so far been done to understand how domains behave in organic and molecular magnets. The advances already gained in this field have originated through developments in synthetic and coordination chemistry, but the whole enterprise is an interdisciplinary effort, involving both physicists and chemists, which promises to remain fast moving and continually surprising.

References

- [1] Ishiguro T, Yamaji K and Saito G 1998 *Organic Superconductors* (Berlin: Springer)
- [2] Rosseinsky M J 1995 *J. Mater. Chem.* **5** 1497
- [3] Tanigaki K and Prassides K 1995 *J. Mater. Chem.* **5** 1515
- [4] Kahn O 1993 *Molecular Magnetism* (Weinheim: Wiley-VCH)
- [5] Miller J S and Drillon M (ed) 2001 *Magnetism: Molecules to Materials* vol 1–3 (Weinheim: Wiley-VCH)
- [6] Lahti P M (ed) 1999 *Magnetic Properties of Organic Materials* (New York: Dekker)
- [7] Kahn O (ed) 1996 *Magnetism: A Supramolecular Function (NATO ASI vol C484)* (Dordrecht: Kluwer)
- [8] Verdaguer M 2001 *Polyhedron* **20** 1115

- [9] Itoh K and Kinoshita M (ed) 2000 *Molecular Magnetism, New Magnetic Materials* (Tokyo: Kodansha), (Amsterdam: Gordon and Breach)
- [10] Day P and Underhill A E (ed) 1999 Metal–organic and organic molecular magnets *Phil. Trans. R. Soc. A* **357** 2851
- [11] Heisenberg W 1928 *Z. Phys.* **49** 613
- [12] Sugano T 2001 *Polyhedron* **20** 1285
- [13] Mukai K 1969 *Bull. Chem. Soc. Japan* **42** 40
- [14] Awaga K, Sugano T and Kinoshita M 1986 *Chem. Phys. Lett.* **128** 587
- [15] Awaga K, Sugano T and Kinoshita M 1986 *J. Chem. Phys.* **85** 1211
- [16] McConnell H M 1967 *Proc. R. A. Welch Found. Chem. Res.* **11** 144
- [17] Awaga K, Sugano T and Kinoshita M 1987 *Chem. Phys. Lett.* **141** 540
- [18] McConnell H M 1963 *J. Chem. Phys.* **39** 1910
- [19] Brown P J, Capiomont A, Gillon B and Schweizer J 1979 *J. Magn. Magn. Mater.* **14** 289
- [20] Saint Paul M and Veyret C 1973 *Phys. Lett. A* **45** 362
- [21] Benoit A, Flouquet J, Gillon B and Schweizer J 1983 *J. Magn. Magn. Mater.* **31–34** 1155
- [22] Chouteau G and Veyret-Jeandey C 1981 *J. Physique* **42** 1441
- [23] Blundell S J, Pattenden P A, Pratt F L, Valladares R M, Sugano T and Hayes W 1995 *Europhys. Lett.* **31** 573
- [24] Blundell S J, Husmann A, Jestadt T, Pratt F L, Marshall I M, Lovett B W, Kurmoo M, Sugano T and Hayes W 2000 *Physica B* **289** 115
- [25] Capiomont A 1972 *Acta Crystallogr. B* **28** 2298
- [26] Sugano T, Blundell S J, Pratt F L, Jestadt T, Lovett B W, Hayes W and Day P 1999 *Mol. Cryst. Liq. Cryst.* **334** 477
- [27] Bramwell S T and Holdsworth P C W 1993 *J. Phys.: Condens. Matter* **5** L53
- [28] Tamura M, Nakazawa Y, Shiomi D, Nozawa K, Hosokoshi Y, Ishikawa M, Takahashi M and Kinoshita M 1991 *Chem. Phys. Lett.* **186** 401
- [29] Nakazawa Y, Tamura M, Shirakawa N, Shiomi D, Takahashi M, Kinoshita M and Ishikawa M 1992 *Phys. Rev. B* **46** 8906
- [30] Kinoshita M 1999 *Phil. Trans. R. Soc. A* **357** 2855
- [31] Le L P, Keren A, Luke G M, Wu W D, Uemura Y J, Tamura M, Ishikawa M and Kinoshita M 1993 *Chem. Phys. Lett.* **206** 405
- [32] Zheludev A, Ressouche E, Schweitzer J, Wan M and Wang H 1994 *J. Magn. Magn. Mater.* **135** 147
- [33] Ressouche E 2001 *J. Phys. Chem. Solids* **62** 2161
- [34] Takahashi M, Turek P, Nakazawa Y, Tamura M, Nozawa K, Shiomi D, Ishikawa M and Kinoshita M 1991 *Phys. Rev. Lett.* **67** 746
- [35] Takahashi M, Turek P, Nakazawa Y, Tamura M, Nozawa K, Shiomi D, Ishikawa M and Kinoshita M 1992 *Phys. Rev. Lett.* **69** 1290
- [36] Takeda K, Konishi K, Tamura M and Kinoshita M 1996 *Phys. Rev. B* **53** 3374
- [37] Mito M, Deguchi H, Tanimoto T, Kawae T, Nakatsuji S, Moromoto H, Anzai H, Nakao H, Murakami Y and Takeda K 2003 *Phys. Rev. B* **67** 024427
- [38] Pratt F L, Valladares R, Caulfield J, Deckers I, Singleton J, Fisher A J, Hayes W, Kurmoo M, Day P and Sugano T 1993 *Synth. Met.* **61** 171
- [39] Blundell S J, Marshall I M, Lovett B W, Pratt F L, Husmann A, Hayes W, Takagi S and Sugano T 2001 *Hyperfine Interact.* **133** 169
- [40] Blundell S J, Sugano T, Pattenden P A, Pratt F L, Valladares R M, Chow K H, Uekusa H, Ohashi Y and Hayes W 1996 *J. Phys.: Condens. Matter* **8** L1
- [41] Blundell S J, Pattenden P A, Valladares R M, Pratt F L, Sugano T and Hayes W 1994 *Solid State Commun.* **92** 569
- [42] Deumal M, Cirujeda J, Veciana J and Novoa J J 1998 *Adv. Mater.* **10** 1461
- [43] Amabilino D B, Cirujeda J and Veciana J 1999 *Phil. Trans. R. Soc. A* **357** 2873
- [44] Watanabe I, Wada N, Yano H, Okuno T, Awaga K, Ohira S, Nishiyama K and Nagamine K 1998 *Phys. Rev. B* **58** 2438
- [45] Awaga K, Okuno T, Yamaguchi A, Hasegawa M, Inabe T, Maruyama W and Wada N 1994 *Phys. Rev. B* **49** 3975
- [46] Wada N, Kobayashi T, Yano H, Okuno T, Yamaguchi A and Awaga K 1997 *J. Phys. Soc. Japan* **66** 961
- [47] Awaga K, Wada N, Watanabe I and Inabe T 1999 *Phil. Trans. R. Soc. A* **357** 2993
- [48] Chiarrelli R, Novak M A, Rassat A and Tholence J L 1993 *Nature* **363** 147
- [49] Shiomi D, Tamura M, Sawa H, Kato R and Kinoshita M 1993 *Synth. Met.* **55–57** 3298
- [50] Hosokoshi Y, Katoh K, Nakazawa Y, Nakano H and Inoue K 2001 *J. Am. Chem. Soc.* **123** 7921

- [51] Slipchenko L V, Munsch T E, Wenthold P G and Krylov A I 2004 *Angew. Chem. Int. Edn Engl.* **43** 742
- [52] Nogami T, Ishida T, Yasui M, Iwasaki F, Takeda N, Ishikawa M, Kawakami T and Yamaguchi K 1996 *Bull. Chem. Soc. Japan* **69** 1841
- [53] Togashi K, Imachi R, Tomioka K, Tsuboi H, Ishida T, Nogami T, Takeda N and Ishikawa M 1996 *Bull. Chem. Soc. Japan* **69** 2821
- [54] Ishida T, Ohira S, Watanabe I, Nogami T and Nagamine K 2001 *Polyhedron* **20** 1545
- [55] Mito M, Kawae T, Hitaka M, Takeda K, Ishida T and Nogami T 2001 *Chem. Phys. Lett.* **333** 69
- [56] Allemand P-M, Srdanov G and Wudl F 1990 *J. Am. Chem. Soc.* **112** 9391
- [57] Neugebauer F A, Fischer H and Krieger C 1993 *J. Chem. Soc. Perkin Trans. 2* **1993** 535
- [58] Takeda K, Hamano T, Kawae T, Hidaka M, Takahashi M, Kawasaki S and Mukai K 1995 *J. Phys. Soc. Japan* **64** 2343
- [59] Mukai K, Konishi K, Nedachi K and Takeda K 1996 *J. Phys. Chem.* **100** 9658
- [60] Itoh K and Kinoshita M (ed) 2000 *Molecular Magnetism, New Magnetic Materials* (Tokyo: Kodansha), (Amsterdam: Gordon and Breach) p 216
- [61] Mukai K, Suzuki K, Ohara K, Jamali J B and Achiwa N 1999 *J. Phys. Soc. Japan* **68** 3078
- [62] Rawson J M and Palacio F 2001 *Struct. Bond.* **100** 93
- [63] Palacio F, Antorrena G, Castro M, Burriel R, Rawson J, Smith J N B, Bricklebank N, Novoa J and Ritter C 1997 *Phys. Rev. Lett.* **79** 2336
- [64] Mito M, Kawae T, Takeda K, Takagi S, Matsushita Y, Deguchi H, Rawson J M and Palacio F 2001 *Polyhedron* **20** 1509
- [65] Pratt F L, Goeta A E, Palacio F, Rawson J M and Smith J N B 2000 *Physica B* **289** 119
- [66] Luzon J, Campo J, Palacio F, McIntyre G J, Goeta A E, Ressouche E, Pask C M and Rawson J M 2003 *Physica B* **335** 1
- [67] Antorrena G, Davies J E, Hartley M, Palacio F, Rawson J M, Smith J N B and Steiner A 1999 *Chem. Commun.* 1393
- [68] Feeder N, Less R J, Rawson J M, Oliete P and Palacio F 2000 *Chem. Commun.* 2449
- [69] Awere E G, Byeford N, Haddon R C, Parsons S, Passmore J, Waszczak J V and White P S 1990 *Inorg. Chem.* **29** 4821
- [70] McManus G D, Rawson J M, Feeder N, Palacio F and Oliete P 2000 *J. Mater. Chem.* **10** 2001
- [71] Fujita W, Awaga K, Nakazawa Y, Saito K and Sorai M 2002 *Chem. Phys. Lett.* **352** 348
- [72] Fujita W and Awaga K 1999 *Science* **286** 261
- [73] Fujita W and Awaga K 2001 *Polyhedron* **20** 1517
- [74] McManus G D, Rawson J M, Feeder N, van Duijn J, McInnes E J L, Novoa J J, Burriel R, Palacio F and Oliete P 2001 *J. Mater. Chem.* **11** 1992
- [75] Fujita W, Awaga K, Matsuzaki H and Okamoto H 2002 *Phys. Rev. B* **65** 064434
- [76] Matsuzaki H, Fujita W, Awaga K and Okamoto H 2003 *Phys. Rev. Lett.* **91** 017403
- [77] Wolmershäuser G, Wortman G and Schnauber M 1988 *J. Chem. Res. (S)* 358
- [78] Fujita W and Awaga K 2002 *Chem. Phys. Lett.* **357** 385
- [79] Fujita W, Awaga K, Takahashi M, Takeda M and Yamazaki T 2002 *Chem. Phys. Lett.* **362** 97
- [80] Allemand P M, Khemani K C, Koch A, Wudl F, Holczler K, Donovan S, Gruner G and Thompson J D 1991 *Science* **253** 301
- [81] Lappas A, Prassides K, Vavakis K, Arcon D, Blinc R, Cevc P, Amato A, Feyerherm R, Gygax F N and Schenck A 1995 *Science* **267** 1799
- [82] Cevc P, Blinc R, Erzen V, Arcon D, Zalar B, Mihailovic D and Venturini P 1994 *Solid State Commun.* **90** 543
- [83] Blinc R, Cevc P, Aron D, Mihailovic D and Venturini P 1994 *Phys. Rev. B* **50** 13051
- [84] Tanaka K, Zakhidov A A, Yoshizawa K, Okahara K, Yamabe T, Yakushi K, Kikuchi K, Suzuki S, Ikemoto I and Achiba Y 1993 *Phys. Rev. B* **47** 7554
- [85] Blinc R *et al* 1996 *Phys. Rev. Lett.* **76** 523
- [86] Aron D, Cevc P, Omerzu A and Blinc R 1998 *Phys. Rev. Lett.* **80** 1529
- [87] Kambe T, Nogami Y and Oshima K 2000 *Phys. Rev. B* **61** R862
- [88] Mrzel A, Cevc P, Omerzu A and Mihailovic D 1996 *Phys. Rev. B* **53** R2922
- [89] Mihailovic D, Arcon D, Venturini P, Blinc R, Omerzu A and Cevc P 1995 *Science* **268** 400
- [90] Tanaka K, Asai Y, Sato T, Kuga T, Yamabe T and Tokumoto M 1996 *Chem. Phys. Lett.* **259** 574
- [91] Narymbetov B, Omerzu A, Kabanov V V, Tokumoto M, Kobayashi H and Mihailovic D 2000 *Nature* **407** 883
- [92] Uemura Y J, Kojima K, Luke G M, Wu W D, Oszlanyi G, Chauvet O and Forro L 1995 *Phys. Rev. B* **52** R6991
- [93] Macfarlane W A, Kiefl R F, Dunsiger S, Sonier J E and Fischer J E 1995 *Phys. Rev. B* **52** R6995
- [94] Cristofolini L *et al* 1995 *J. Phys.: Condens. Matter* **7** L567
- [95] Takenobu T, Muro T, Iwasa Y and Mitani T 2000 *Phys. Rev. Lett.* **85** 381

- [196] Makarova T L, Sundqvist B, Hohne R, Esquinazi P, Kopelevich Y, Scharff P, Davydov V A, Kashevarova L S and Rakhmanina A V 2001 *Nature* **413** 716
- [197] Wood R A, Lewis M H, Lees M R, Bennington S M, Cain M G and Kitamura N 2002 *J. Phys.: Condens. Matter* **14** L385
- [198] Narozhnyi V N, Müller K-M, Eckert D, Teresiak A, Dunsch L, Davydov V A, Kashevarova L S and Rakhmanina A V 2003 *Physica B* **329–333** 1217
- [199] FitzHugh E W (ed) *Artists' Pigments: A Handbook of Their History and Characteristics* vol 3 (Oxford: Oxford University Press)
- [100] Hoden A N, Matthias B T, Anderson P W and Lewis H W 1956 *Phys. Rev.* **102** 1463
- [101] Bozorth R M, William H J and Walsh D E 1956 *Phys. Rev.* **103** 572
- [102] Mallah T, Thiebalt S, Verdaguer M and Veillet P 1993 *Science* **262** 1554
- [103] Entley W R and Girolami G S 1995 *Science* **268** 397
- [104] Miller J S 2000 *MRS Bull.* (November) 33
- [105] Ferlay S, Mallah T, Ouhahes L, Veillet P and Verdaguer M 1995 *Nature* **378** 701
- [106] Hatlevik Ø, Buschmann W E, Zhang J, Manson J L and Miller J S 1999 *Adv. Mater.* **11** 914
- [107] Holmes S D and Girolami G S 1999 *J. Am. Chem. Soc.* **121** 5593
- [108] Ohkoshi S, Abe Y, Fujishima A and Hashimoto K 1999 *Phys. Rev. Lett.* **82** 1285
- [109] Ohkoshi S, Hozumi T and Hashimoto K 2001 *Phys. Rev. B* **64** 132404
- [110] Miller J S and Manson J L 2001 *Acc. Chem. Res.* **34** 563
- [111] Batten S R, Jensen P, Moubaraki B, Murray K S and Robson R 1998 *Chem. Commun.* 439
- [112] Kurmoo M and Kepert C J 1998 *New J. Chem.* **22** 1515
- [113] Kurmoo M and Kepert C J 1999 *Mol. Cryst. Liq. Cryst.* **334** 693
- [114] Batten S R, Jensen P, Kepert C J, Kurmoo M, Moubaraki B, Murray K S and Price D J 1999 *J. Chem. Soc. Dalton Trans.* 2987
- [115] Kurmoo M 1999 *Chem. Mater.* **11** 3370
- [116] Manson J L *et al* 1998 *Chem. Mater.* **10** 2552
- [117] Lappas A, Wills A S, Green M A, Prassides K and Kurmoo M 2003 *Phys. Rev. B* **67** 144406
- [118] Kmety C R, Manson J L, Huang Q, Lynn J W, Erwin R W, Miller J S and Epstein A J 1999 *Phys. Rev. B* **60** 60
- [119] Kmety C R, Huang Q, Lynn J W, Erwin R W, Manson J L, McCall S, Crow J E, Stevenson K L, Miller J S and Epstein A J 2000 *Phys. Rev. B* **62** 5576
- [120] Batten S R and Murray K S 2003 *Coord. Chem. Rev.* **246** 103
- [121] Blundell S J 2001 *Magnetism in Condensed Matter* (Oxford: Oxford University Press)
- [122] Gütlich P, Garcia Y and Goodwin H A 2000 *Chem. Soc. Rev.* **29** 419
- [123] Decurtins S, Gütlich P, Köhler C P, Spiering H and Hauser A 1984 *Chem. Phys. Lett.* **105** 1
- [124] Scheidt W R and Reed C A 1981 *Chem. Soc. Rev.* **81** 543
- [125] Willembacher N and Spiering H 1988 *J. Phys. C: Solid State Phys.* **21** 1423
- [126] Kahn O and Martinez C J 1998 *Science* **279** 44
- [127] Létard J-F, Guionneau P, Codjovi E, Lavastre O, Bravic G, Chasseau D and Kahn O 1997 *J. Am. Chem. Soc.* **119** 10861
- [128] Daubric H, Cantin C, Thomas C, Kliava J, Létard J-F and Kahn O 1999 *Chem. Phys. Lett.* **244** 75
- [129] Briois V, Cartier dit Moulin C, Sainctavit P, Brouder C and Flank A-M 1995 *J. Am. Chem. Soc.* **117** 1019
- [130] Ksenofontov V, Spiering H, Reiman S, Garcia Y, Gaspar A B, Moliner N, Real J A and Gütlich P 2001 *Chem. Phys. Lett.* **348** 381
- [131] Guionneau P, Létard J-F, Yufit D S, Chasseau D, Bravic G, Goeta A E, Howard J A K and Kahn O 1999 *J. Mater. Chem.* **9** 985
- [132] Ksenofontov V, Levchenko G, Spiering H, Gutlich P, Létard J-F, Bouhedja Y and Kahn O 1998 *Chem. Phys. Lett.* **294** 545
- [133] Kahn O, Sommier L and Codjovi E 1997 *Chem. Mater.* **9** 3199
- [134] Lanfranc de Panthou F, Beloriki E, Calenczuk R, Luneau D, Marcenat C, Ressouche E, Turek P and Rey P 1995 *J. Am. Chem. Soc.* **117** 11247
- [135] Adams D M, Dei A, Rheingold A L and Hendrickson D N 1993 *J. Am. Chem. Soc.* **115** 8221
- [136] Capes L, Létard J-F and Kahn O 2000 *Chem. Eur. J.* **6** 2246
- Létard J F, Capes L, Chastanet G, Moliner N, Létard S, Real J A and Kahn O 1999 *Chem. Phys. Lett.* **313** 115
- [137] Marcén S, Lecren L, Capes L, Goodwin H A and Létard J-F 2002 *Chem. Phys. Lett.* **358** 87
- [138] Belitto C and Day P 1978 *J. Chem. Soc. Chem. Commun.* 511
- [139] Day P 1979 *Acc. Chem. Res.* **12** 236
- [140] Belitto C, Fair M J, Wood T E and Day P 1980 *J. Phys. C: Solid State Phys.* **13** L627

- [141] Hauser A 1986 *Chem. Phys. Lett.* **124** 543
- [142] Ogawa Y, Koshihara S, Koshino K, Ogawa T, Urano C and Takagi H 2000 *Phys. Rev. Lett.* **84** 3181
- [143] Tayagaki T and Tanaka K 2001 *Phys. Rev. Lett.* **86** 2886
- [144] Sato O, Iyoda T, Fujishima A and Hashimoto K 1996 *Science* **272** 704
- [145] Sato O, Hayami S, Gu Z, Takahashi K, Nakajima R and Fujishima A 2002 *Chem. Phys. Lett.* **355** 169
- [146] Liu H W, Matsuda K, Gu Z Z, Takahashi K, Cui A L, Nakajima R, Fujishima A and Sato O 2003 *Phys. Rev. Lett.* **90** 167403
- [147] Pejaković D A, Manson J L, Miller J S and Epstein A J 2000 *Phys. Rev. Lett.* **85** 1994
- [148] Halder G J, Kepert C J, Moubaraki B, Murray K S and Cashion J D 2002 *Science* **298** 1762
- [149] Chittipeddi S, Cromack K R, Miller J S and Epstein A J 1987 *Phys. Rev. Lett.* **58** 2695
- [150] Chakraborty A, Epstein A J, Lawless W N and Miller J S 1989 *Phys. Rev. B* **40** 11422
- [151] Huang Z J, Chen F, Ren Y T, Xue Y Y, Chu C W and Miller J S 1993 *J. Appl. Phys.* **73** 6563
- [152] Zheludev A, Grand A, Ressouche E, Schweizer J, Morin B, Epstein A J, Dixon D A and Miller J S 1994 *J. Am. Chem. Soc.* **116** 7243
- [153] Uemura Y J, Keren A, Le L P, Luke G M, Sternlieb B J and Wu W D 1994 *Hyperfine Interact.* **85** 133
- [154] Yee G T, Manriquez J M, Dixon D A, McLean R S, Groski D M, Flippen R B, Narayan K S, Epstein A J and Miller J S 1991 *Adv. Mater.* **3** 309
- [155] Miller J S and Epstein A J 1994 *Angew. Chem. Int. Edn Engl.* **33** 385
- [156] Narayan K S, Morin B G, Miller J S and Epstein A J 1992 *Phys. Rev. B* **46** 6195
- [157] Manriquez J M, Yee G T, McLean R S, Epstein A J and Miller J S 1991 *Science* **252** 1415
- [158] Pokhodnya K I, Peterson N and Miller J S 2002 *Inorg. Chem.* **41** 1996
- [159] Raebinger J W and Miller J S 2002 *Inorg. Chem.* **41** 3308
- [160] Miller J S 2000 *Inorg. Chem.* **39** 4392
- [161] Candela G A, Swartzendruber L, Miller J S and Rice M J 1979 *J. Am. Chem. Soc.* **101** 2755
- [162] Broderick W E, Thompson J A, Day E P and Hoffman B M 1990 *Science* **249** 401
- [163] Clérac R, O'Kane S, Cowen J, Ouyang X, Heintz R, Zhao H, Bazile M J Jr and Dunbar K R 2003 *Chem. Mater.* **15** 1840
- [164] Ueda K *et al* 1996 *Chem. Phys. Lett.* **261** 295
- [165] Painelli A, Pecile C and Girlando A 1986 *Mol. Cryst. Liq. Cryst.* **134** 1
- [166] Kuoroda N *et al* 2003 *Synth. Met.* **133/134** 535
- [167] Kato R 2000 *Bull. Chem. Soc. Japan* **73** 515
- [168] Hiraoka M, Sakamoto H, Mizoguchi K and Kato R 2002 *Phys. Rev. B* **65** 174413
- [169] Garrigou-Lagrange Ch, Róžański S A, Kurmoo M, Pratt F L, Macéno G, Delhaès P, Lequan M and Lequan R M 1988 *Solid State Commun.* **67** 481
- [170] Umeya M, Kawata S, Matsuzaka H, Kitagawa S, Nishikawa H, Kikuchi K and Ikemoto I 1998 *J. Mater. Chem.* **8** 295
- [171] Coomber A T, Beljonne D, Friend R H, Bredas J L, Charlton A, Robertson N, Underhill A E, Kurmoo M and Day P 1996 *Nature* **380** 144
- [172] Rovira C *et al* 1997 *Angew. Chem. Int. Edn Engl.* **36** 2324
- [173] Rovira C 2000 *Chem. Eur. J.* **6** 1723
- [174] Arcon D, Lappas A, Margadonna S, Prassides K, Ribera E, Veciana J, Rovira C, Henriques R T and Almeida M 1999 *Phys. Rev. B* **60** 4191
- [175] Nakamura T, Takahashi T, Aonuma S and Kato R 2001 *J. Mater. Chem.* **11** 2159
- [176] Tamura M and Kato R 2002 *J. Phys.: Condens. Matter* **14** L729
- [177] Tanaka H, Okano Y, Kobayashi H, Suzuki W and Kobayashi A 2001 *Science* **291** 285
- [178] Tanaka H, Kobayashi H and Kobayashi A 2002 *J. Am. Chem. Soc.* **124** 10002
- [179] Stumpf H O, Ouahab L, Pei Y, Grandjean D and Kahn O 1993 *Science* **261** 447
- [180] Stumpf H O, Ouahab L, Pei Y, Bergerat P and Kahn O 1994 *J. Am. Chem. Soc.* **116** 3866
- [181] Kurmoo M, Kumagai H, Green M A, Lovett B W, Blundell S J, Ardavan A and Singleton J 2001 *J. Solid State Chem.* **159** 343
- [182] Rujjwatra A, Kepert C J, Claridge J B, Rosseinsky M J, Kumagai H and Kurmoo M 2001 *J. Am. Chem. Soc.* **123** 10584
- [183] Kurmoo M, Kumagai H, Hughes S M and Kepert C J 2003 *Inorg. Chem.* **42** 6709
- [184] Tamaki H, Zhong Z J, Matsumoto N, Kida S, Koikawa M, Achiwa N, Hashimoto Y and Okawa H 1992 *J. Am. Chem. Soc.* **114** 6974
- [185] Coronado E, Galán-Mascarós J R, Gómez-García C J, Enslin J and Gütlich P 2000 *Chem. Eur. J.* **5** 52
- [186] Akutsu H *et al* 2002 *J. Am. Chem. Soc.* **124** 12430
- [187] Coldea A I, Bangura A F, Singleton J A, Ardavan A, Akutsu-Sato A, Akutsu H, Turner S S and Day P 2004 *Phys. Rev. B* **69** 165103

- [188] Day P 1993 *Phys. Scr.* T **49** 726
- [189] Singleton J 2000 *Rep. Prog. Phys.* **63** 1111
- [190] Wosnitza J 1996 *Fermi Surfaces of Low-Dimensional Organic Metals and Superconductors* (Berlin: Springer)
- [191] Mori T 2002 *J. Solid State Chem.* **168** 433
- [192] Kawakami T, Taniguchi T, Nakano S, Kitagawa Y and Yamaguchi K 2003 *Polyhedron* **22** 2051
- [193] Enoki T, Umeyama T, Enomoto M, Yamaura J, Yamaguchi K, Miyazaki A, Ogura E, Kuwatani Y, Iyoda M and Kikuchi K 1999 *Synth. Met.* **103** 2275
- [194] Day P *et al* 1992 *J. Am. Chem. Soc.* **114** 10722
- [195] Kurmoo M, Day P, Guionneau P, Bravic G, Chasseau D, Ducasse L, Allan M L, Marsden I D and Friend R H 1996 *Inorg. Chem.* **35** 4719
- [196] Kurmoo M *et al* 1995 *J. Am. Chem. Soc.* **117** 12209
- [197] Coronado E, Galán-Mascarós J R, Gómez-García C J and Laukhin V 2000 *Nature* **408** 447
- [198] Kobayashi A, Udagawa T, Tomita H, Naito T and Kobayashi H 1993 *Chem. Lett.* 2179
- [199] Tanaka H, Kobayashi A, Sato A, Akutsu H and Kobayashi H 1999 *J. Am. Chem. Soc.* **121** 760
- [200] Kobayashi H, Tomita H, Naito T, Kobayashi A, Sakai F, Watanabe T and Cassoux P 1996 *J. Am. Chem. Soc.* **118** 368
- [201] Cepas O, McKenzie R H and Merino J 2002 *Phys. Rev. B* **65** 100502
- [202] Uji S, Shinagawa H, Terashima T, Yakabe T, Terai Y, Tokumoto M, Kobayashi A, Tanaka H and Kobayashi H 2001 *Nature* **410** 908
- [203] Balicas L B, Brooks J S, Storr K, Uji S, Tokumoto M, Tanaka H, Kobayashi H, Kobayashi A, Barzykin V and Gor'kov L P 2001 *Phys. Rev. Lett.* **87** 067002
- [204] Jaccarino V and Peter M 1962 *Phys. Rev. Lett.* **9** 260
- [205] Tanatar M A, Ishiguro T, Tanaka H and Kobayashi H 2002 *Phys. Rev. B* **66** 134503
- [206] Houzet M, Buzdin A, Bulaevskii L and Maley M 2002 *Phys. Rev. Lett.* **88** 227001
- [207] Fulde P and Ferrell R A 1964 *Phys. Rev.* **135** A550
- [208] Larkin A I and Ovchinnikov Yu N 1964 *Zh. Eksp. Teor. Fiz.* **47** 1136
Larkin A I and Ovchinnikov Yu N 1965 *Sov. Phys.—JETP* **20** 762 (Engl. Transl.)
- [209] Bulaevskii L, Buzdin A and Maley M 2003 *Phys. Rev. Lett.* **90** 067003
- [210] Uji S *et al* 2003 *Synth. Met.* **137** 1183
- [211] Kobayashi H, Kobayashi A and Cassoux P 2000 *Chem. Soc. Rev.* **29** 325
- [212] Pratt F L, Lee S L, Blundell S J, Marshall I M, Uozaki H and Toyota N 2003 *Synth. Met.* **133** 489
- [213] Hotta C and Fukuyama H 2000 *J. Phys. Soc. Japan* **69** 2577
- [214] de Jongh L J and Miedama A R 1974 *Adv. Phys.* **23** 1
- [215] Ami T, Crawford M K, Harlow R L, Wang Z R, Johnston D C, Huang Q and Erwin R W 1995 *Phys. Rev. B* **51** 5994
- [216] Motoyama N, Eisaki H and Uchida S 1996 *Phys. Rev. Lett.* **76** 3212
- [217] Haldane F D M 1983 *Phys. Rev. Lett.* **50** 1153
- [218] Kojima K M *et al* 1997 *Phys. Rev. Lett.* **78** 1787
- [219] Bonner J C and Fisher M E 1964 *Phys. Rev.* **135** A640
- [220] Eggert S, Affleck I and Takahashi M 1994 *Phys. Rev. Lett.* **73** 332
- [221] Takeda K, Konishi K, Nedachi K and Mukai K 1995 *Phys. Rev. Lett.* **74** 1673
- [222] Haines D N and Drumheller J E 1987 *Phys. Rev. Lett.* **58** 2702
- [223] Bordallo H N, Chapon L, Manson J L, Ling C D, Qualls J S, Hall D and Argyriou D N 2003 *Polyhedron* **22** 2045
- [224] Manson J L 2003 *Inorg. Chem.* **42** 2602
- [225] Landee C P, Turnbull M M, Galeriu C, Giantsidis J and Woodward F M 2001 *Phys. Rev. B* **63** 100402
- [226] Caneschi A, Gatteschi D and Sessoli R 1993 *Inorg. Chem.* **32** 4612
- [227] Caneschi A, Gatteschi D, Rey P and Sessoli R 1991 *Inorg. Chem.* **30** 3936
- [228] Caneschi A, Gatteschi D, Renard J P, Rey P and Sessoli R 1989 *Inorg. Chem.* **28** 3314
- [229] Caneschi A, Gatteschi D, Rey P and Sessoli R 1988 *Inorg. Chem.* **27** 1756
- [230] Benelli C, Caneschi A, Gatteschi D, Pardi L and Rey P 1990 *Inorg. Chem.* **29** 4223
- [231] Caneschi A, Gatteschi D, Renard J P, Rey P and Sessoli R 1989 *Inorg. Chem.* **28** 1976
- [232] Villain J and Loveluck J M 1977 *J. Physique Lett.* **38** L77
- [233] Caneschi A, Gatteschi D and Lelirzin A 1994 *J. Mater. Chem.* **4** 319
- [234] Benelli C and Gatteschi D 2002 *Chem. Rev.* **102** 2369
- [235] Benelli C, Caneschi A, Gatteschi D, Pardi L and Rey P 1989 *Inorg. Chem.* **28** 3230
- [236] Benelli C, Caneschi A, Gatteschi D and Sessoli R 1993 *Inorg. Chem.* **32** 4797
- [237] Benelli C, Caneschi A, Gatteschi D and Sessoli R 1992 *Adv. Mater.* **4** 504

- [238] Lascialfari A, Ullu R, Affronte M, Cinti F, Caneschi A, Gatteschi D, Rovai D, Pini M G and Rettori A 2003 *Phys. Rev. B* **67** 224408
- [239] Bartolomé F, Bartolomé J, Benelli C, Caneschi A, Gatteschi D, Paulsen C, Pini M G, Rettori A, Sessoli R and Volokitin Y 1996 *Phys. Rev. Lett.* **77** 382
- [240] Affronte M, Caneschi A, Cucci C, Gatteschi D, Lasjaunias J C, Paulsen C, Pini M G, Rettori A and Sessoli R 1999 *Phys. Rev. B* **59** 6282
- [241] Villain J 1998 *Ann. Isr. Phys. Soc.* **2** 565
- [242] Bray J W, Interrante L V, Jacobs I S and Bonner J C 1983 *Extended Linear Chain Compounds* vol 3 (New York: Plenum) p 353
- [243] Lovett B W, Blundell S J, Pratt F L, Jestadt T, Hayes W, Tagaki S and Kurmoo M 2000 *Phys. Rev. B* **61** 12241
- [244] Huizinga S, Kommandeur J, Sawatzky G A, Thole B T, Kopinga K, de Jonge W J M and Roos J 1979 *Phys. Rev. B* **19** 4723
- [245] Bulaevskii L N 1969 *Sov. Phys.—Solid State* **11** 921
- [246] Bray J W, Hart H R, Interrante L V, Jacobs I S, Kasper J S, Watkins G D, Wee S H and Bonner J C 1975 *Phys. Rev. Lett.* **35** 744
- [247] Jacobs I S, Bray J W, Hart H R, Interrante L V, Kasper J S, Watkins G D, Prober D E and Bonner J C 1976 *Phys. Rev. B* **14** 3036
- [248] Obertelli S D, Friend R H, Talham D R, Kurmoo M and Day P 1989 *J. Phys.: Condens. Matter* **1** 5671
- [249] Parker I D, Friend R H, Kurmoo M and Day P 1989 *J. Phys.: Condens. Matter* **1** 5681
- [250] Kurmoo M, Green M A, Day P, Bellitto C, Staulo G, Pratt F L and Hayes W 1993 *Synth. Met.* **55–57** 2380
- [251] Ducasse L, Coulon C, Chasseau D, Yagbasan R, Fabre J M and Gouasmia A K 1988 *Synth. Met.* **27** B543
- [252] Liu Q, Ravy S, Pouget J P, Coulon C and Bourbonnais C 1993 *Synth. Met.* **55–57** 1840
- [253] Hase M, Terasaki I and Uchinokura K 1993 *Phys. Rev. Lett.* **70** 3651
- [254] Konno M, Kobayashi H, Marumo F and Saito G 1973 *Bull. Chem. Soc. Japan* **46** 1987
- [255] Hase M, Terasaki I, Sasago Y, Uchinokura K and Obara H 1993 *Phys. Rev. Lett.* **71** 4059
- [256] Kang W, Hannahs S T and Chaikin P M 1993 *Phys. Rev. Lett.* **70** 3091
- [257] Le L P *et al* 1993 *Phys. Rev. B* **48** 7284
- [258] Mataga N 1968 *Theor. Chim. Acta* **10** 372
- [259] Rajca A, Wongsriratanakul J and Rajca S 2001 *Science* **294** 1503
- [260] Néel L 1949 *C. R. Acad. Sci.* **34** 3397
- [261] Morrish A H and Yu S P 1956 *Phys. Rev.* **102** 670
- [262] Bean C P and Livingstone J D 1959 *J. Appl. Phys.* **30** 120S
- [263] Caldeira A O and Leggett A J 1981 *Phys. Rev. Lett.* **46** 211
- [264] Leggett A J, Chakravarty S, Dorsey A T, Fisher M P A, Garg A and Zwerger W 1987 *Rev. Mod. Phys.* **59** 1
- [265] Dumestre F, Chaudret B, Amiens C, Renaud P and Fejes P 2004 *Science* **303** 821
- [266] Jamet M, Wernsdorfer W, Thirion C, Mailly D, Dupuis V, Melinon P and Perez A 2001 *Phys. Rev. Lett.* **86** 4676
- [267] Winpenny R E P 2002 *J. Chem. Soc. Dalton Trans.* **1**
- [268] Gatteschi D, Caneschi A, Pardi L and Sessoli R 1994 *Science* **265** 1054
- [269] Sessoli R, Gatteschi D, Caneschi A and Novak M A 1993 *Nature* **365** 141
- [270] Friedman J R, Sarachik M P, Tejada J and Ziolo R 1996 *Phys. Rev. Lett.* **76** 3830
- [271] Thomas L, Lioni F, Ballou R, Gatteschi D, Sessoli R and Barbara B 1996 *Nature* **383** 145
- [272] Sangregorio C, Ohm T, Paulsen C, Sessoli R and Gatteschi D 1997 *Phys. Rev. Lett.* **78** 4645
- [273] Aubin S M J, Wemple M W, Adams D M, Tsai H L, Christou G and Hendrickson D N 1996 *J. Am. Chem. Soc.* **118** 7746
- [274] Brechin E K, Soler M, Davidson J, Hendrickson D N, Parsons S and Christou G 2002 *Chem. Commun.* 2252
- [275] Goodwin J C, Sessoli R, Gatteschi D, Wernsdorfer W, Powell A K and Heath S L 2000 *J. Chem. Soc. Dalton Trans.* 1835
- [276] Andres H *et al* 2002 *Chem.—Eur. J.* **8** 4867
- [277] Tejada J 2001 *Polyhedron* **20** 1751
- [278] Brechin E K, Soler M, Christou G, Davidson J, Hendrickson D N, Parsons S and Wernsdorfer W 2003 *Polyhedron* **22** 1771
- [279] Park K, Pederson M R and Hellberg C S 2004 *Phys. Rev. B* **69** 014416
- [280] Mirebeau I, Hennion M, Caslata H, Andres H, Güdel H U, Irodova A V and Caneschi A 1999 *Phys. Rev. Lett.* **83** 628
- [281] Hill S, Perenboom J A A J, Dalal N S, Hathaway T, Stalcup T and Brooks J S 1998 *Phys. Rev. Lett.* **80** 2453
- [282] Pederson M R, Bernstein N and Kortus J 2002 *Phys. Rev. Lett.* **89** 097202
- [283] Sushkov A B, Jones B R, Musfeldt J L, Wang Y J, Achey R M and Dalal N S 2001 *Phys. Rev. B* **63** 214408

- [284] Chudnovsky E M and Garanin D A 2001 *Phys. Rev. Lett.* **87** 187203
- [285] Cornia A, Sessoli R, Sorace L, Gatteschi D, Barra A L and Daiguebonne C 2002 *Phys. Rev. Lett.* **89** 257201
- [286] del Barco E, Kent A D, Rumberger E M, Hendrickson D N and Christou G 2003 *Phys. Rev. Lett.* **91** 047203
- [287] Pontillon Y, Caneschi A, Gatteschi D, Sessoli R, Ressouche E, Schweitzer J and Lelievre-Berna E 1999 *J. Am. Chem. Soc.* **121** 5342
- [288] Barra A L, Debrunner P, Gatteschi D, Schulz C E and Sessoli R 1996 *Europhys. Lett.* **35** 133
- [289] Perenboom J A A J, Brooks J S, Hill S, Hathaway T and Dalal N S 1998 *Phys. Rev. B* **58** 330
- [290] Garg A 1993 *Europhys. Lett.* **22** 205
- [291] Wernsdorfer W and Sessoli R 1999 *Science* **284** 133
- [292] Berry M V 1984 *Proc. R. Soc. A* **392** 45
- [293] Loss D, DiVincenzo D P and Grinstein G 1992 *Phys. Rev. Lett.* **69** 3232
- [294] Barnes S E 2001 *Phys. Rev. Lett.* **87** 167201
- [295] Prokof'ev N V and Stamp P C E 1998 *Phys. Rev. Lett.* **80** 5794
- [296] Prokof'ev N V and Stamp P C E 2000 *Rep. Prog. Phys.* **63** 669
- [297] Wernsdorfer W, Ohm T, Sangregorio C, Sessoli R, Mailly D and Paulsen C 1999 *Phys. Rev. Lett.* **82** 3903
- [298] Ohm T, Sangregorio C and Paulsen C 1998 *Europhys. J. B* **6** 195
- [299] Wernsdorfer W, Caneschi A, Sessoli R, Gatteschi D, Cornia A, Villar V and Paulsen C 2000 *Phys. Rev. Lett.* **84** 2965
- [300] Wernsdorfer W, Sessoli R and Gatteschi D 1999 *Europhys. Lett.* **47** 254
- [301] Alonso J J and Fernández J F 2001 *Phys. Rev. Lett.* **87** 097205
- [302] Fernández J F and Alonso J J 2003 *Phys. Rev. Lett.* **91** 047202
- [303] Tupitsyn I S and Stamp P C E 2004 *Phys. Rev. Lett.* **92** 119701
- [304] Fernández J F and Alonso J J 2004 *Phys. Rev. Lett.* **92** 119702
- [305] Bellessa G, Vernier N, Barbara B and Gatteschi D 1999 *Phys. Rev. Lett.* **83** 416
- [306] Luis F, Mettes F L, Tejada J, Gatteschi D and de Jongh L J 2000 *Phys. Rev. Lett.* **85** 4377
- [307] Chiorescu I, Giraud R, Jansen A G M, Caneschi A and Barbara B 2000 *Phys. Rev. Lett.* **85** 4807
- [308] Mettes F L, Luis F and de Jongh L J 2001 *Phys. Rev. B* **64** 174411
- [309] Mertes K M, Suzuki Y, Sarachik M P, Paltiel Y, Shtrikman H, Zeldov E, Rumberger E, Hendrickson D N and Christou G 2001 *Phys. Rev. Lett.* **87** 227205
- [310] Kim G-H and Kim T-S 2004 *Phys. Rev. Lett.* **92** 137203
- [311] Hendrickson D N *et al* 1992 *J. Am. Chem. Soc.* **114** 2455
- [312] Wemple M W, Adams D M, Hagen K S, Folting K, Hendrickson D N and Christou G 1995 *Chem. Commun.* 1591
- [313] Wemple M W, Adams D M, Folting K, Hendrickson D N and Christou G 1995 *J. Am. Chem. Soc.* **117** 7275
- [314] Barra A L, Caneschi A, Cornia A, de Biani F F, Gatteschi D, Sangregorio C, Sessoli R and Sorace L 1999 *J. Am. Chem. Soc.* **121** 5302
- [315] Brechin E K, Yoo J, Nakano M, Huffman J C, Hendrickson D N and Christou G 1999 *Chem. Commun.* 783
- [316] Wernsdorfer W, Allaga-Alcalde N, Hendrickson D N and Christou G 2002 *Nature* **416** 406
- [317] Hill S, Edwards R S, Aliaga-Alcalde N and Christou G 2003 *Science* **302** 1015
- [318] Wernsdorfer W, Bhaduri S, Hendrickson D N and Christou G 2002 *Phys. Rev. Lett.* **89** 197201
- [319] Tiron R, Wernsdorfer W, Aliaga-Alcalde N and Christou G 2003 *Phys. Rev. B* **68** 140407
- [320] Tiron R, Wernsdorfer W, Foguet-Albiol D, Aliaga-Alcalde N and Christou G 2003 *Phys. Rev. Lett.* **91** 227203
- [321] van Hemmen J L and Sütö S 1986 *Europhys. Lett.* **1** 481
- [322] Wernsdorfer W, Bhaduri S, Boskovic C, Christou G and Hendrickson D N 2002 *Phys. Rev. B* **65** 180403
- [323] Morello A, Mettes F L, Luis F, Fernandez J F, Krzystek J, Aromi G, Christou G and de Jongh L J 2003 *Phys. Rev. Lett.* **90** 017206
- [324] Gatteschi D, Pardi L, Barra A L, Müller A and Doring J 1991 *Nature* **354** 463
- [325] Chiorescu I, Wernsdorfer W, Müller A, Miyashita S and Barbara B 2003 *Phys. Rev. B* **67** 020402
- [326] Powell A K, Heath S L, Gatteschi D, Pardi L, Sessoli R, Spina G, Delgiallo F and Pieralli F 1995 *J. Am. Chem. Soc.* **117** 2491
- [327] Affronte M, Lasjaunias J C, Wernsdorfer W, Sessoli R, Gatteschi D, Heath S L, Fort A and Rettori A 2002 *Phys. Rev. B* **66** 064408
- [328] Benelli C, Cano J, Journaux Y, Sessoli R, Solan G A and Winpenny R E P 2001 *Inorg. Chem.* **40** 188
- [329] Mabbs F E, McInnes E J L, Murrie M, Parsons S, Smith G M, Wilson C C and Winpenny R E P 1999 *Chem. Commun.* 643
- [330] Sun Z M, Grant C M, Castro S L, Hendrickson D N and Christou G 1998 *Chem. Commun.* 721
- [331] Barra A L, Gatteschi D and Sessoli R 1997 *Phys. Rev. B* **56** 8192
- [332] Barra A L, Brunel L C, Gatteschi D, Pardi L and Sessoli R 1998 *Acc. Chem. Res.* **31** 460

- [333] Park K, Novotny M A, Dalal N S, Hill S and Rikvold P A 2002 *Phys. Rev. B* **66** 144409
- [334] Hill S, Maccagnano S, Park K, Achey R M, North J M and Dalal N S 2002 *Phys. Rev. B* **65** 224410
- [335] Park K, Novotny M A, Dalal N S, Hill S and Rikvold P A 2002 *Phys. Rev. B* **65** 014426
- [336] Hill S, Edwards R S, Jones S I, Dalal N S and North J M 2003 *Phys. Rev. Lett.* **90** 217204
- [337] Lascialfari A, Gatteschi D, Borsa F, Shastri A, Jang Z H and Carretta P 1998 *Phys. Rev. B* **57** 514
- [338] Lascialfari A, Jang Z H, Borsa F, Carretta P and Gatteschi D 1998 *Phys. Rev. Lett.* **81** 3773
- [339] Kubo T, Goto T, Koshihara T, Takeda K and Awaga K 2002 *Phys. Rev. B* **65** 224425
- [340] Furukawa Y, Watanabe K, Kumagai K, Borsa F, Sasaki T, Kobayashi N and Gatteschi D 2003 *Phys. Rev. B* **67** 064426
- [341] Salman Z, Keren A, Mendels P, Sculler A and Verdager M 2000 *Physica B* **289** 106
- [342] Salman Z, Keren A, Mendels P, Marvaud V, Sculler A, Verdager M, Lord J S and Baines C 2002 *Phys. Rev. B* **65** 132403
- [343] Blundell S J, Pratt F L, Lancaster T, Marshall I M, Steer C A, Heath S L, Létard J F, Sugano T, Mihailovic D and Omerzu A 2003 *Polyhedron* **22** 1973
- [344] Lancaster T, Blundell S J, Pratt F L, Brooks M L, Manson J L, Brechin E K, Cadon C, Law D, McInnes E J L and Winpenny R E P 2004 *J. Phys.: Condens. Matter* submitted
- [345] Taft K L, Delfs C D, Papaefthymiou G C, Foner S, Gatteschi D and Lippard S J 1994 *J. Am. Chem. Soc.* **116** 823
- [346] Brechin E K, Cador O, Caneschi A, Cadiou C, Harris S G, Parsons S, Vonci M and Winpenny R E P 2002 *Chem. Commun.* 1860
- [347] Affronte M, Cornia A, Lascialfari A, Borsa F, Gatteschi D, Hinderer J, Horvatic M, Jansen A G M and Julien M H 2002 *Phys. Rev. Lett.* **88** 167201
- [348] Waldmann O, Koch R, Schromm S, Muller P, Bernt I and Saalfrank R W 2002 *Phys. Rev. Lett.* **89** 246401
Waldmann O, Koch R, Schromm S, Muller P, Bernt I and Saalfrank R W 2002 *Phys. Rev. Lett.* **90** 229904 (erratum)
- [349] Affronte M *et al* 2003 *Phys. Rev. B* **68** 104403
- [350] Normand B, Wang X, Zotos X and Loss D 2001 *Phys. Rev. B* **63** 184409
- [351] Schnack J and Luban M 2000 *Phys. Rev. B* **63** 014418
- [352] Waldmann O 2002 *Europhys. Lett.* **60** 302
- [353] Chiolero A and Loss D 1998 *Phys. Rev. Lett.* **80** 169
- [354] Meier F and Loss D 2001 *Phys. Rev. Lett.* **86** 5373
- [355] Honecker A, Meier F, Loss D and Normand B 2002 *Eur. Phys. J. B* **27** 487
- [356] Meier F and Loss D 2001 *Phys. Rev. B* **64** 224411
- [357] Lascialfari A, Gatteschi D, Cornia A, Balucani U, Pini M G and Rettori A 1998 *Phys. Rev. B* **57** 1115
- [358] Waldmann O, Guidi T, Carretta S, Mondelli C and Dearden A L 2003 *Phys. Rev. Lett.* **91** 237202
- [359] Waldmann O, Hassmann J, Müller P, Hanan G S, Volkmer D, Schubert U S and Lehn J-M 1997 *Phys. Rev. Lett.* **78** 3390
- [360] Koch R, Waldmann O, Muller P, Reimann U and Saalfrank R W 2003 *Phys. Rev. B* **67** 094407
- [361] Zhao L A, Matthews C J, Thompson L K and Heath S L 2000 *Chem. Commun.* 265
- [362] Zhao L, Xu Z Q, Thompson L K, Heath S L, Miller D O and Ohba M 2000 *Angew. Chem. Int. Edn Engl.* **39** 3114
- [363] Waldmann O, Zhao L and Thompson L K 2002 *Phys. Rev. Lett.* **88** 066401
- [364] Waldmann O, Carretta S, Santini P, Koch R, Jansen A G M, Amoretti G, Caciuffo R, Zhao L and Thompson L K 2004 *Phys. Rev. Lett.* **92** 096403
- [365] Leuenberger M N and Loss D 2001 *Nature* **410** 789
- [366] Grover L K 1997 *Phys. Rev. Lett.* **79** 325
Grover L K 1997 *Phys. Rev. Lett.* **79** 4709
Grover L K 1998 *Phys. Rev. Lett.* **80** 4329
- [367] Leuenberger M N, Loss D, Poggio M and Awschalom D D 2002 *Phys. Rev. Lett.* **89** 207601
- [368] Meier F, Levy J and Loss D 2003 *Phys. Rev. B* **68** 134417
- [369] Meier F, Levy J and Loss D 2003 *Phys. Rev. Lett.* **90** 047901
- [370] Bose S 2003 *Phys. Rev. Lett.* **91** 207901
- [371] Cavallini M, Biscarini F, Gomez-Segura J, Ruiz D and Veciana J 2003 *Nano Lett.* **3** 1527
- [372] Hayward M A, Cussen E J, Claridge J B, Bieringer M, Rosseinsky M J, Kiely C J, Blundell S J, Marshall I M and Pratt F L 2002 *Science* **295** 1882
- [373] Lehn J-M 2004 *Rep. Prog. Phys.* **67** 249